Characterization and Modeling of Dispersed Synthetic Fibers in Dense Graded Asphalt Mixtures

A Dissertation

Presented in Partial Fulfillment of the Requirements for the

Degree of Doctor of Philosophy

with

a Major in Civil Engineering

in the

College of Graduate Studies

University of Idaho

by

Ahmed M. Muftah

Major Professor: Fouad Bayomy, Ph.D.

Committee Members: Emad Kassem, Ph.D.; Kevin Chang, Ph.D.; Gabriel Potirniche, Ph.D.

Department Chair: Patricia Colberg, Ph.D.

December 2016

Authorization to Submit Dissertation

This dissertation of Ahmed M. Muftah, submitted for the degree of Doctor of Philosophy with a Major in Civil Engineering and titled "**Characterization and Modeling of Dispersed Synthetic Fibers in Dense Graded Asphalt Mixtures**" has been reviewed in final form. Permission, as indicated by the signatures and dates below, is now granted to submit final copies to the college of Graduate Studies for approval.

Major Professor: Date:

_____ _____

Fouad Bayomy Ph.D.

Committee Members: Date:

_____ _____

Emad Kassem, Ph.D.

Date:

_____ _____

Gabriel Potirniche, Ph.D.

Date:

_____ _____

Kevin Chang, Ph.D.

Department

Chair: Date:

_____ _____

Patricia Colberg, Ph.D.

Abstract

The premature deterioration of hot mix asphalt pavements is one of the common issues concern many transportation agencies. Innovative solutions are needed to enhance the serviceable life of pavement. Various solutions are widely utilized, and one of the common techniques is fiber reinforcement.

Fibers have been used extensively in Portland Cement Concrete (PCC) since 1950's. However, use of fibers in asphalt mixtures is relatively new. There are limited studies that investigate the effect of fibers in asphalt mixtures. Some laboratory testing showed that fibers improved the resistance of asphalt mixtures to rutting and fatigue. However, these investigations did not provide comprehensive understanding of the interaction mechanism between asphalt mixture constituents and fibers. The goal of this research was to evaluate and quantify the effect of fibers on the asphalt mix performance characteristics. Furthermore, the research aimed at evaluating the healing characteristics, developing a method to detect the fiber dispersion in the mix and to develop a finite element model (FEM) to study the resistance of fiber-modified asphalt mixtures to permanent deformation.

Three types of synthetic fibers were used. Fiber #1 (aramid and polyolefin fibers), fiber #2 (a wax treated aramid fiber) and fiber #3 (glass fiber). A number of laboratory tests were conducted on laboratory-prepared test samples and extracted field cores. A FEM model to simulate the accelerated performance test was developed and was calibrated using material parameters from direct laboratory testing. X-ray tomography was used to evaluate and quantify the level of fiber dispersion in the mix.

The results show slightly improved performance at higher fiber contents than those recommended by the manufacturers. Asphalt healing study revealed that presence of fibers has increased healing rate and consequently delayed fatigue damage. The developed finite element model (FEM) can be used to predict long-term rutting performance of asphalt pavements. It was found out that X-ray tomography was not suitable to detect fiber dispersion. An optical image processing technique in conjunction with lab-based method using UV light was developed and found to be more successful to evaluate the fiber dispersion in the mix.

Acknowledgments

In the name of God the most merciful, the most compassionate.

I would like to express my deepest gratitude and appreciation to my advisor, Dr. Fouad Bayomy, who has offered me the great opportunity pursuing my Doctor of Philosophy degree at University of Idaho. I would never have been able to finish this dissertation without all his support, guidance, patience and encouragement.

I would also like to thank my committee members; Dr. Emad Kassem for his guidance, support, feedback, and providing continued supervision through this study; Dr. Kevin Chang for his help, support, and feedback. In addition, I would like to thank Dr. Gabriel Potirniche for his help, support, and feedback.

My research assistantship that supported my PhD study at the University of Idaho was mainly funded through series of research projects sponsored by the Idaho Transportation Department (ITD) and the Federal Highway Administration (FHWA). Many individuals at ITD have provided valuable help and assistance. Their support is greatly appreciated.

All lab work conducted at the University of Idaho material laboratories was not possible without the great help of Mr. Donald Parks, the Lab supervisor at the Department of Civil Engineering. I am so thankful to Don for always being there to assist when problems arise. Some of the tests performed during my research was conducted at the Washington State University (WSU) pavement laboratories. Special thanks are due to my friend Amir Bahadori, Graduate Student at WSU, for his help and assistance in the tests conducted at WSU.

Dedication

This dissertation is dedicated to my family, especially my wonderful mom (Fatma) and my great dad (Milad) in appreciation of their endless love, support and prayers; and to my brilliant, lovely and supportive wife, Joanna (Asia) for being at my side every step of the way. This is for all of you…

Table of Contents

List of Figures

List of Tables

1. Introduction

1.1 Backgroud

Technologies for fiber-reinforced Portland Cement Concrete (PCC) mixes have been widely developed, and they play a significant role in mitigating concrete cracks and increasing strength. On the other hand, research on fibers additives to improve the performance of Hot Mix Asphalt (HMA) for pavement applications is rather limited. A recent NCHRP Synthesis No. 475 summarized the state of practice for fibers in asphalt pavement (McDaniel, 2015). The report indicated that most of the states in the U.S. have used fibers in open graded mixtures. A limited number of states have used fibers in dense graded asphalt mixes. Types of fibers used included mineral, glass, cellulose, and synthetic polymer fiber. The design procedure of the fiber mixes is the same as of the conventional mixes; however, the purpose of using fibers is different. In the stone matrix asphalt (SMA) and open graded friction courses (OGFCs) or porous friction courses (PFCs), the primary use of fibers is to control the draindown of the binder in the mix. In the case of dense graded mixes, fibers are used to enhance the mix performance. Some studies suggested that the enhancement in mix performance could be linked to the extra tensile strength due to the addition of fibers and from the interconnection between aggregates, which allows the material to gain additional strain energy before cracking or fracture happens (Mahrez et al., 2011). Different types of fibers have been tested including glass, polyester, polypropylene, asbestos, carbon, cellulose, Kevlar and recycled waste fibers. (Chem et al., 2009; De S. Bueno et al., 2003).

Additionally, fiber modified HMA has evolved to include a blend of different fibers to achieve different performance aspects.

During the last decade many models have been developed to simulate the behavior of different types of fibers and fabrics in the PCC. However, when it comes to the HMA, the research lacks these models. This project focuses on the principles that have been employed to develop fiber reinforced concrete (FRC) models and use them to develop a FE model that simulate the behavior of fiber modified asphalt mixtures.

1.2 Problem Statement and Research Goal

As we make every effort to construct durable pavements with extended service life, we stand in need of materials with better performance than the conventional resources used today. Considering the massive investment in the highways system there is even greater necessity to sustain it, therefore, researchers are looking for better materials to a new construction and rehabilitation of flexible pavements. Since we hit the limits of the aggregates and binder performance, it seems the alternative way to achieve better performance is through additives. One of the innovative constituents is synthetic fibers which can be added to the asphalt mixtures to improve rutting resistance and reduce cracking. Fiber modified Asphalt Concrete (FRAC) seems to be a promising solution for achieving better performance. However, the main concern is that we don't have a comprehensive understanding of how fibers interact with the asphalt mixture and behave as one composite material. The reason is that factors such as fiber type, length, quantity, and even fibers' diameter play an important role on this composite material's behavior. The primary goal of this research was evaluate the evaluate the effect of adding fibers to the hot

mix asphalt (HMA) using well established laboratory tests, developing a model that allows for quantification of the effect of fibers on improving rutting performance, and develop a lab method to quantify the fiber dispersion in the asphalt mix.

1.3 Objectives

To achieve the primary goal of the study, the following set of objectives have been established:

1. Investigate the effect of fiber content and type on mechanical properties of asphalt mixtures.
2. Optimize the fiber content with asphalt mix design for superior performance at the reasonable cost.
3. Develop a procedure to quantify the dispersion of fibers in asphalt mixtures to ensure uniformity.
4. Develop a test procedure to evaluate the healing characteristics of asphalt mixtures with and without fibers.
5. Develop a FE model to study the resistance of fiber-modified asphalt mixtures to rutting.

1.4 Research Approach

The research was performed in six phases:

1. Review of the literature and current practice that relate to use of fibers in the asphalt mixes. The review also included the developments and advancements if the use of fibers in PCC mixes.

2. Material and Fiber Characterization: Among different types of fibers, three types from different manufactures were selected for this study, mixtures and samples preparations for different type of testing included in this phase.
3. Experimental Testing: Different performance testing protocols have been conducted to obtain the desired parameters for characterizing the viscoelastic-viscoplastic fiber modified asphalt mixtures. Tests were performed at different loading modes, various temperatures, and loading time to capture the effect of fibers on the performance of asphalt mixtures. These tests evaluated stiffness, rutting and cracking resistance potential for the proposed fiber types.
4. Evaluation of Healing Characteristic of Asphalt Mixtures: the effect of fibers on healing characteristics of asphalt mixtures has been studied. This part of the work focused on the microcrack healing of fiber modified asphalt concrete during rest periods and how that can reduce the accumulated damage. In addition, a combined effect of thermal treatment and rest period has been studied to investigate and evaluate the fibers' effect on healing. A new laboratory test protocol was developed for this objective.
5. Modeling of Fiber Modified HMA: Under this task, a Finite Element Model (FEM) has been developed to study the rutting performance of asphalt mixture modified with different fiber contents.
6. Evaluation of Fiber Dispersion in the Mix: Several methods were examined including chemical extraction method, X-ray Computed Tomography (X-ray CT) and Ultraviolet light. Indices have been developed to quantify the dispersion of fiber in the mixtures.

2. Literature Review of Fiber Modified Asphalt Mixtures

This chapter presents a literature review of relevant studies on modified fiber asphalt mixtures. A recent NCHRP Synthesis No. 475 summarized the state of practice of the use of fibers in asphalt pavements (McDaniel, 2015). The report indicated that most of the states have used fibers in open graded mixtures. A limited number of states have used fibers in dense graded asphalt mixes. The materials used in those projects are mineral, glass, cellulose, and synthetic polymer fiber. The design procedure of the fiber mixes is the same as of the conventional mixes; however, the purpose of using fibers is different. In the stone matrix asphalt (SMA) and open graded friction courses (OGFCs) or porous friction courses (PFCs); the primary use of fibers is to control the draindown of the binder in the mix. In the case of dense graded mixes, the use of fibers is to enhance the mix performance. Nevertheless, the results have shown the benefits of fibers are inconsistent. In some studies, the fibers improved the mix resistance to rutting and cracking, but in others, no significant difference was observed in the fiber-reinforced mixes. The following literature presents different results of the performance of fiber modified asphalt mixes.

2.1 Rutting Potential

Some studies indicated that adding fibers to the hot asphalt mixture may improve the rutting resistance. Jahromi and Khodai (2008) conducted a study evaluating the properties of modified carbon fibers asphalt mixtures. The laboratory tests included: marshal stability, repeated load indirect tensile test, creep compliance, indirect tension, and. The findings indicated that adding carbon fibers resulted in decrease in flow and increased air voids.

Nevertheless, the addition of carbon fibers to the mix improved Marshall Stability, increased rut resistance and fatigue life.

Mahrez and Karim (2003) stated that addition of glass fibers into stone mastic asphalt (SMA) produced variable Marshall Stability data, and a decrease in stiffness and stability of the mixture. In a following study, the authors evaluated the rutting resistance and creep of glass fiber-reinforced SMA mixtures by using wheel tracking test. They reported that mixtures containing glass fibers had higher resilient modulus and more resistance to rutting.

Bueno et al. (2003) conducted a study on evaluating the effect of randomly distributed synthetic fiber on the mechanical response of a cold-mixed densely graded asphalt mixtures. The laboratory investigation included Marshall, static and cyclic tri-axial tests. The evaluated properties included density, air voids, Marshall Stability and flow, elastic, and resilient moduli. The asphalt mixtures were treated with different staple polypropylene fibers lengths (10, 20, and 40 mm long), and fiber content of 0.1 and 0.25%. The findings indicated that presence of fibers in a mix is the main reason for a small variation in mixture shear strength tri-axial parameters, as well as for significant drops in the mixture resilient moduli when compared to control mixtures. It did not, however, affect the permanent strains of the mixtures. Also, addition of fibers to cold densely graded emulsified asphalt mixes reduced Marshall Stability and the dry density of the mix.

Chen et al. (2008) investigated the effect of different types of fibers on the volumetric and mechanical properties asphalt mixtures. Four different fibers were used: polyester, polyacrylonitrile, lignin, and asbestos fibers. They used Marshall Stability tests to measure the mechanical and volumetric properties of asphalt mixtures. Moisture susceptibility and

dynamic stability tests were used to examine the performance of the mixes. The results showed that generally, presence of fibers in the mixtures decreased the bulk specific gravity, while increased the optimum asphalt content, air void, voids in mineral aggregate and Marshall Stability. Optimum asphalt content, Marshall Stability, and dynamic stability increased initially and then decreased with increasing fiber content. It also showed that the polyacrylonitrile and polyester fibers had higher stability due to their higher networking effect. On the other hand, the asbestos and lignin fibers increased the optimum asphalt content due to their higher absorption. The test results using a fiber content of 0.35% by mass of mixture for the polyester fiber were used for final proportions.

Tapkin (2008) investigated the effect of polypropylene fibers on the behavior of the asphalt mixture. The fibers were added up to 0.3%, 0.5% and 1% by weight of the mix. For fiber-reinforced specimens it was observed that the Marshall Stability values increased and flow values decreased in an obvious manner. The fatigue life of these specimens was improved as well. The properties of asphalt concrete were enhanced due to adding polypropylene fibers. The fiber-reinforced asphalt mixture reflected good resistance to rutting, prolonged fatigue life and better reflection cracking resistance.

Ayyed et al. (2013) stated that among various modifiers used to improve the performance of asphalt-concrete (AC) mixtures, fibers have a leading position due their unique potential. His work focused on polypropylene (PP) and glass fibers as a novel concept of hybrid reinforcement of AC mixtures. Since both glass fiber modified AC and PP fiber modified AC mixtures exhibited improved performance compared to other fibers, these two types of fibers were used together to investigate possible additive improvement in the

performance of the AC mixtures. PP fibers with the length of 12 mm were blended with bitumen at different percentages, and glass fibers with the length of 12 mm were also added to aggregates. A combination of 0.1% of glass fiber plus 0.6% of PP presented the best hybrid reinforcement. Hybrid reinforced asphalt concrete (HRAC) samples were prepared using a Superpave gyratory compactor and tested for Marshall Stability. Volumetric analysis was done following the standard procedures. In the case of the normal bituminous specimens, penetration, softening point and ductility tests were carried out. Because of the tacky property of PP fiber around its melting point and the high modulus of glass fiber, the hybrid mixture increased stability and decreased flow. These results supported the idea that PP can significantly affect the properties and improve the consistency of the mixture. Therefore, this novel HRAC approach was suitable for use in hot regions due to growth in the void total mix (VTM) and stability.

Taher (2013) declared that due to the environmental conditions, construction, design errors, and more importantly due to the increase in the number of vehicles, especially those with high axle loads, two major distresses occur in road pavement: fatigue cracking and rutting. Using additives such as different types of polymer and fiber in asphalt concrete (AC) could be a solution to prolong the service life of asphalt pavement. His work also included summarized previous research that had been done on the effects of using different types of additives and aggregate gradation. The finding of his research as well as his review indicated that fatigue and rutting resistance can be enhanced by addition of fibers increasing the amount of strain energy absorbed during fatigue and fracture process of the mix in the resulting composite. Moreover, polymers and fibers provided 3D networking effect in

asphalt concrete and significantly stabilized the binder on surface of aggregate, thus, successfully prevented from any movement at higher temperature.

Su and Hachiya (2008) investigated the use of fiber reinforcement with recycled asphalt pavement (RAP) in airfield surface course pavements. The authors declared that adding of cellulose fibers increased the optimum binder content, and this led to improved Marshall Stability and provided less mass loss by the Cantabro test. The improvement of fibers was more noticeable when modified binder was used rather than virgin binder. The conclusion of their study was that the fiber addition to RAP containing modified binder increased the dynamic stability (wheel tracking test) making it suitable for airports with heavy loading.

2.2 Resistance to Fatigue Cracking

A research project by Federal Highway Administration studied the performance of fiber modified asphalt mixture in the laboratory and using full-scale accelerated pavement testing (Gibson et al., 2012). In one of twelve test lanes in the FHWA's accelerated loading facility (ALF), polyester fibers were added to the mix. The concentration of the fibers was 0.3 % by aggregate mass. The results indicated that the fatigue cracking of the fiber modified section was considerably less than those of the polymer modified and unmodified sections. Fatigue results in the lab did not match the full scale performance using an earlier variation of an axial fatigue (push-pull) methodology that was not conducted in an AMPT where the analysis used slightly different analytical mathematics along with a conventional 50% modulus reduction failure criteria.

In a following study, Gibson et al. (2015) examined the cracking resistance of two independent sets of mixtures from the FHWA full-scale accelerated loading facility and a Pennsylvania DOT trial section. Both sets had the same materials; a control mixture and a mixture with SBS modified binder. The same mix with synthetic (polyester) fiber reinforcement. Two methods of cracking characterization were evaluated; direct tension monotonic strength and simplified viscoelastic continuum damage. The results of dynamic modulus test indicated that the polymer modification has more effect than fiber modification. Cyclic fatigue test results showed both fiber modified mixes and SBS have better performance than the control mix in both sets of materials. In the cyclic fatigue tests, the fiber mixes performed better at higher fatigue stains, however, the SBS modified mix performed better under small fatigue strains.

Guo et al. (2007) conducted a research study that focused on the use of polyester fiber modified asphalt mixtures. The goal of this study was to examine the influence of fibers on the durability of asphalt pavement. Two types of asphalt mixtures were used. One was a densely graded asphalt mixture with 0.2% fibers, and the other was stone matrix asphalt (SMA) with 0.1% fibers. The results showed that adding fibers reduces the pavement crack propagation. It was concluded that, polyester fiber modified mixtures behaved much better in the fatigue resistance than that of non-fiber mixtures.

Lee et al. (2005) studied the influence of fibers on the fatigue cracking resistance of asphalt concrete. The fatigue resistance was based on the fracture energy. The recycled carpet fibers (Nylon) were used in this study. The experimental program was designed with two phases: the single fiber pull-out test which to determine the critical length of the fiber,

and that was 9.2 mm. Then the indirect tension strength tests were conducted on samples with two different fiber lengths 6 and 12 mm. The concentration of the fibers was 0.25, 0.5, and 1%. The results indicated that mixes with 1% and 12 mm results in 85% higher fracture energy than control specimens. The increased fracture energy shows a potential for better asphalt fatigue life.

Pyeong (2011) studied the characteristics of plastic fiber modified Hot-Mix asphalt mixtures. He concluded that in order to enhance the fatigue life of any mixture, the structural integrity of that mixture must be improved. Since a conventional asphalt mixture may have performance limitations, many geosynthetic fabric approaches have evolved such as: geogrid, geotextile, or geomembrane layers at the bottom the mixture or on the top of a subgrade. Although these interlayer techniques allow for improvement in the HMA pavements' performance by mitigating ruts or delaying reflective cracks, other parameters such as toughness, tensile strength, and shear strength of HMA mixtures need to be enhanced. The issue with these fabrics is its inability to mix with the asphalt mixtures. On the other hand, utilizing new plastic fibers within asphalt mixtures, as shown in the study enhances the structural integrity of the entire mixture which leads to significant improvements in phenomenological toughness and fatigue life. The improved performance of fiber modified mixtures over conventional hot-mix asphalt mixtures was measured by indirect cyclic fatigue tests in loading-control modes and four-point bending beam tests in displacement-control modes as the author indicated.

Alrajhi (2012) at Arizona State University studied the effect of adding different fiber quantities on the asphalt mixture and binder performance. The laboratory evaluation was

conducted by using sixteen different amounts and blends of the fibers with several combinations of aramid and polypropylene fibers. The asphalt mixture tests included the indirect tensile strength and the dynamic modulus. The binder tests included: softening point, penetration, and Brookfield viscosity tests. The binder test results showed that the best viscosity temperature susceptibility performance would be from the fiber blend of 75% polypropylene and 25% aramid, the dynamic modulus test results confirmed this finding as well. Generally, adding fibers to the HMA resulted in an increase in the stiffness of the mix. From the indirect tensile strength results, the aramid fibers showed more effect on post peak failure than the polypropylene fibers as manifested by higher fracture energy.

Putman (2011) investigated the effects of finishes applied to polyester fibers during the manufacturing on the asphalt binders and mastics properties. In this research, asphalt binders were blended with finishes that were extracted from the fibers. The mastics were similarly made with binder and fibers, with and without the finish, to separate the effects of the finish. The findings of this research indicated that the source of the asphalt crude plays a significant role on how the fiber finish affects the binders and mastics. Also, different finishes had different effects on binder properties. The main outcome of this research is that different polyester fibers, even from the same producer, may not always have the same performance in the asphalt mix. It is essential to use fibers that are compatible with the specific asphalt binder because of the effect of the binder source on the interaction between the binder and the finish.

2.3 Resistance to thermal cracking

Ahmed (2012) declared that the type and quantity of asphalt mixtures directly affect highways quality. Different types of additives and modifiers have been used in asphalt mixtures to mitigate the distresses that lead to the pavement failure. One of the most extensively studied additives is fiber which provides additional tensile strength in the resulting composite and potentially can increase the amount of strain absorbed during the fatigue and fracture process of the mixture. Although the increase in track axle loads, tire pressure, and the difference in pavement temperature led to the severity of permanent deformation and thermal cracking, mixtures with polypropylene fibers seem to be a promising solution to provide additional tensile strength in the resulting composite. In this study, using Marshall Methodology, indirect tensile strength, indirect creep test, and ultrasonic testing, several parameters of asphalt mixtures were evaluated: polypropylene fiber content, asphalt cement content, aggregate gradation and testing temperature. The obtained results confirmed that the addition of (0.3%) polypropylene fiber by weight of total mix with type (A) aggregate grading improved the performance of asphalt mixtures. Thus they were significantly more resistant to permanent deformation and thermal cracking.

Xu et al. (2010) studied the reinforcing effects and mechanisms of fibers on asphalt concrete (AC) mixtures with respect to temperature and water effects. The four different types of fibers included: polyester, polyacrylonitrile, lignin and asbestos were evaluated. Laboratory tests were conducted on the fiber modified mixtures to determine its strength, strain and fatigue behavior. Results show that fibers have substantially improved the asphalt mixture resistance to permanent deformation as well as fatigue life and toughness. The

flexural strength and ultimate flexural strain, and the split indirect tensile strength at low temperature were similarly enhanced. The polyester and polyacrylonitrile fibers improved rutting resistance and fatigue life more significantly than lignin and asbestos fibers. That might be as a result of their greater networking function. Unlike lignin and asbestos fibers that result in greater flexural strength and ultimate flexural strain, this networking function might result in greater asphalt stabilization effect. Furthermore, the researchers concluded that a 0.35% fiber content by mass of mixture achieved the optimum performance outputs of permanent deformation resistance and split indirect tensile test for polyester fiber.

Huang et al. (2009) investigated the influence of the conductive additives on the mechanical performance of asphalt. The test results of this study showed the variation of electrical and mechanical properties versus conductive additives such as steel and carbon fibers. In Huang et al.'s tests, steel fibers significantly improved rutting resistance, but not the fracture energy and strength of the mix.

2.4 Field Performance

Jiang and McDaniel (1992) investigated the field performance of asphalt overlays with various thicknesses. The overlays were on pavements with and without cracking and seating of the existing concrete surface. Polypropylene fibers with a concentration of 0.3% by weight of the mix were used in the intermediate and base layers of the overlays. The evaluation of eight years' field performance showed that adding fibers to the base and intermediate layers of a normal overlay section did not reduce cracking because reflective cracking is caused by horizontal and vertical movements. However, the researchers declared that fibers delayed and reduced cracking on both cracked and seated sections. Also, there was no noticeable

difference between the cracked and seated sections with fibers only in the base versus the in base and intermediate layers.

A study in Indiana conducted by McDaniel and Shah (2003) was to evaluate the use of seven different asphalt additives or modifiers. These additives included: polymers, gelled asphalt, and crumb rubber, as well as polyester fibers. The polyester fibers were added to an asphalt overlay over jointed concrete pavement. The fibers content was 0.3% by weight of the mix. The mixing of fibers was done in both dry and wet mixing processes with 30 s and 35 s mixing time in a batch plant, respectively. The results showed that polymerized asphalt cement (PAC), styrene butadiene rubber (SBR), and asphalt rubber mixtures were the most effective to resist cracking. Polyester fiber had slightly more cracking than the other additives. All the mixes including the control mix did not show significant rutting under heavy interstate traffic. The outcome of this research suggested that additives were not necessary to accomplish good performance.

One of the studies initiated in 1985 and conducted by Oregon DOT was on six test sections with fibers and polymer modified binders. There were two control sections and two fiber sections. One section included polypropylene fibers and another included polyester fibers. The structure of the test sections was 1.5 to 2 in of HMA layer with an unmodified base course (4 to 4.5 in.) over an existing pavement with severe alligator and thermal cracks. The performance for 10 years and application of more than 1.5 to 1.7 million equivalent single-axle loads showed that both fiber sections were comparable to the controls, with average rut depths of 13 to 16 mm. Similarly, for the fatigue cracking, the fiber sections performed comparably to the control one. However, the polypropylene fibers had better

performance than the polyester fibers in terms of block cracking, and both of them performed better than the control (Edger, 1998).

In a study for the New Jersey DOT, Bennert compared the performance of plant produced mixes with and without a combination of polyolefin and aramid fibers. The mix design was for traffic of 3 to 10 million equivalent single axle load. The lab performance tests included dynamic modulus, Flow number, beam fatigue test, and cycles to failure in the overlay tester. The results showed that fiber mixes had lower modulus values at high temperatures compared to the control mix. At low temperatures the control mixes were slightly stiffer than the fiber mixes. Phase angle results showed that control mixes were more elastic than the fiber mixes. The flow number test also indicated that control mixes had better resistance to rutting than fiber mixes by achieving higher number of cycles to 5% strain. The results of the beam fatigue test showed comparable results, however, the overlay test results revealed that the fiber mix had much greater resistance to crack propagation than the control one (Bennert, 2012).

Huang and White (1996) tested cores and slabs taken from test sections that were constructed on two high traffic ways in 1990 in Indiana. The test sections contained polypropylene fiber modified asphalt overlays. The lab testing included complex modulus testing on cores, and fatigue testing of beams cut from the pavement slabs. Dynamic modulus test results indicated that the fibers decreased the modulus, but did not affect the phase angle. However, beam fatigue testing showed that the use of fiber mixes had better fatigue life than the control one. On the other hand, the extraction of the fibers from the mixes showed that the actual fiber contents in the plant-produced mixes varied from the

target content in most samples (4% to 43% from the target). Although the other properties of the mix were within the specifications, the field densities were low. The air void contents of the fiber mixes were higher than those of the controls indicating that fibers could make the compaction harder.

2.5 Reviews of modeling fiber reinforced PCC

Most of the literature available on modeling of fiber-reinforced mixes are on Portland cement Concrete Mixes. Therefore, the following part of the review conducted as an effort to summarize the work that has been done in this field. Portland Cement Concrete is strong in compression but weak in tension. Its tensile strength is about 10% of the compressive strength. To overcome the tensile strength weakness, concrete must be reinforced by materials that can withstand tension such as steel and fibers. During its service life, a reinforced concrete structure is expected to have minor cracks in the tension zone which may affect the structural performance. This performance deteriorates due to repeated loads and exposure to extreme environments. The need for more sustainable transportation infrastructure such as pavements and bridges is the driving force toward tougher concrete structures. Fiber Reinforced Concrete (FRC) is sometimes employed to strengthen the aging structures. FRC offers higher strength and fatigue resistance than normal concrete which is attractive for highways.

Analytical models and numerical simulations have been used to examine the micromechanics of fiber reinforced concrete and describe the mechanical behavior of this composite material. Mainly, modeling fibers and fabrics in concrete can be classified into three levels based on the scale of the modeling. Microstructure modeling is commonly the

focus of the fiber cement matrix interface to explain the pullout mechanism between the fabrics and cement matrix and to simulate the bonding between fabrics and cement paste. Meso-scale modeling is used to link the responses at the micromechanics level to structural responses in the macroscopic leveling studying the crack evolution and tension responses of the fiber reinforced cement composites. Macro-scale modeling of fiber reinforcement is used to simulate the flexural response of structural elements (Mobasher, 2003).

The initial stiffness of the concrete is much higher than the post crack stiffness, and this reduction in the stiffness causes excessive deformation due to the application of loads. For this reason, the ability of reinforced concrete composites to carry loads after cracking is a very important issue. At the crack locations, even though the concrete has lost most of its tensile strength, it is still able to carry some tension forces between two parallel cracks, causing the material response to appear stiffer than the expected response of an assumed zero concrete tensile strength. This improvement in the stiffness depends upon the cracking mechanisms in reinforced members such as crack width, crack spacing, and the bonding between reinforcing materials such as fibers and matrix. The tension stiffening is observed in all reinforcing materials including fibers, and it is typically evaluated by three main approaches: experimental, analytical, and numerical (Soranakom, 2008). It is an important phase in material research to conduct experimental programs and establish empirical equations for specific set of factors that need to be studied. The obtained experimental data can provide important information of material behaviors that can be explained by empirical equations to show the relationship between the input variables and measured responses.

A Numerical Approach is commonly used when the behavior of the material is complex. Many factors are required to develop the mathematical models. Using several parameters may lead to long derivative equations that are not easy to solve. Finite element method is the most extensively used numerical tool to solve these complex equations. It has been used to simulate cracking and tensile behavior and bond mechanism of different materials. Mobasher et al. (1996) studied the toughening mechanisms in the brittle matrix composites. In this study, both finite element method and non-linear fracture mechanics were used. In the finite element analysis approach, the fibers were modeled by means of spring elements which resist the opening of existing cracks in the matrix. These nonlinear spring elements can be imposed with load deformation responses obtained from fiber pullout tests. Barros et al. developed a constitutive model based on non-linear analysis of the steel fiber reinforced concrete slabs supported on soil (Barros et al., 2008). The fiber reinforcement influences the energy absorption capacity which needs to be taken into account in the material constitutive relationship. To deal with the elasto-plastic behavior of concrete, the theory of plasticity was applied. Additionally, to simulate the concrete cracking behavior as well as soil non-linear behavior, the researchers utilized a smeared-crack model and springs on orthogonal direction to the slope, respectively. Also, the loss of contact between the slab and the soil was taken into account to create a reliable performance model based on the results of the experimental research.

An analytical approach can be employed to explain physical behaviors of crack evolution in tension specimens. The analytical models can be formulated on the basis of the relationship between the bond stress and crack patterns, and several of these models have

been developed. A model to predict the stresses and forces of reinforced concrete beam with glass fiber reinforced plastic (GFRP) was proposed by Anderson in 1995. In order to accurately assess the behavior of the beam, the research focused on five performance assumptions 1) linear strain distribution throughout the beam; 2) small deformations; 3) tensile strength of concrete was ignored; 4) shear deformation was ignored; 5) perfect bond between concrete and GFRP. The researchers used classical flexural theory and strain compatibility to evaluate effects of variables such as material strength, modulus of elasticity, and reinforcement ratios of the steel and GFRP. Then those data were compared with experimental results**.** Another model was developed by Sakai and Suzuki in which the stress distributions are functions of both the crack opening and crack ligament length by using exponentially decaying parameters. R-Curves were then used to account for increased energy dissipation and simulate the crack growth in the matrix response subjected to the closing pressure. Mobasher et al. indicated that this approach can be used to model the effect of fiber content on the flexural response of concrete reinforced with AR glass fibers. This can be achieved by developing a nonlinear curve fit model to the experimental data for the flexural load-CMOD response. One can back calculate the stress-strain response of the composite required to satisfy the experimentally obtained load-CMOD response (Mobasher et al., 2003).

The analytical models for fiber pullout tests are classified into three approaches: 1) perfect interface model; 2) fracture mechanical model; and 3) cohesive interface model.

Perfect interface model (Stress Approach)

This model was originally developed by Cox in 1952. The model assumes bonding between the fiber and matrix was perfect, which means the displacements and tractions were continuous at the interface. The interface can be seen as an axis-symmetry problem which simplifies the problem to 2D problem rather than 3D problem. Many other researchers later used the elastic equations for an axis symmetric stress state to formulate the pullout model. However, their solutions were very difficult and in many cases they were too complex. A further simplification from 2D to 1D problem was done to obtain better results. Nayfeh (1977) derived the second order differential equation for the fiber force distribution in the fiber for the pull-push test. The interface between the fiber and matrix was defined by the shear lag parameter which was dependent on the Young's modulus and shear modulus of the fiber and matrix.

Fracture mechanical model (Energy Approach)

According to the stress approach, the debonding of mixes starts when shear stress is greater than the shear strength limit. However, a fracture at the interface of the fiber and matrix occurs differently. Once the energy in the system exceeds the energy limit, the crack surfaces along the fiber direction are created as a consequence of the release of the energy. The relation of the energy required for crack propagation and the increase of surface energy was first described by Griffith in 1920 (Li, 1992). The law of energy conservation used in the fracture mechanic can be written as

$$W=U+KE+Us$$

where W is the external energy, U is the internal energy which consist of elastic and inelastic deformation, KE is the Kinetic energy, and Us is the surface energy due to crack propagation.

According to static or quasi-static pullout test, KE is insignificant and can be omitted; thus, the energy equilibrium can be presented as proposed by Li (1992).

$$W = Ue + Uf + Us$$

where Ue is the elastic strain energy in the bonded region and Uf is the inelastic energy due to friction in the debond region.

It has been proposed that the entire interface is divided into two regions: the bonded area containing two intact materials and the debonded region where damages occur at different degrees. The constant fraction bond strength in damaged region is treated as a shear stress. Based on this assumption, researchers derive expressions for the energy release rate G. However, the other realistic models for bond behaviors at the interface and the analytical forms are challenging and hard to achieve.

Cohesive interface Model (Stress Approach)

Theoretically, two composite materials are assumed to be perfectly bonded at the interface to ensure the highest material performance, nevertheless, it is almost impossible to achieve in many composite materials. For example, concrete reinforced by steel fiber contains a thin interphase layer between concrete matrix and fibers and creates a transition zone containing calcium hydroxide, a porous layer of calcium silicate hydrates, and ettringite. Due to different material properties other than the matrix materials, this transition zone has a strength that 30% lower than the matrix materials. Because this zone

extends from the surface of the fiber up to only 50 micrometers, it was renamed to an interface (with zero thickness). This approximation leads to the displacement discontinuity between the reinforcing elements and matrix itself. As a consequence, the shear stress at the interface represents only a function of local slip and shall be called bond stress versus slip relation (BSR). In this principle, the cement based matrix is connected to the fiber by an independent BSR model. The pullout boundary value problem can be expressed by second order differential equations. The most accurate BSR model that starts with elastic response and followed by nonlinear portion up to the peak, then continued by the softening post peak response is very complex and not easy to derive for the analytical equation (Mobasher, 2003; Soranakom, 2008).

2.6 Summary

There are different types of fibers that can be used as additive to the HMA such as: polypropylene, steel, polyester, cellulose, fabric and carpet, carbon, and aramid fibers. Based on different laboratory tests and analysis data, there are general findings about the benefits of adding fibers to the HMA, but they are inconsistent. For the studies that showed improved performance of asphalt mixtures, all kind of synthetic fibers showed the same trend. At high temperature, modified fiber asphalt mixtures are stiffer and that result in better rut resistance. In terms of fatigue cracking, most of the studies also showed that fiber modified mixes perform better than non-reinforced mixes. The reason may be that fibers provide additional tensile strength in the resulting composite and potentially can increase the amount of strain absorbed during the fatigue and fracture process of the mixture. However, at low temperatures, some studies indicated no difference between the reinforced

and non-reinforced mixes, and the performance of both mixes is comparable. The type of fiber should be compatible with the binder to get the best performance. The widely used and recommended fiber types are polypropylene and aramid fibers.

Different models have been established to simulate the behavior of fibers in Portland cement concrete. The models aim to determine the effect of fibers on the tensile stress strain response and the fracture toughness of the composite. They were developed for the PCC, but they are not compatible with the HMA due to the sensitivity of HMA to the temperature change. The performance of PCC at a range of temperatures is comparable. Though, for the HMA, the behavior is drastically different due to the change in the material stiffness caused by the change in the asphalt binder viscosity. Also, most of the models in PCC were developed for fabrics or continues fibers. In the case of the fiber application in HMA, fibers are short in length and randomly dispersed in the mix. The alternative approach for simulating the fibers in HMA was to get direct measurements for stress-strain results from laboratory experimentation, and to develop a numerical solution using the finite element method.

3. Mix Design and Fiber Characterization

This chapter presents the results of fiber characterization and mix design. The fibers are characterized based on their types and content. The mix design and the volumetric properties of these mixes are described below.

3.1 Mix Design

The mix type that used in this research is SP5 as per Idaho Transpiration department (ITD) classification. It had ¾ in. nominal maximum aggregate size (NMAS), and the gradations of the mix is shown in Table 1. The optimum asphalt content of the project mix was 4.8%. The virgin binder added to the mix was only 1.97%, and the rest was contributed by the RAP binder. Table 2 shows a summary of the mix volumetric properties. More details about the mix design and job mix formula is shown in Appendix A.

The purpose for selecting this mix is that ITD has constructed four test sections with three different synthetic fibers, the same fiber types selected for this research. The mix design of the control and the three fiber sections is the same. The assumption is that the dosages of fibers added to this mix in the field did not affect the mechanical properties of the mix. The evaluation of samples that were taken during the construction by ITD quality control showed no significant change in VMA, VFA, and other mix properties, and they remain within the specified production limits. The mix also contained 47% RAP which was milled from the existing pavement of the same project. This situation was unique for the project since only one source of RAP is introduced in the mix design, which minimizes the variability of RAP materials. The performance grade of the RAP binder was PG 64-28 which is lower than the virgin binder that has a performance grade of PG70-28.

Table 1 Blended and RAP aggregates Gradation

Sieve Size (mm)	25.0	19.0	12.5	9.5	4.75	2.36	1.18	0.6	0.3	0.15	0.075
Blended Agg. (% Passing)	100	99	83	66	39	26	20	16	12	8	4.9
RAP Agg. (% Passing)	100	98	87	73	44	29	21	17	14	10	5.7
Virgin Agg. (%Passing)	100	100	79	60	35	24	19	15	10	5.6	4.2

Table 2 Volumetric Properties and ITD Requirements

	Control mix	ITD Specs.
Optimum AC (%) (In Total)	4.8	---
Virgin Asphalt added (%)	1.97	---
Air Voids (%)	4	4
%Gmm @ Ndes	95.9	96
VMA (%)	13.6	13 min
VFA (%)	70.40%	65-75
Dust-to-Asphalt Ratio	1.1	0.8-1.6
%Gmm @ Nmax	97.6	$\leqslant$ 98.0
Laboratory Mixing Temperature (deg in F)	300 deg.	-
Laboratory compacting Temperature (deg in F)	275 deg.	-
Avg. Plant Mixing Temperature (deg in F)	320 deg.	

3.2 Fiber Characterization

Three different fibers from different vendors were used in this study. The first type was a blend of polyolefin and aramid fibers from Forta Fi, the second was aramid fibers that is treated from Surface Tech and referred to as ACE fibers, and the third was a glass fiber

from Nycon. The three different fibers are referred in order as fiber #1, #2 and #3. All fibers have comparable lengths which are ¾" to ½" (19mm to 13 mm). The amounts of fibers added to the mix were primarily based on the vendors' recommendations. These initial percentages were 1lb/ton, 0.28 lb/ton, and 3 lb/ton of HMA, respectively. Further research has been conducted to evaluate the mixes performance at higher fiber content.

Fiber #1 (polyolefin and Aramid)

Fiber #1 is a blend of aramid fibers and polyolefin fibers. Both fibers have the same length of ¾" (19mm). The specific gravities are 1.44 and 0.91 respectively. The tensile strength of the aramid fibers is up to 400 ksi with a decomposition or break down temperature of 800 ^{o}F. However, the polyolefin fibers has a much lower tensile strength, 70 ksi, and a break down temperature of 315 ^{o}F. Figure 1 shows the shape and the color of the fiber blend.

Figure 1 Fiber #1 (Polyolefin & Aramid)

Kaloush et al. (2010) conducted a laboratory performance evaluation of fiber-reinforced asphalt mixtures in a comparison with control mixture from a field test section in

Tempe, Arizona. This mixture includes fiber #1 (polypropylene and aramid). The researchers reported less shear deformation and higher residual strength in the triaxial strength test. Rutting performance tests indicated that fiber modified asphalt mixtures accumulated less permanent strain and showed higher flow numbers than the control mixture. A significant increase in the dynamic modulus values of FRAC was detected at high temperatures. However, at lower temperatures the FRAC mixture were comparable to the control mix. Also, FRAC mixtures exhibited higher tensile strength, total fracture energy and slower crack propagation according to the Indirect Tensile Strength test (IDT) and C* line integral test, respectively. Finally, the FRAC showed better fatigue resistance at 40° F; however, the control outperformed the FRAC mixture at high strain levels at 70 °F.

On the other hand, Mondschein et al. (2011) examined the effect of fiber #1 on laboratory produced asphalt mixture performance in terms of permanent deformation and fatigue. Four different asphalt mixes were used. The fibers were dosed in the mixture in quantities of 1 lb per 1 ton of asphalt mixture. The laboratory findings of this study declared that "the compaction of the mixture is not negatively affected by the application of fibers. The better understanding of the behavior of 3D reinforcement will need a wider scope of testing, ideally in trial sections to be long term monitored along with the traffic loads and weather conditions."

Fiber #2 (Aramid)

Fiber #2 consists only of aramid fibers with ¾" (19 mm) in length, and have a specific gravity of 1.44 with a tensile strength of 400 ksi. The break down temperature is 800 ^{o}F. These fibers were treated with melted wax to provide more control of fiber mixing and

weighing down the fibers due to its light weight. Figure 2 presents the aramid fibers with the Wax treatment. No published scientific research has been performed yet on fiber #2. However, brochures from Surface Tech Company, the producer of the fibers, shows a Texas

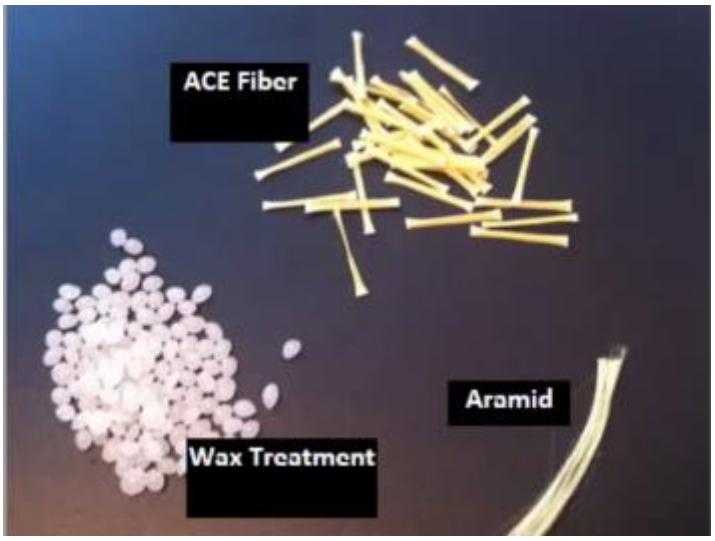

Figure 2 Fiber #2 (Aramid)

Overlay Test on fiber modified sample. The results indicate that there is an increase in the number of the cycles from 500 cycles to 1,200 cycles for the overlay tester. Also, the Hamburg Wheel tracking test shows the number of cycles to rut failure is 8000 in the control mix and 14,000 cycles for the fiber mix. There isn't much information about the amount of the fibers in these mixes. So far, the ACE fibers have been used in some projects in Oregon and Washington State.

Fiber #3 (Glass)

Fiber #3 is made of glass fiber as shown in Figure 3, and provided by Nycon Company. The fibers' length is ½" (13mm) and has a specific gravity of 2.7. The tensile strength is 300 ksi. It is known that the melting of the fiber glass is 2075 ^{o}F for these fibers. The water absorption is less than 1%. There is some research about a successful use of the glass fibers in the Portland Cement Concrete (PCC). However, there is no research published on the effect of Nycon type E glass fibers on HMA performance.

Figure 3 Fiber #3 (Glass)

Test Sections and Field Production

Four test sections were constructed by ITD as indicated earlier. The fiber-modified sections adopted the same mix design without any alteration, and the fibers were added at the asphalt plant as per each vendor's specifications. The four construction sections at US-30 (south of Idaho state) project are: Section 1 (from MP 435.281 to 436.01) was the

unmodified control; Section 2 (from MP 436.01 to 436.8) was the fiber #1-modified with a rate of one lb/ton; Section 3 (from MP 436.8 to 437.6) was fiber #2-modified with a rate of one third lb/ton; and Section 4 (from MP 437.6 to 438.376) was fiber #3-modified with a rate of three lb/ton. The rate of fibers addition was specified by the vendors. The method of fiber addition of all three types was the same. The asphalt plant was a continuous production plant and the fibers were blown into the drum dryer at the inlet of the RAP (Figure 4). Analysis of the production quantities in the project construction reports indicated the average actual rate of fiber addition for each mix was very close to the designated rate specified. The actual quantities for the sections are 1.04, 0.28 and 3.11 lb/ton for fiber #1, #2 and #3 respectively. These contents are close to the specified amount by the vendors, and are roughly equivalent to 0.05%, 0.01% and 0.16% by the HMA mix weight.

Field samples of the plant mix of each section were collected by ITD personnel in accordance to ITD standard procedures. Plant mix samples were collected mid-way from each section to insure that it is an average representative of the laid mix. This was also to avoid any possible overlap between types of fibers at the boarder of sections. In addition to the loose plant mix samples, field cores were extracted for density and volumetric analysis as per ITD standard procedures. Additional cores were extracted from the shoulders to have sufficient number of core samples for lab testing.

Figure 4 Process of blowing fibers into the HMA plan

4. Laboratory Performance Evaluation

This chapter presents methods and results of laboratory performance tests including: rutting resistance, fatigue cracking resistance, and low temperature thermal cracking resistance.

4.1 Rutting Resistance

Rutting resistance of mixes was tested by dynamic modulus, flow number, and Hamburg wheel tracking test. Those tests are used to characterize different aspects of mixes for rutting resistance. Dynamic modulus of mixes is the indicator of stiffness of mixes, while flow number is to describe lateral shear resistance of mixes. Hamburg wheel test is conducted to indicate the resistance to consolidation type of rutting.

Dynamic Modulus and Flow Number

The dynamic modulus test was conducted in accordance with AASHTO T 342-11. The test was conducted on standard 6 inches Gyratory compacted samples. Specimens were fabricated by Pine-AFG1 Superpave gyratory compactor to achieve a height of 6.7 inches (170 mm). Trial and error were used to determine the number Gyrations that lead to the target height. After compaction, the specimens were cored and saw cut to the size of 5.9 inches (150mm) in height and 4 inches (100mm) in diameter with air voids level of 7±0.5 %. *AASHTO T209, Standard Method of Test for Determining the Theoretical Maximum Specific Gravity (G_{mm}), and AASHTO T166, Standard Method of Test for Determining the Bulk Specific Gravity (G_{mb})* were the test methods that used to conduct the volumetric analysis of the samples. The prepared samples were tested in the Asphalt Mixture Performance Tester

(AMPT), which meets the AASHTO T 342-11 requirements. The temperatures used for dynamic modulus test were:
40 ^{o}F, 70 ^{o}F, 100 ^{o}F, and 130 ^{o}F. At each temperature, six different loading frequencies: 25, 10, 5, 1, 0.5, 0.1 Hz, were applied. For each mixture, a total of three specimens were fabricated and tested in order to confirm the results. After the raw data was obtained, the dynamic modulus values of all samples was averaged at each combination of temperature and frequency sets, standard deviation (STD) and coefficient of variance (COV) were calculated for each temperature and frequency. The averaged data of all tested samples were used to calculate the dynamic modulus master curve for each mixture. The computed E* master curve is used in the AASHTOWare Pavement ME Design to predict the mechanistic responses of pavement under various combinations of pavement temperature and vehicle speed in order to find the influence of fiber content on the pavement behavior.

The flow number test was conducted using a loading cycle of 1.0 second in duration, which consists of a 0.1 second haversine load followed by a 0.9 second rest at a testing temperature of 130 ^{o}F. As shown in Figure 5, the flow number is the number of load repetitions when the permanent deformation rate reaches a minimum This test is typically conducted at the end of the E* test, which is performed at the same temperature, 130 ^{o}F. However, in this research the Flow Number test was conducted on new samples to avoid the consolidation effect from the dynamic modulus test. The Flow point and cycles were automatically calculated and recorded by using the Simple Performance Tester software UTS005 version 1.33. This protocol is in accordance with *AASHTO TP79-13, Standard Method of Test for Determining the Dynamic Modulus and Flow Number for Hot Mix Asphalt (HMA)*

Using the Asphalt Mixture Performance Tester (AMPT). The researchers then compared measured flow numbers to the minimum flow number values that were developed in NCHRP Project 9-33 for hot mix asphalt (HMA) as shown below in table 3.

Table 3 NCHRP Project 9-33 Recommended Minimum Flow Number Requirements

Traffic Level, Million ESALs	Minimum Flow Number, Cycles (HMA)	Minimum Flow Number, Cycles (WMA)
<3	-	-
3 to <10	50	30
10 to <30	190	105
Equal or >30	740	415

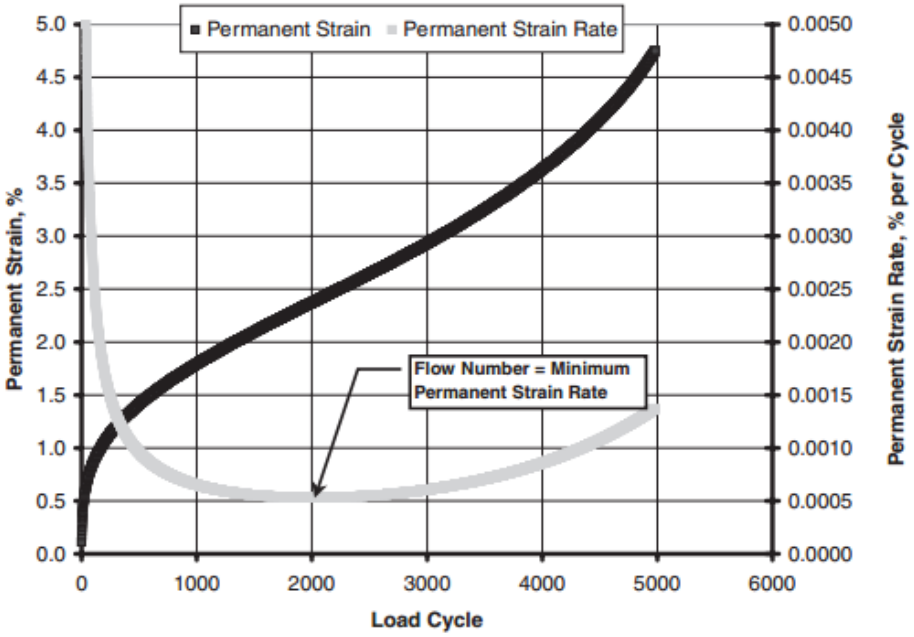

Figure 5 Schematic of Typical Flow Number Test Data

Hamburg Wheel Tracking

The Hamburg Wheel Tracking Device (HWTD), can be used to evaluate rutting and stripping potential. The test conducted in accordance with Tex-242-F. The HWTD tracks a loaded steel wheel back and forth directly on a HMA sample. The test was typically conducted on Superpave Gyratory Compactors (SGC) compacted samples using three replicates for each mix type. Each sample has an air void level of $7\pm0.5\%$ and size of 2.3 ± 0.1 in. (58 ± 2mm) in height and 5.9 in. (150mm) in diameter. Most commonly, the 1.85 inch (47 mm) wide wheel is tracked across a submerged (underwater) sample for 20,000 cycles (or until 20 mm of deformation occurs) using a 158 lb (705 N) load. Rut depth is measured continuously with a series of LVDTs on the sample. Three replicates have been used for each mix.

4.2 Fatigue Cracking Resistance

Indirect Tension Test

The concept of fracture work density and vertical failure deformation from indirect tensile test (IDT) was used to evaluate mixture resistance for bottom-up cracking and top-down cracking, respectively. The definition of fracture work density was as fracture work divided by sample volume, and fracture work was determined as the entire area under the load versus the vertical displacement curve (Wen et al., 2002). And vertical failure deformation was defined as vertical displacement under the peak load, which could indicate ductility of mixes, as illustrated in Figure 6.

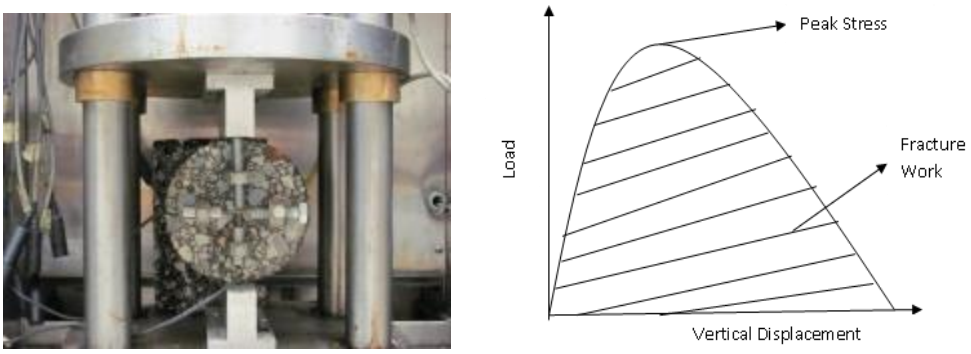

(a) (b)

Figure 6 Indirect Tensile Test (a) Indirect Tensile Test Set-up and (b) Load-Displacement Curve of Indirect Tensile Test

A servo-hydraulic Geotechnical Consulting Testing System (GCTS) with an environmental chamber was used to test the samples. Four linear variable differential transformers (LVDTs) were mounted on the front and back of sample to measure the deformations during the tests. Once the LVDTs are attached, the specimen is placed in a loading apparatus, which consists of top and bottom plates with loading strips of the proper curvature to load the specimens, shown in Figure 6. Fatigue tests were performed at 68 ^{o}F with a deformation rate of 2 inches per minutes by the GCTS ram. The deformation was continued until the load on the sample achieved a value close to zero. Three samples for each type of mix were tested, and the average value and coefficient of variation (COV) were calculated and presented.

Fracture Parameter, J_c

Another indicator of fracture resistance is referred to as J_c. and read as (J-sub-c). The J_c parameter is defined as a path independent integration of strain energy density, traction, and displacement along an arbitrary contour path around the crack (Bayomy, 2010). The test

is conducted at room temperature of approximately 68±2°F (20 ±1°C) as a bending test on a notched semi-circle samples as shown in Figure 7. The Value of J_c was determined from the applied load versus the vertical deformation relationship. The strain energy U, which is equal to the area underneath the load-deformation curve, was determined. After determining the strain energy, the ratio of the strain energy to the specimen thickness, U/b, for each specimen was plotted against the notch depth, a. The value of J_c was obtained from the slope of the U/b versus a best straight line fit. Four data points used to develop such a line fit, and therefore, three specimens with different notch depth (0, 0.25, 0.5, and 0.75 in.) were tested for the J_c calculation. For each notch depth, three replicate specimens were used to evaluate test repeatability. All the samples were compacted in the lab from field loose mixes. More details about J_c sample preparation is well described in previous research project (Bayomy, 2007).

Figure 7 Fracture Test using Semicircular Notched Samples in Bending (J_c)

4.3 Low Temperature Cracking Resistance

The low temperature property of the mixture was characterized by the test of creep compliance and indirect tensile (IDT) strength. The nondestructive creep compliance test for each sample was conducted first at temperature of -4 ^{o}F, 14 ^{o}F and 32 ^{o}F with loading duration of 100s. And then IDT strength test was carried out under temperature of 14 ^{o}F at a displacement rate of 0.1 inch/min. The deformation was continued until the load on the sample achieved a value of zero and the specimens completely split. The value of creep compliance and IDT strength were used for MEPDG thermal cracking model to predict mixture performance which is presented later in chapter six. And fracture work density of mixture from IDT strength test at 14^{o}F was calculated to compare the resistance of thermal cracking performance of mixtures with different types and percentages of fibers.

Since the resistance of low temperature thermal cracking was also considered as long-term performance of the mixtures, samples used for thermal cracking test were prepared following the same procedure as IDT fatigue test.

4.4 Results and Discussion

In order to study the effect of fibers under various conditions of loading and temperatures as explained earlier, the testing plan was developed as shown table 4 below.

Table 4 Laboratory Testing Matrix

Testing	Control Mix	Fiber #1				Fiber #2	Fiber #3
	No Fibers	0.05%	0.20%	0.30%	0.40%	0.015%	0.16%
Dynamic Modulus	X	X	X	X	X	X	X
Flow Number	X	X	X	X	X	X	X
HWT	X	X	X	X	X	X	X
Jc	X	X				X	X
SCB	X		X	X	X		
IDT (Fatigue)	X	X				X	X
IDT (Thermal)	X	X	X	X	X	X	X
Creep Compliance	X	X				X	X
Healing testing	X		X		X		

Stiffness (Dynamic modulus test)

Results of the dynamic modulus (E*) at all designated temperatures are presented in table 5 respectively. Even though the field mixes have different fiber types and contents, the dynamic modulus values indicated that at high frequency (or low temperature) level at which the dynamic modulus is not sensitive to variation of asphalt binder, all field mixes were comparable to each other. At low frequency (or high temperature) level at which the dynamic modulus is sensitive to the asphalt binder, the results also indicated that there is no significant difference among the field mixes as shown in table 17 in Appendix B. At intermediate temperatures, the lowest dynamic modulus values were observed in the

control mix. Among the fiber mixes, the results indicated that field fiber #1-modified mix increased the dynamic modulus values at 70 ^{o}F and 100 ^{o}F. Fiber #2 showed the same trend at 70 ^{o}F only. But, there was no significant difference between the control and fiber #3 mix. This finding showed that fibers may not add significant improvement to the mix performance at low and at high temperatures with the designated fiber contents. Additional testing were performed on samples that were prepared in the laboratory with fiber#1. The dosages of fibers increased to 0.2%, 0.3% and 0.4%. Results of dynamic modulus test indicate that there is a slight improvement in the stiffness of the samples at 0.2% fiber content.

Table 5 Dynamic modulus test results

Dynamic modulus, ksi									
Temp, ^{o}F	40 ^{o}F	70 ^{o}F	100 ^{o}F	130 ^{o}F	Temp, ^{o}F	40 ^{o}F	70 ^{o}F	100 ^{o}F	130 ^{o}F
Freq. (Hz)	**Control, Unmodified HMA**				Freq. (Hz)	**Lab mix Fiber #1_0.2%**			
25	2,268	984	266	77	25	1,952	905	304	91
10	2,059	795	190	49	10	1,780	745	226	57
5	1,896	665	138	37	5	1,658	635	172	38
1	1,505	402	60	16	1	1,353	407	81	15
0.5	1,345	320	41	11	0.5	1,224	335	58	10
0.1	979	168	20	6	0.1	921	184	26	5
Freq. (Hz)	**Field Mix Fiber #1_0.05%**				Freq. (Hz)	**Lab mix Fiber #1_0.3%**			
25	2,241	1,057	316	98	25	1,828	835	270	96
10	2,052	874	226	59	10	1,662	685	200	65
5	1,905	742	165	43	5	1,537	580	153	44
1	1,551	468	73	18	1	1,245	371	71	17
0.5	1,399	379	51	13	0.5	1,123	303	51	11
0.1	1,058	204	22	7	0.1	843	170	22	5
Freq. (Hz)	**Field Mix Fiber #2_0.01%**				Freq. (Hz)	**Lab mix Fiber #1_0.4%**			
25	2,305	1,061	311	93	25	1,949	919	265	116
10	2,099	875	220	56	10	1,785	751	191	79
5	1,950	744	160	37	5	1,659	636	143	54
1	1,584	470	70	16	1	1,342	407	66	22
0.5	1,428	379	49	11	0.5	1,204	335	47	15
0.1	1,073	200	22	6	0.1	907	185	19	7
Freq. (Hz)	**Field Mix Fiber #3_0.16%**								
25	2,342	1,084	307	88					
10	2,141	881	218	51					
5	1,948	746	158	34					
1	1,605	465	71	16					
0.5	1,403	373	50	13					
0.1	1,024	201	23	7					

Rutting Resistance (Flow Number test)

According to the National Cooperative Highway Research Program (NCHRP) Report 702, the recommended minimum flow numbers under 210kPa deviator creep stress, and based on the traffic levels for the project (10-30 million ESALs) is 190. The results as presented in Figure 8 showed that all of the mixes satisfy this criterion. A comparison of the flow numbers of the fiber mixes indicates that the fiber mixes had higher numbers than the control mix, which means higher resistance to rutting. In addition, the development of rut depth as shown by the micro-strain versus cycles plots in Figure 9 which showed that the three different types of fibers that were mixed in the field did not show any significant difference statistically in terms of rutting resistance, as shown in table 19 in the appendix, and this is due to their low fiber contents. However, the laboratory developed mixes showed that fiber modified mixes that has a minimum fiber content of 0.3% has better rutting resistance.

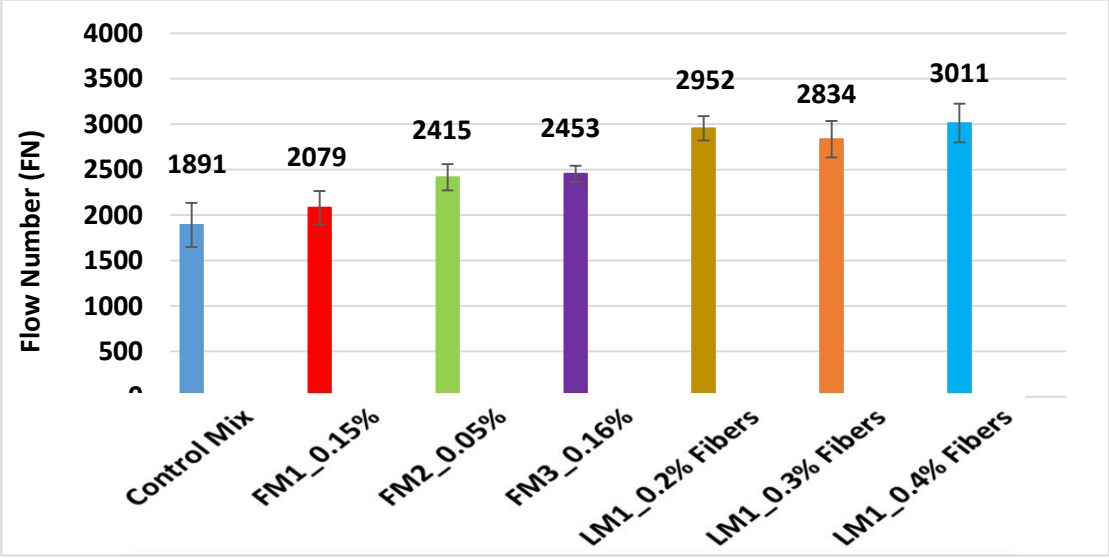

Figure 8 Average Flow Number test results of mixes

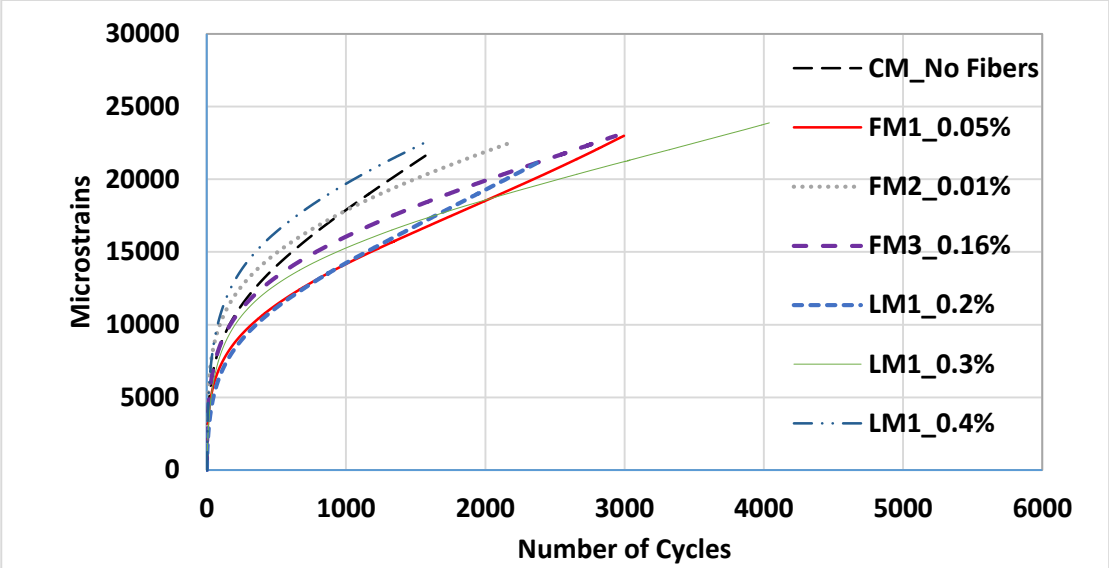

Figure 9 Average Micro-Strain vs. Number of Cycles of the flow number test

Rutting Resistance (Hamburg Wheel Track test)

Figure 10 presents the results of Hamburg Wheel Track (HWT) tests for the field and laboratory mixes. Each line indicates the average of four samples. The results of ANOVA analysis as shown in table 20 for the final rut depth at 20,000th cycle revealed no significant difference among field mixes in terms of rutting based on HWT test results. It is to be noted that in this analysis ANOVA was used rather than ANCOVA since HWT testing was done on lab samples where air voids were under control. ANCOVA was used on analysis of core samples to suppress the effect of air voids variability. Although Figure 10 indicates that the utilization of fiber showed slight improvement in the rutting performance of asphalt mixes this improvement is not significant statistically. Possible reason could be due to the non-uniform distribution of fiber during mixing procedure. However, the results demonstrated that the laboratory mixtures with higher fiber contents (0.2%, 0.3%, and 0.4%) exhibited better rutting resistance.

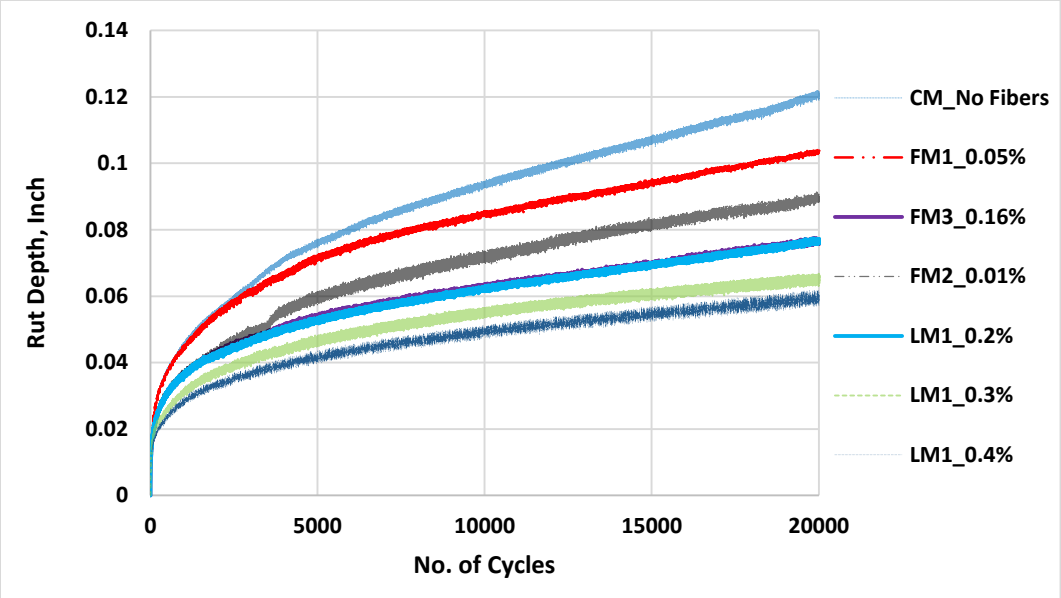

Figure 10 Hamburg Wheel Track test (HWT) results

Fatigue Cracking Resistance

Figure 11 presents the results of fracture work density, vertical failure deformation and tensile strength at 68 °F for the different types of mixes. For each mix type, the average value of three replicates is presented. The mixes statistically have comparable fracture work density and vertical failure deformation. The ANCOVA analysis in table 21 and 22 revealed that no significant difference is evident among different types of mixes in terms of fracture work density and vertical failure deformation.

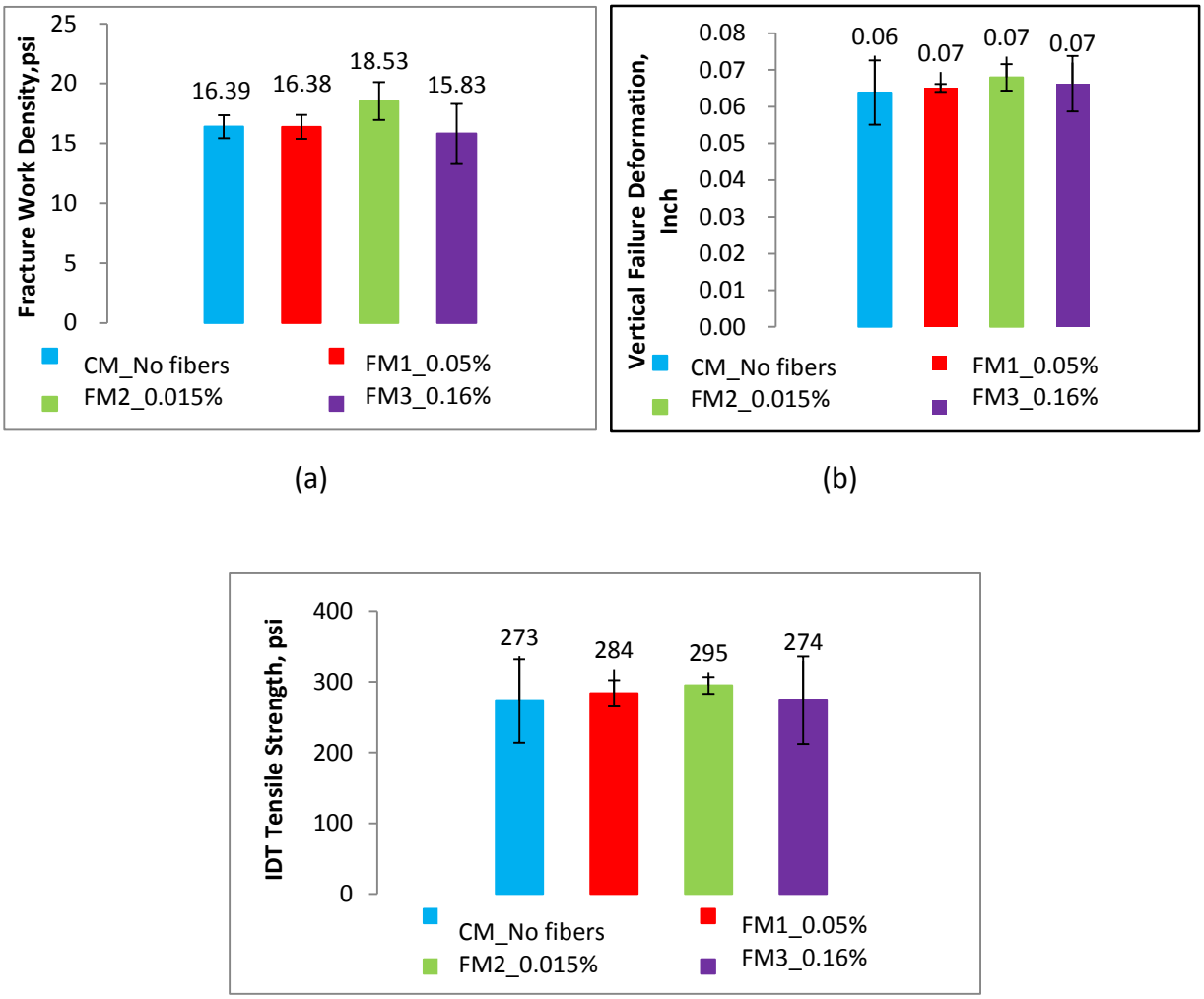

Figure 11 (a) Fracture Work Density, and (b) Vertical Failure Deformation (at 68℉) (c) IDT Tensile Strength

Figure 12 presents the results of J_c test of the all mixes at 68°F. The J_c is an indicator of fatigue cracking resistance. The higher the J_c value is, the better the cracking resistance. The results showed that fiber #3 modified mix had the highest result, which means better resistance to fracture, followed by fiber #1 and fiber #2 mixes. The statistical analysis of the ANCOVA as presented in Table 28 in Appendix B points out this difference is not significant.

That means all field mixes behaved the same in terms of fatigue cracking resistance, and no superior performance was observed in the field fiber-reinforced mixes.

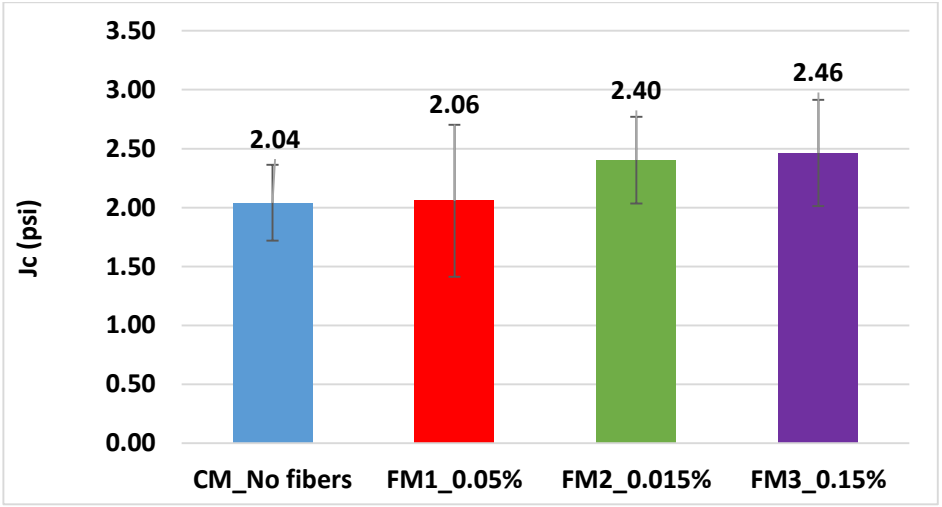

Figure 12 J_c test results of the field fiber mixes at 68 °F

The fracture test for the laboratory mixes were tested at only one notch depth, but different temperatures. The results of the Semi-Circular Bending (SCB) test is presented in Figure 13. The figure shows an example of the load-displacement curve from the SCB test as well the calculated fracture energy per unit width of test samples at different temperatures. Although the fiber decreased the peak load, the displacement at the failure point was greatly increased leading to an overall increase of the fracture energy. An increase of the fracture energy was associated with the improved overall performance. The results indicate that, after reaching the peak load, fibers resist crack propagation through the bridging mechanism in which fibers carry part of applied tensile stress. It should be noted that fibers are short in length and randomly dispersed inside the mixture. Therefore, there must be a minimum

fraction (threshold) of fibers to resist cracking once initiated. If the fiber content is less than the effective threshold, no significant difference in performance is expected.

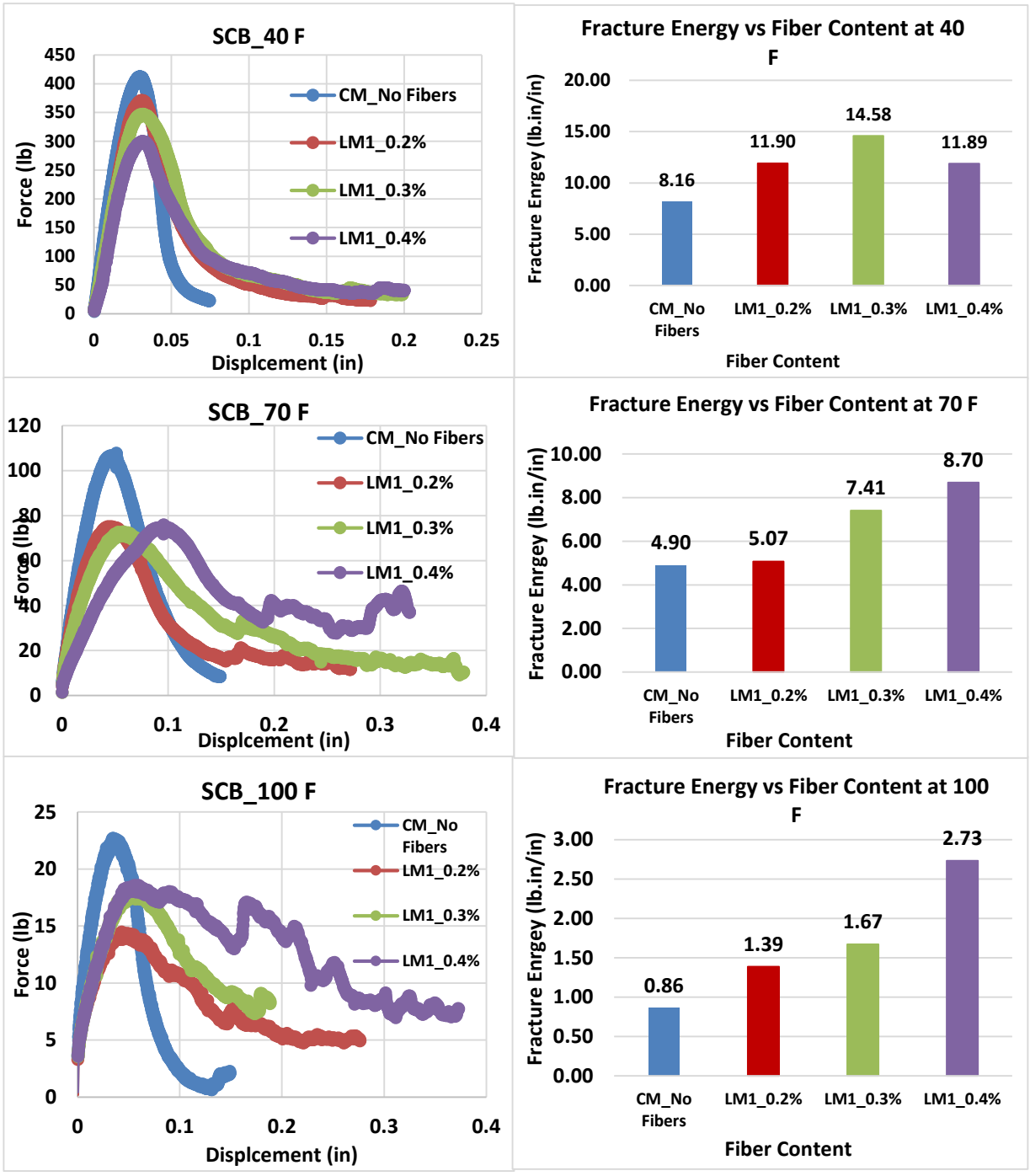

Figure 13 Fracture test results using Semi Circular Bending test at 40 °F, 70 °F, and 100 °F

Low Temperature Thermal Cracking Resistance

Figure 14 presents the results of fracture work density for IDT test at low temperature. Fracture work density values among different types of mixes are statistically comparable. This indicates samples with fiber do not have advantageous performance in comparison to control mixes against thermal cracking. This may be explained by non-uniform distribution of fiber in the plant mix procedure which caused some field cores to have a low amount of fiber.

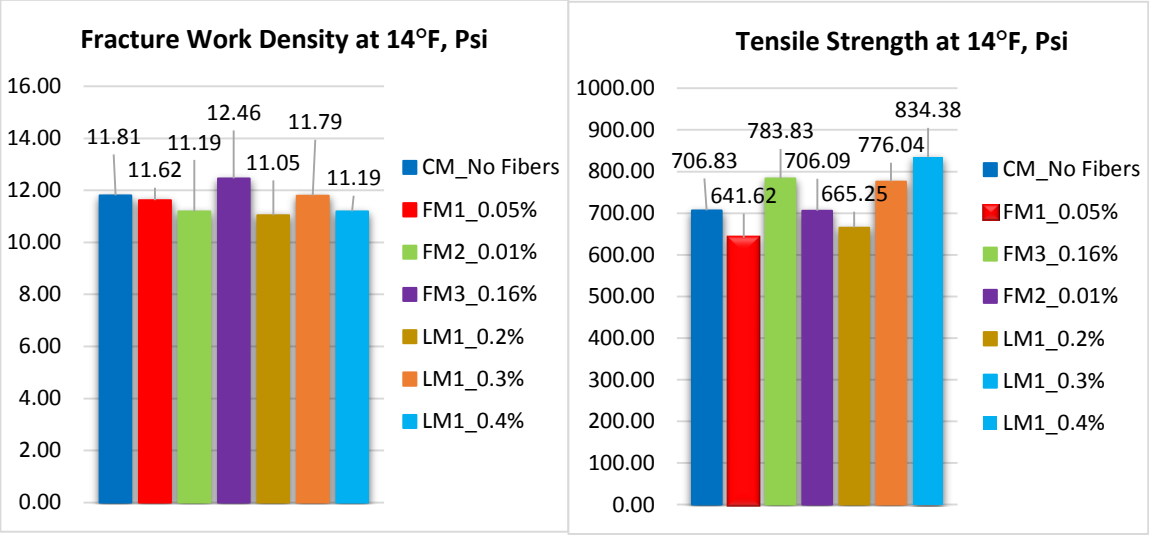

Figure 14 Fracture Work Density at 14°F

Creep Compliance Test

Table 6 presents the creep compliance results for asphalt mixes. Each data indicates the average of three replicates. As can be seen, average creep compliance data for four filed mixes are close. Furthermore, the slopes of creep compliance master curves which are an appropriate indicator to thermal cracking resistance are comparable for four types of mixes.

Table 6 Results of Creep Compliance Tests

	Creep Compliance, psi^{-1}		
Temp, ^oF	-4 ^oF	14 ^oF	32 ^oF
Time (sec)	**Control Mix_No Fibers**		
1	2.3429E-07	3.1152E-07	4.6487E-07
2	2.4551E-07	3.2866E-07	5.1872E-07
5	2.5770E-07	3.5670E-07	5.9865E-07
10	2.6857E-07	3.8326E-07	6.9049E-07
20	2.8102E-07	4.1429E-07	8.1131E-07
50	2.9914E-07	4.6442E-07	1.0332E-06
100	3.1880E-07	4.9792E-07	1.2520E-06
Time (sec)	**Field Mix Fiber #1_0.05%**		
1	2.2408E-07	2.6375E-07	4.0762E-07
2	2.2480E-07	2.7362E-07	4.3711E-07
5	2.4498E-07	2.9768E-07	5.0617E-07
10	2.5203E-07	3.1722E-07	5.8406E-07
20	2.6241E-07	3.3412E-07	6.9117E-07
50	2.8395E-07	3.6179E-07	8.4379E-07
100	2.9868E-07	3.8535E-07	1.0305E-06
Time (sec)	**Field Mix Fiber #2_0.015%**		
1	2.1900E-07	3.0429E-07	4.7990E-07
2	2.3118E-07	3.1929E-07	5.3684E-07
5	2.4333E-07	3.4529E-07	6.3838E-07
10	2.5509E-07	3.6926E-07	7.4094E-07
20	2.6566E-07	4.1386E-07	8.7041E-07
50	2.8119E-07	4.6428E-07	1.1111E-06
100	2.9274E-07	5.3444E-07	1.3613E-06
Time (sec)	**Field Mix Fiber #3_0.16%**		
1	2.3691E-07	3.0930E-07	4.6009E-07
2	2.4663E-07	3.1984E-07	5.1150E-07
5	2.5837E-07	3.4382E-07	5.8198E-07
10	2.7055E-07	3.7186E-07	6.6206E-07
20	2.7880E-07	4.0746E-07	7.7422E-07
50	3.0067E-07	4.5152E-07	9.6666E-07
100	3.1584E-07	5.0818E-07	1.1656E-06

The creep compliance values at low, intermediate, and high time-temperature combination levels are shown in Figures 15 through 17. The ANCOVA analysis results as shown in Table 31 indicate that no significant difference is evident among different types of mixes in terms of creep compliance in these levels.

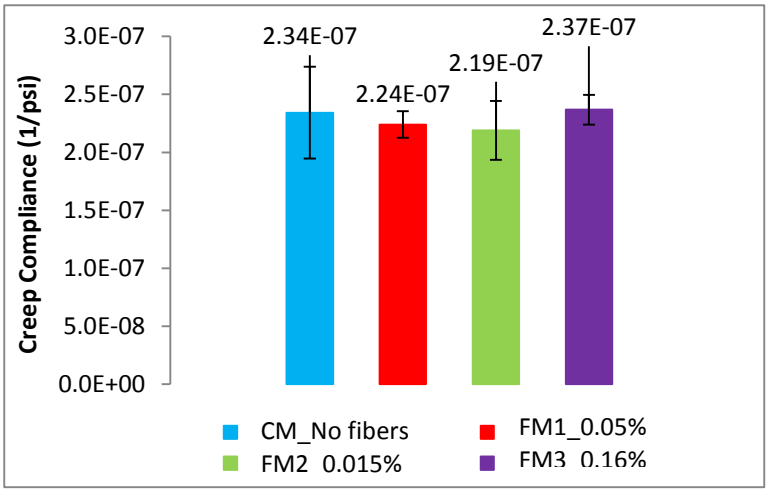

Figure 15 Creep Compliance at Low Time-Temperature Level (-4°F and 1s)

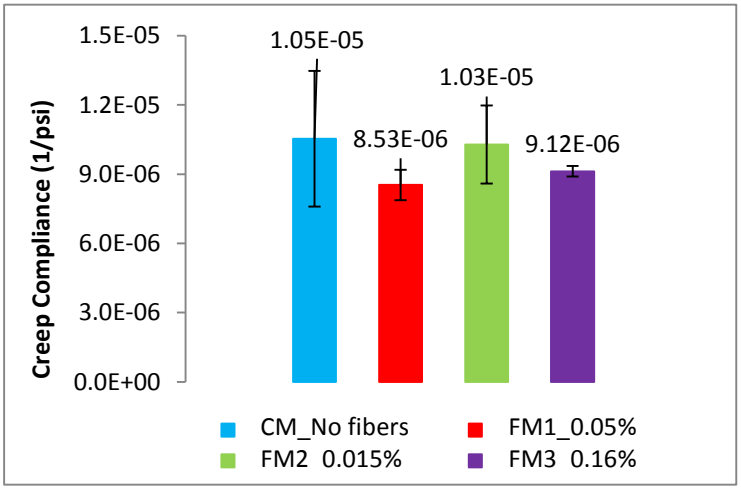

Figure 16 Creep Compliance at Intermediate Time-Temperature Level (68°F and 10s)

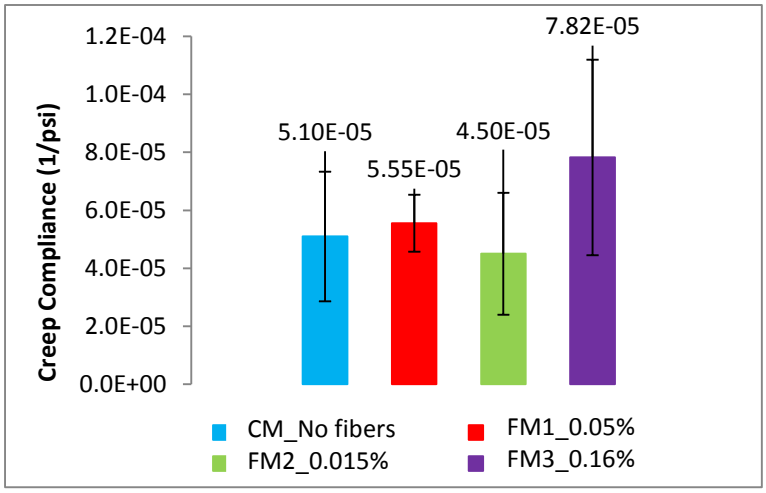

Figure 17 Creep Compliance at High Time-Temperature Level (68°F and 100s)

4.5 Summary

This chapter summarizes the laboratory performance evaluation of fiber modified asphalt mixes in terms of rutting resistance, fatigue cracking resistance and low temperature thermal cracking resistance. Based on the test results, it is concluded that the field fiber modified mixtures' rutting resistance to lateral shear failure, indicated by the flow number, did not increase significantly by adding fibers to the mix. The Hamburg Wheel Tracking tests also indicated the presence of fibers in the field mixes did not add significant value to the mix resistance to rutting. At higher fiber contents (0.2%, 0.3%, 0.4%) rutting resistance improved as indicated by flow number and Hamburg wheel tracking test.

Fatigue cracking resistance was evaluated by the fracture work density measured in the indirect tension test and the J_c parameter from the semicircular bending test of notched samples. Both test results indicated that the field mixes performed comparably and that no

significant difference is expected in the resistance to fatigue. Laboratory mixes that contains higher fiber contents showed better resistance in the region of the postpone cracking.

Fracture work density test performed at Low Temperature also indicated that the fiber mixes had similar fracture work values to resist thermal cracking and no significant improvement was observed.

5. Evaluation of Healing Characteristics

Asphalt mixture experience several distresses such as fatigue cracking, permanent deformation or rutting, and moisture damage. Cracking of asphalt pavement could occur due to mechanical loading and/or temperature variations. Once the asphalt concrete is subjected to a mechanical loading, microcracks develop triggering a microstructural damage. These cracks occur ahead of the macrocrack tip, forming a damage zone. Propagation and rebonding of these microcracks in the damage zone affect the macrocrack growth and healing. And thus it affects the fatigue life of asphalt concrete (Kim, 2009; Bhasin, 2009).

When an asphalt concrete pavement is subjected to repetitive applications of different load levels and several intervals of rest duration, three main mechanisms follow: fatigue, which occur due to damage accumulation during loading; time-dependent behavior related to the viscoelastic nature of asphalt concrete; and healing take a place during rest periods and temperature increases.

The main objective of this part of the study was to evaluate the effectiveness of fibers in accelerate healing in asphalt mixtures. The advantage of accelerated healing is to reverse part of the cumulative fatigue damage developed in asphalt mixtures. Since some of the laboratory testing did not detect the effect of fibers on the mixtures' performance, the author developed a new test protocol to evaluate the healing of fiber modified mixtures using a semi-circular bending test. The new proposed test protocol involved a combination of introducing a rest periods and thermal treatment during the test to evaluate the fiber effect on healing. This section discusses the proposed testing protocol and main findings.

5.1 Test Protocol

Three different asphalt mixes were evaluated in this task. Each of asphalt mixtures has different fiber content; a control mix and two fiber#1 mixes with 0.2% and 0.4% fiber content.

The test specimens were prepared using the Superpave Gyratory Compactor (SGC). The samples were compacted to N_{design} of 100 gyrations as per the mix design. The size of the compacted samples was 150 mm in diameter and 115 mm in height with air voids of 4±0.5%. The cylindrical sample from each mix was cut into four Semi Circle sample that has a thickness of 44.45 mm (1.75 in) and a 12.7mm (0.5 in) notch depth as shown in Figure 18.

Mechanical test was performed in indirect tension mode. The AMPT machine used to apply a dynamic creep loading at the top of a SCB sample to simulate the growth of the fatigue cracks due to the bending stress at the bottom surface of the sample. To enable testing in bending stress mode, a steel plate with fixtures were placed at the bottom of the specimen. A loading cycle of 1.0 second in duration that consists of a 0.1 second haversine load followed by a 0.9 second rest period. The test was conducted at a temperature of 21.1 ^{o}C (70 ^{o}F). The schematic of testing is shown in Figure 18.

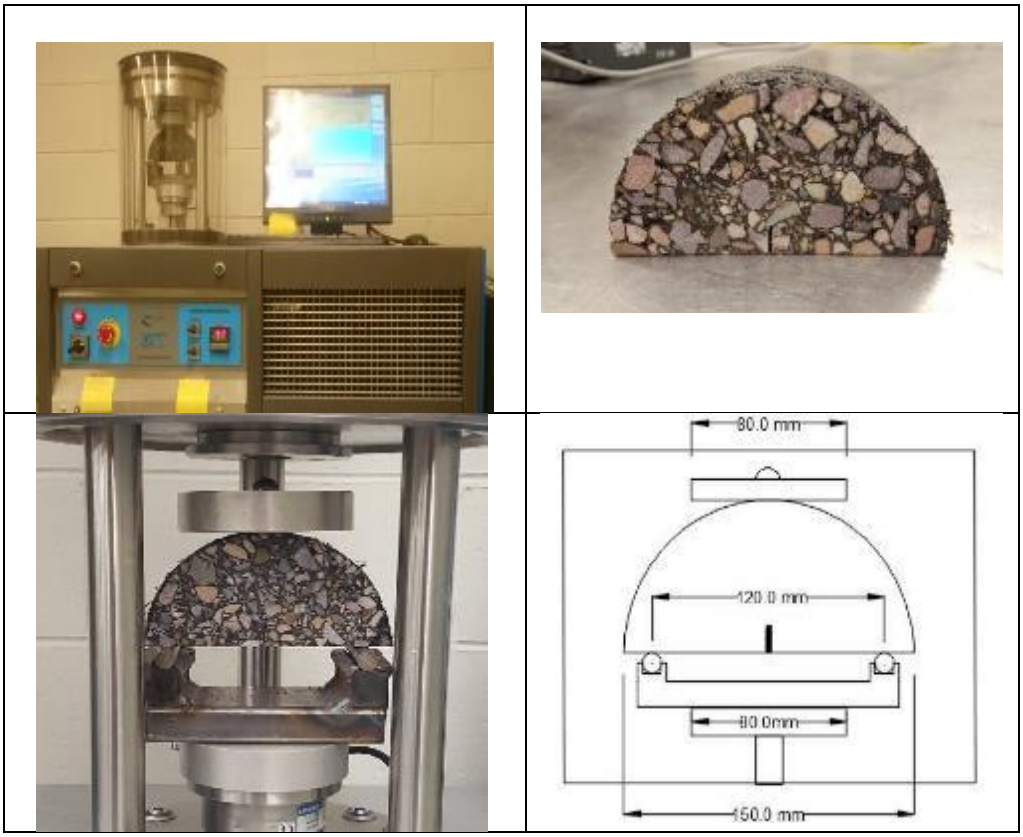

Figure 18 Indirect Tensile Test Set-up and Load Displacement Curve of Indirect Tensile Test

To investigate the effect of fibers on healing, three different types of stress-controlled fatigue tests were conducted for every mix. In each of them, Semi-Circular notched specimens were prepared from the same cylindrical compacted samples to reduce the variability among samples. Below is the description of the three different types of tests.

Test 1, in this test, the dynamic creep stress was conducted without applying any long rest period. This test was performed to measure the fatigue cracking life of the asphalt mixes. Samples were tested by applying stress controlled impulse loading for 0.1 second followed by 0.9 second rest period at 21.1 °C (70 °F). The indirect tension stress amplitude

selected so the test samples fail in a reasonable period of time (8,000 to 16,000 cycles) to avoid a prolonged test. The same optimized stress amplitude was applied for all tested mixes.

Test 2: The dynamic creep test at indirect tension mode was performed similar to Test 1; however, in this test, an intermediate rest period of two-hour duration were introduced. Samples were subjected for the rest period after reaching 50% of their average fatigue life defined by Test 1. For example, if the average fatigue life of a sample was 12,000 cycles, the rest period applied at 6,000 cycles. Then the test is continued for another 6,000 cycles, and a second rest period is applied. At that point the test is continued until sample fail.

Test 3: this testing is similar test 2 with the exception that the samples were exposed to thermal treatment during the two hour rest period. The temperature was manually adjusted. The process was to increase the temperature in the inner chamber until reach 45 °C at the beginning of the rest period and held for 30 minutes, after which heating was stopped and once the temperature in the inner chamber matched up that of the outer chamber, the cooling process was conducted for 30 minutes. In the remaining 40 minutes, the inner chamber temperature was dropped and maintained at 21.1°C until next the dynamic load application.

Each type of test was followed by collection of data (e.g., load, defamation, temperature) from the AMPT machine. The self-healing effect was evaluated based on the improved fatigue life or the number of cycles until failure.

5.2 Results

Figure 19 presents the total number of load cycles to failure for the three asphalt mixtures. Results revealed that all mixtures experienced healing. The average fatigue life of the control mixture increased by 33% during the two hours' rest period in test 2, and 60% with the thermal treatment that was provided during this rest period in test 3. The same trend can be observed for the other two mixtures with fiber reinforcement. The average fatigue life increased by 64% during the rest period and by 92% with applying the thermal treatment during the rest period for the mixture with 0.2% fibers. At 0.4% fiber content, fatigue life increased by 16% during the rest period and 44% when thermal treatment applied at the rest period. The results clearly demonstrated that fiber improved the healing and extended the fatigue life of asphalt mixtures. In addition, the thermal treatment expedited the healing rate of asphalt mixtures.

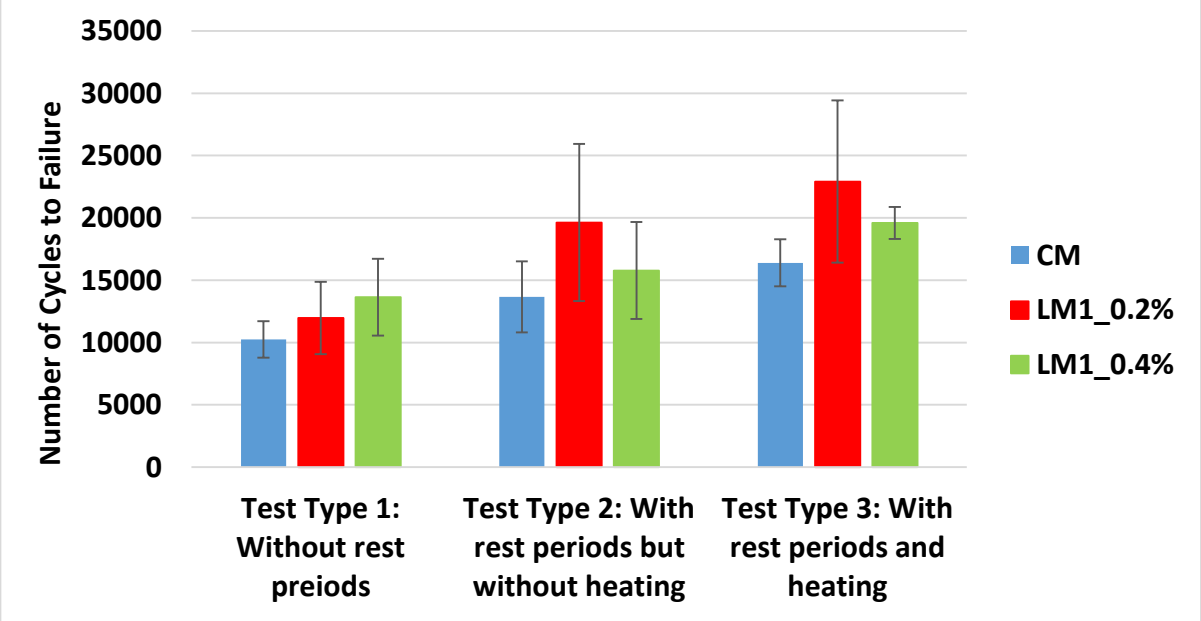

Figure 19 Number of Cycles to Failure for the three types of tests

Table 7 presents the percentage of increase in fatigue life for each mix relative to the control mix during first type of testing. This comparison has been made to isolate the effect of fibers on accelerated healing. As shown in the table, fiber reinforcement at level of 0.2% increased the fatigue life by 58% during the rest period only and 64% when thermal treatment was applied. Also, adding 0.4% fibers increased the fatigue life by 21% and 31% when rest period was applied without and with thermal treatment, respectively. The result indicated that healing can be accelerated in asphalt mixtures by adding dispersed fibers at the designated dosage of 0.2%, and thus the fatigue life can be extended.

Table 7 Comparison of the number of Cycles to Failure relative to the control mix

Type of Mixture	Number of Cycles to Failure		
	Test Type 1: Without rest periods	**Test Type 2: With rest periods but without heating**	**Test Type 3: With rest periods and heating**
Control	-	33%	60%
0.2% Fibers	97%	91%	124%
0.4% Fibers	109%	54%	91%

6. Performance Modeling and Prediction

The laboratory test results and the material properties of all mixes were presented earlier. In order to evaluate the predicted field performance, consideration of traffic and climate conditions were employed in the AASHTOWare Pavement ME Design software. Furthermore, a Finite Element Model (FEM) was developed to simulate the rutting performance in the Hamburg Wheel Tracking (HWT) test. The purpose of this evaluation is to grasp the effects of fibers on pavement performance based on the identified properties of the mixes.

6.1 AASHTOWare Performance Prediction

The pavement structure of the sections was modeled as of 4.8 inches of new asphalt layer over 4.8 inches of old existing asphalt. The sublayers were assigned 7.2 inches of crushed base material over 19.2 inches of crushed sub-base. The class of asphalt material was SP5; the 0.75 inch maximum size crushed base material had an estimated R-value of 80; and the subgrade soil consists mainly of gravel with silt and sand with an assigned R-value of 60. Figure 47 in Appendix C presents the details of the layers' structure. The FWD values obtained from ITD were used to back calculate the resilient modulus of the existing HMA layer. All data related to the layers properties is in Appendix C.

Analysis

The input data needed for the AASHTOWare Pavement ME Design analysis were either provided by the ITD or measured directly in the laboratory. For the predicted pavement performance, the reliability was 90 percent for a design life of 20 years. The performance

prediction characteristics for the pavements include fatigue, rutting, thermal cracking, and roughness. The climatic data are based on weather station in Pocatello, ID. The ITD measured the AADTT which is presented in Figure 45 in the Appendix. Vehicle class distribution and the adjustment factors were obtained from the ITD and shown in Tables 36 and 37. As of this writing, the State of Idaho's local calibration factors for the AASHTOWare Pavement ME Design are not available. Accordingly, the nationally calibrated distress models in the AASHTOWare Pavement ME Design software were used. The AASHTOWare Pavement ME Design requires complex shear modulus and phase angle data for RTFO-aged binder residue at several temperatures for Level 1 and Level 2 asphalt inputs. Table 35 in Appendix C provides details of the Level 1 inputs of the binder.

Results

Figures 20a through 20f present the predicted rut depths, top-down fatigue cracking, bottom-up fatigue cracking, and thermal cracking, and IRI results of the control and fiber pavements, respectively. The predicted rut depths of the asphalt layers after 20 years indicated that the control mix had a rut depth slightly higher than the others, and all the fiber mixes had the same level of rutting. This is due to the rutting model for asphalt layers in AASHTOWare Pavement ME Design being based on the dynamic modulus values, and since there was no significant difference among fiber mixes modulus values at high temperature there was no difference in performance. Figures 20c and 20d present the predicted top-down and bottom-up fatigue cracking results, respectively. The same trend of the fiber mixes can be seen in the bottom up cracking. Again, these outcomes are due to the fact that the top-down and bottom-up fatigue cracking models in AASHTOWare Pavement

ME Design are based on the dynamic modulus. High modulus values of an asphalt mix lead to less fatigue cracking in this model. Fiber #1 pavement section showed poor resistance to thermal cracking compared to the other sections, as shown in Figure 20e. This may be due to the low m-values of the creep compliance (which describes the ability to relieve stress), which is similar to the m-values for the creep stiffness of binder in Superpave binder specifications. In AASHTOWare Pavement ME Design, the thermal cracking model is based on IDT strength, creep compliance, and the slope of the creep compliance master curve.

Generally, the predicted performance follows the material properties measured in the laboratory after considering traffic and climate. This result is expected, because the distress models are based on these material properties and the traffic and climate conditions are kept the same for pavements with different Fibers. In addition, because this study used nationally calibrated distress models, the absolute values for predicted distresses may not be representative of true pavement performance without the local calibration of these models. However, the ranking of the performance of the four different pavements should hold true.

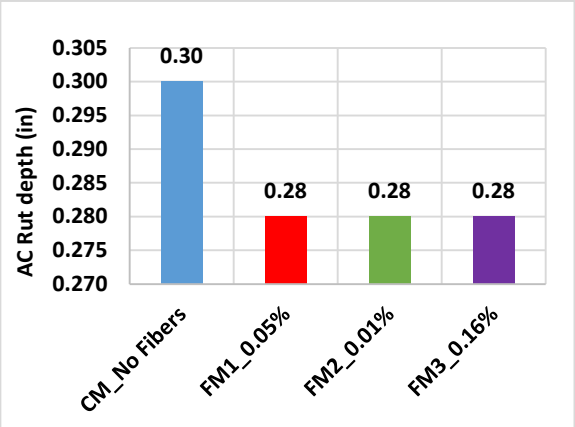

(a) HMA layer rut depth, in.

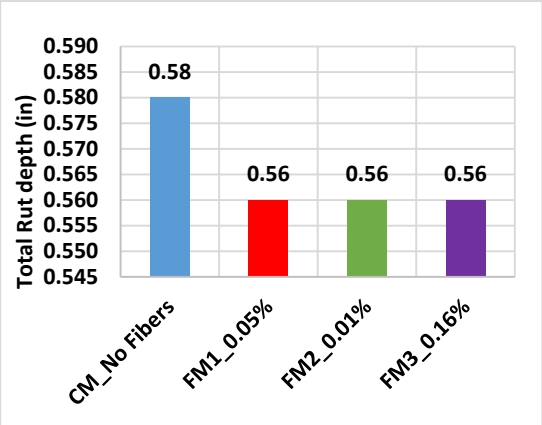

(b) Total rut depth, in.

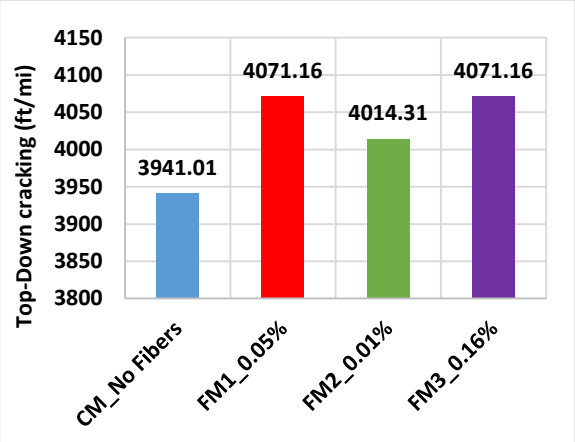

(c) Top-Down cracking (ft/mile)

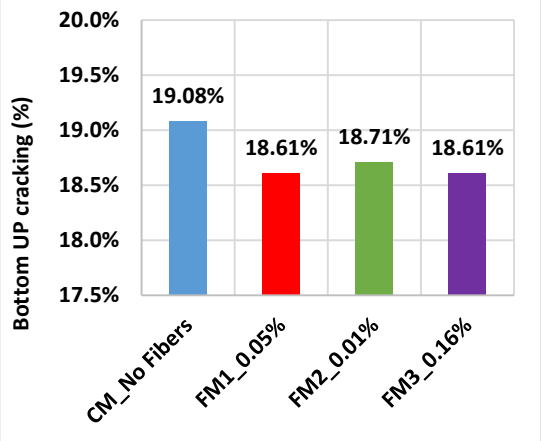

(d) Bottom Up cracking (%)

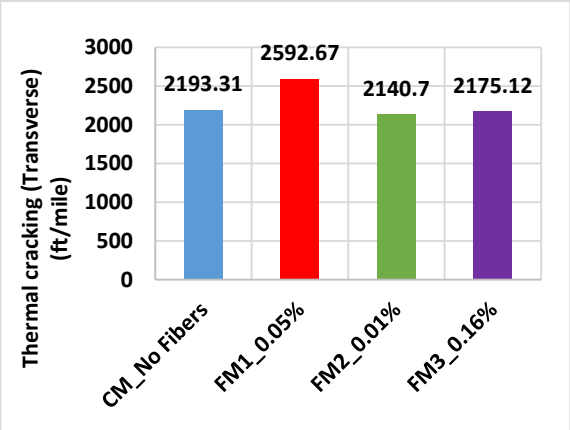

(e) Thermal cracking (ft/mile)

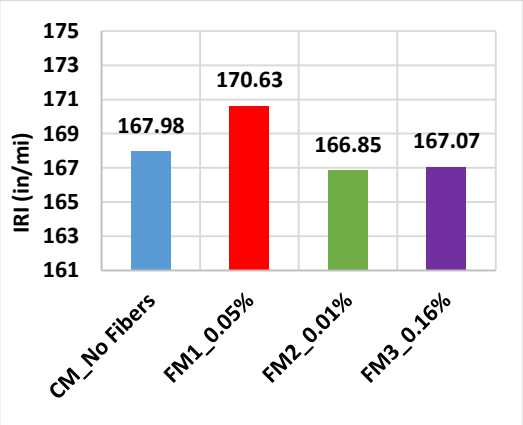

(f) IRI (in/mile)

Figure 20 (a) to (F) AASHTOWare Pavement ME Predicted Distresses of the Fiber pavements

S

6.2 Fatigue life

Expected fatigue life for bottom-up cracking was calculated based on phenomenological fatigue model outlined by Wen (2013). Below is the fracture work density model.

$$N_f = 3.75 \times 10^{-5}(\frac{1}{\varepsilon_t})^{0.147}(FWD)^{1.92}h^{0.135} \quad (1)$$

N_f is the number of repetitions to fatigue; ε_t is the tensile strain at critical location, microstrain; FWD is the fracture work density, psi; h is the thickness of asphalt layer, in. Tensile strain at the bottom of asphalt concrete overlay was calculated for the standard 18 kip single axle load by Everstress software. Everstress is a linear elastic layer program developed by the Washington State Department of Transportation. Table 8 presents the details of pavement structure for the test section. Modulus values for the surface layers are assigned based on the results in this research, where the layer moduli of the base and subgrade were assigned based on the R-values of these layers.

Table 8 Generalized Pavement Structure for Test Section

Layer Number	Type of Layer	Thickness(Inch)	Modulus(ksi)
1	AC Overlay	4.8	564^{C}-$655^{F\#1}$-$575^{F\#2}$-$595^{F\#3}$
2	Existing AC	4.8	350
3	Base:3/4” aggregate	7.2	45.40
4	Subbase: granular	19.2	34.30
5	Subgrade	-	15.43

Table 9 presents the fatigue life for different fiber modified mixes and control mix. As shown, fiber #2 section indicates higher fatigue life in comparison to other fiber modified sections. That relates to a high fracture work density of these mixes. It should be noted that

this model was calibrated based on the Accelerated Load Facility (ALF) data at the FHWA Turner-Fairbank Highway Research Center. Hence, its prediction values may not be valid for the field performance of asphalt concrete pavements.

Table 9 Fatigue life for Bottom-UP Cracking

Mix	Strain(Micro)	FWD(psi)	h(inch)	N_f
CM_No fibers	38.11	38.11	4.8	211493
FM1_0.05%	39.87	39.87	4.8	209702
FM2_0.015%	38.68	38.68	4.8	267156
FM3_0.16%	39.02	39.02	4.8	197193

6.3 Finite Element modeling

Finite element method (FEM) is a powerful method to develop numerical solutions of complex problems. In the FEM, the structure body is divided into an equivalent system of many smaller units (finite elements) interconnected at points called nodes with boundary lines or surfaces. Elements may have physical properties such as density, Young's modulus, Poisson's ratio.

A commercially available finite element program, Abaqus, was used in this study to model asphalt mixture behavior with different dosages of fibers in the Hamburg wheel tracking test. The software consists of powerful engineering simulation codes that has the capability of solving relatively simple problems to complicated nonlinear problems.

In the software, it is required for the user to go with a logical sequence to create a model. In many circumstances the user must follow a natural progression to complete the modeling task. The following is a brief summary on the steps: The user should create

individual parts and sketching their geometry, create section and define material properties and select the material models, choose the required field and history output, create and assemble part instances, define the analysis steps including the time period for each step, define the load type and boundary conditions, select the finite element type and mesh the part, create a job and submit the data for analysis. Then analysis of results and selected model data can be viewed (Abaqus 6.12 User's manual, 2012).

The essential goal of FE modeling in this part of the research was to simulate the effect of the HWT test on the fiber modified asphalt mixtures. One of the common concerns related to Abaqus is the computation or the analysis time. To reduce the analysis time, a two dimensional plane space model was designated with deformable solid features. This reduced the computation time considerably without significant effect on the results' accuracy. Hua, 2000, used a simplified method to simulate the loading time during the HWT test, the same approach used in this study.

Developing material parameters

The power law creep model which is available in Abaqus to describe the plasticity of the material was selected for this task. This model considered to be appropriate for describing the creep behavior of the asphalt mixture and simulate rutting (White 2002).

$$\dot{\varepsilon} = A\sigma^n t^m \quad (2)$$

where

$\dot{\varepsilon}$ = uniaxial equivalent creep strain rate

σ = uniaxial equivalent deviator stress

t = total time

A, n, m = material parameters

The Hamburg wheel tracking test's temperature is based on the high performance grade of the asphalt binder. Since the used asphalt binder is PG 70-28, the temperature that has been used for the test was 55 ^{o}C. For this reason, it is required to determine the modulus of elasticity and Poisson's ratio for the asphalt mixtures at this temperature. The modulus was determined at 1 Hz from the dynamic modulus test, and the Poisson's ratio was determined from the Mechanical-Empirical Pavement Design Guide.

$$\Upsilon_{ac} = 0.15 + \frac{0.35}{1+e^{(-1.63+3.84x10^{-6}E_{ac})}} \quad (3)$$

Υ_{ac} = Poisson's ratio of asphalt mix at a specific temperature

E_{ac} = modulus of asphalt mixture at a specific temperature (psi)

The result of the Poisson's ratio found to be 0.43 at all asphalt mixtures. The effect of the dynamic modulus results was miner at the designated temperature. The material parameters A, m and n in the creep power law model should be defined to simulate the development of the rut depth. The visco-plastic axial strain versus time relationship at the range of the secondary zone in the flow number test used to determine the initial parameters for all the fiber mixes. The dynamic creep test was conducted at 210 kPa stress level. Since the stress level was constant, parameter n held constant for all mixtures. Table 10 below shows the initial parameters for all mixes.

Table 10 Initial material parameters of fiber modified asphalt mixtures

Mix	Initial material properties		
	A	n	m
Control Mix	0.00130	1.45	-0.381
FM1_0.15%	0.00093	1.45	-0.395
FM2_0.05%	0.00180	1.45	-0.450
FM3_0.16%	0.00160	1.45	-0.489
LM1_0.2% Fibers	0.00140	1.45	-0.431
LM1_0.3% Fibers	0.00110	1.45	-0.301
LM1_0.4% Fibers	0.00128	1.45	-0.378

Modeling of Hamburg Wheel Tracking test

The footprint of the HWT is solid steel wheel on the surface of asphalt mix samples, measured at a testing temperature of 55 ^{o}C as shown in Figure 21 below. The average width of the wheel is 47 mm with applied load of 705 N during the test.

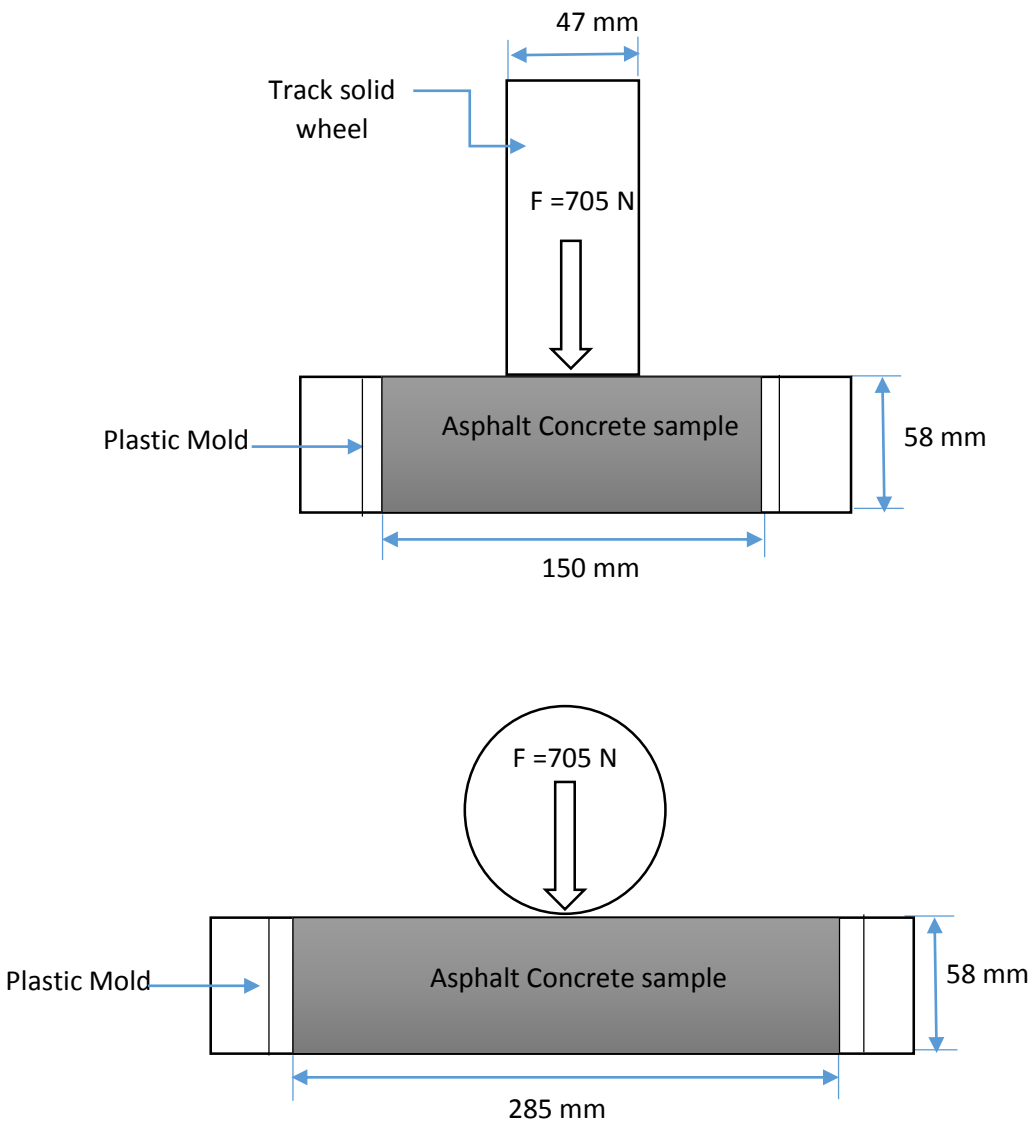

Figure 21 Schematic of Hamburg Wheel Tracking Test

Hua (2000) analyzed the wheel movement at the top of the sample surface in the HWRT test. The loading time in one pass was about 0.14 sec. The time of loading conversion described in Figure 22 used for the HWT simulation. The average time from T0 to T1 is 0.07 sec. which was similar to the average time from T2 to T3. The period from T2-T3 is 0.14 sec. The converted loading time in one pass was 0.21 sec. To accommodate the total number of passes, the time of loading in the HWT for 20,000 cycles converted to 4,200 sec (Uzarowski, 2007).

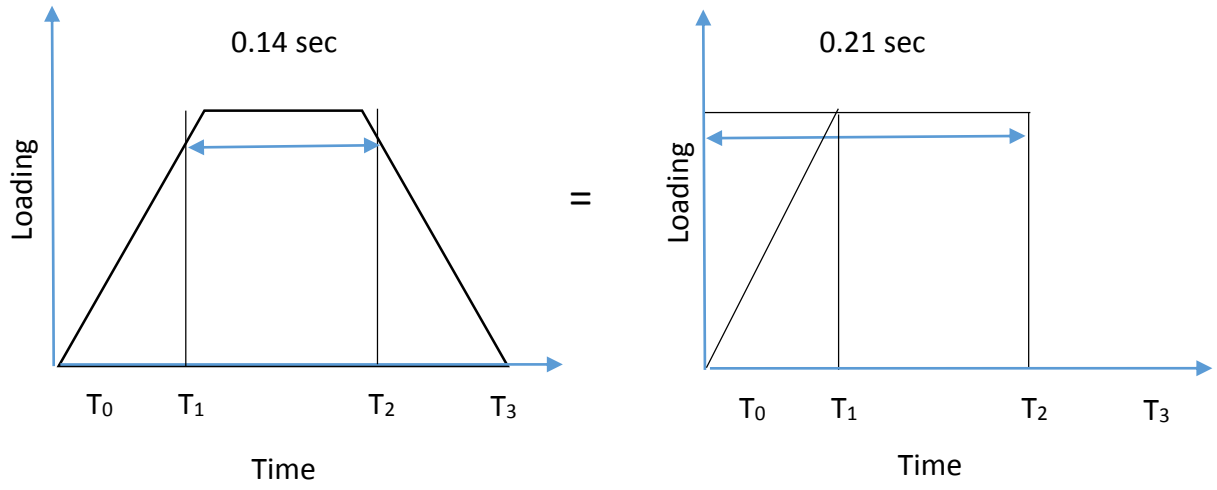

Figure 22 Conversion of Load duration in HWTT (Hua, 2000)

Figure 23 shows the mesh distribution, loading and boundary conditions. There is no vertical or horizontal movements allowed along the bottom or side edges.

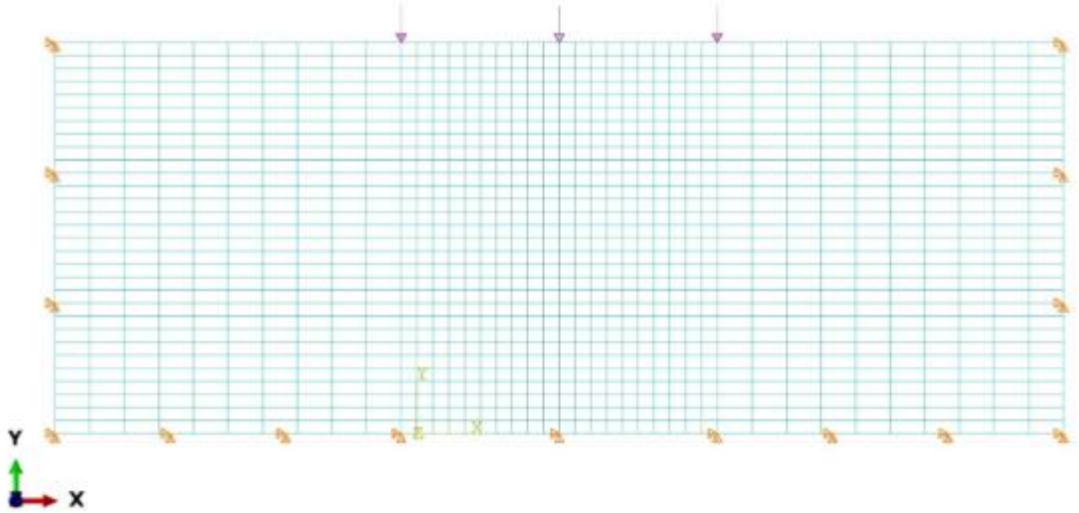

Figure 23 Mesh distribution, loading and Boundary Conditions of the Model

The Mises stress is used in the calculation of the creep rate in the creep model. Figure 24 shows the Mises stress in the control mix calculated in Abaqus at the end of the HWT test. Figure 25 shows the deformed shape and the vertical deformation (U2) of the control mix after 20,000cycles.

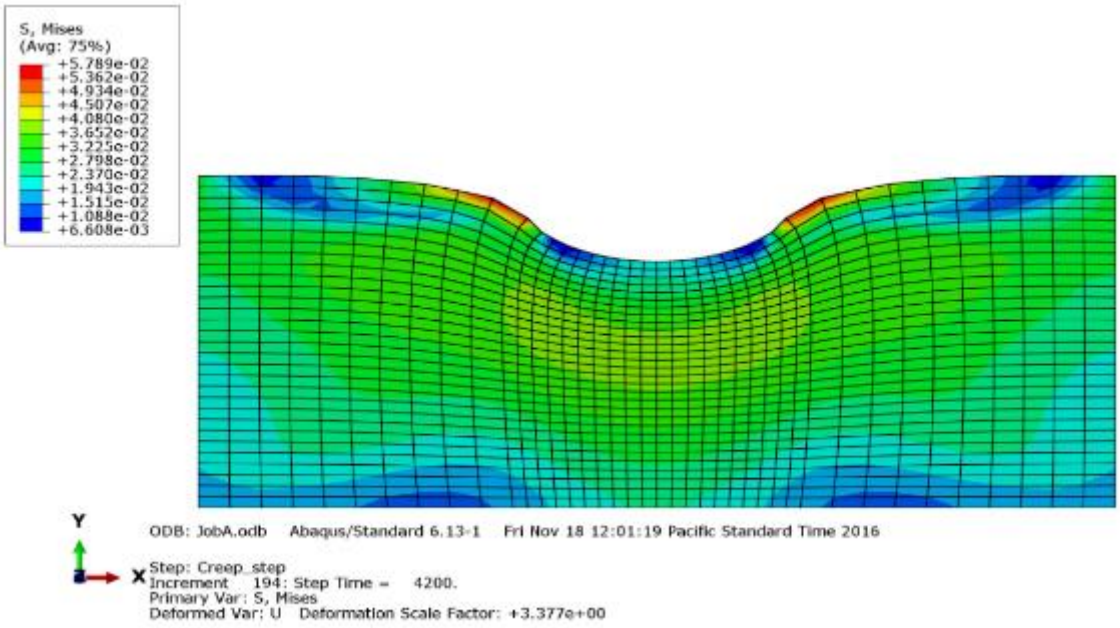

Figure 24 Von Mises Stress in HWT after 20,000 cycles for the Control mix

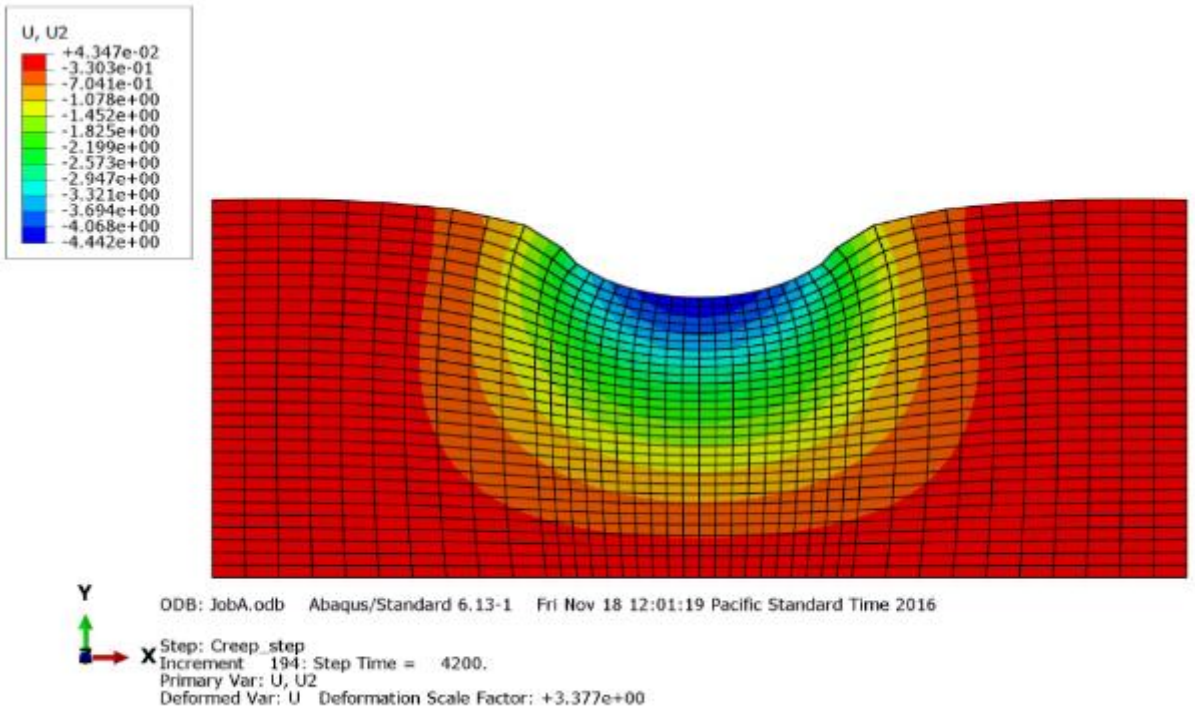

Figure 25 Predicted vertical deformation in the Control mix after 20,000 cycles

The permanent deformation predicted by Abaqus simulation was compared to the real measured values in the HWT test. Table 11 shows that the predicted rutting was higher than the measured. As it can be seen, the software is over predicting the rutting depths. The liner trend line for the relationship as seen in Figure 26 has R^2 equal 0.68.

Table 11 Initial material parameters with Measured Rutting vs. Predicted Rutting after 20,000 cycles

Mix	Rutting Depth (in) measured in HWTT	Rutting Depth (in) Predicted by Abaqus
Control Mix	0.122	0.175
FM1_0.15%	0.104	0.115
FM2_0.05%	0.089	0.158
FM3_0.16%	0.078	0.098
LM1_0.2% Fibers	0.077	0.118
LM1_0.3% Fibers	0.066	0.102
LM1_0.4% Fibers	0.060	0.177

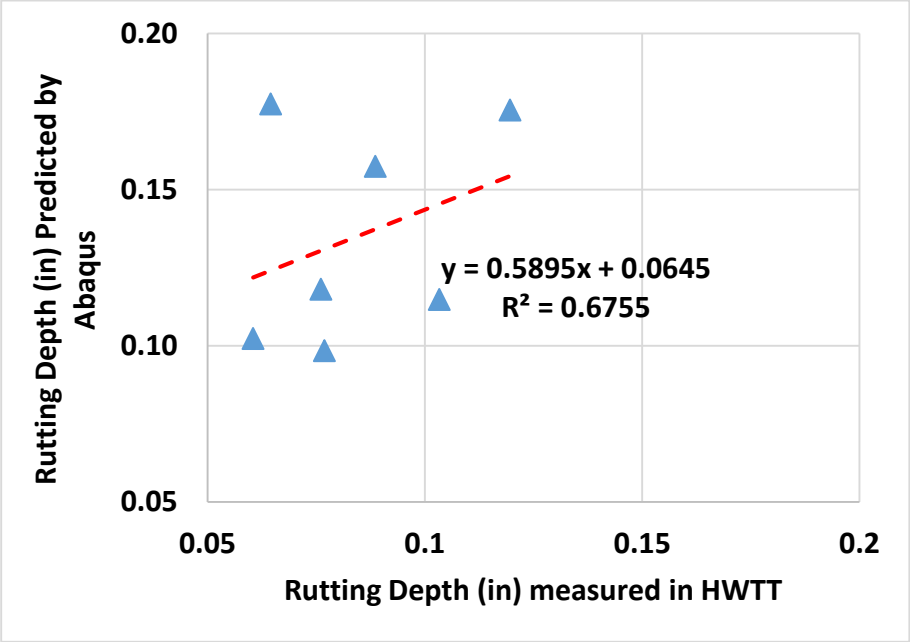

Figure 26 Measured vs. Predicted Rutting at different with the initial material parameters

Since the model is over predicting the rut depth, the measured values from the Hamburg Wheel test used to calibrate the creep parameters. Parameters A and m were adjusted by trial and error until obtaining a good fit. The rut depths were compared at

different number of cycles. Figure 27 shows the rut depths comparison after calibrating the material parameters for fiber #1 field modified mix at different loading times.

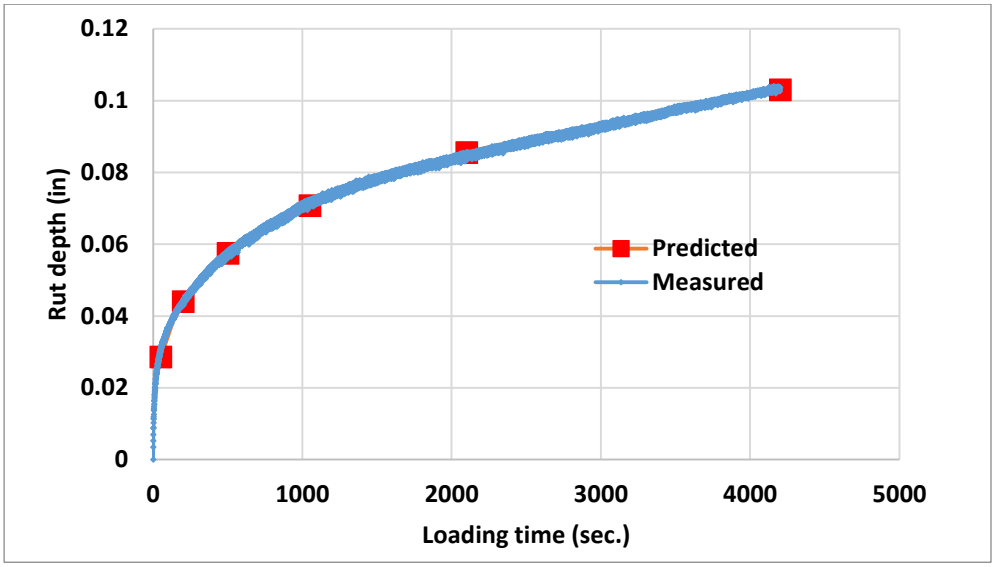

Figure 27 Measured vs. Predicted rut depth at various loading times of FM1_0.05%

Figures 28 to 34 show the rut depths in (mm) as predicted in Abaqus at the end of the test.

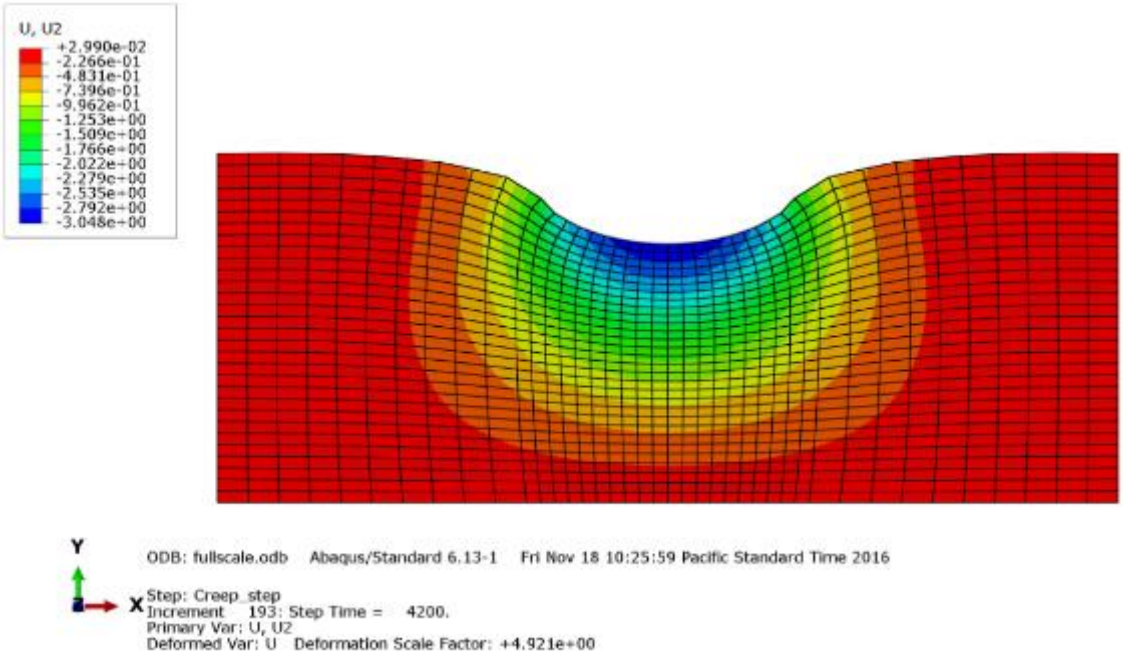

Figure 28 Predicted vertical deformation in the Control mix after 20,000 cycles

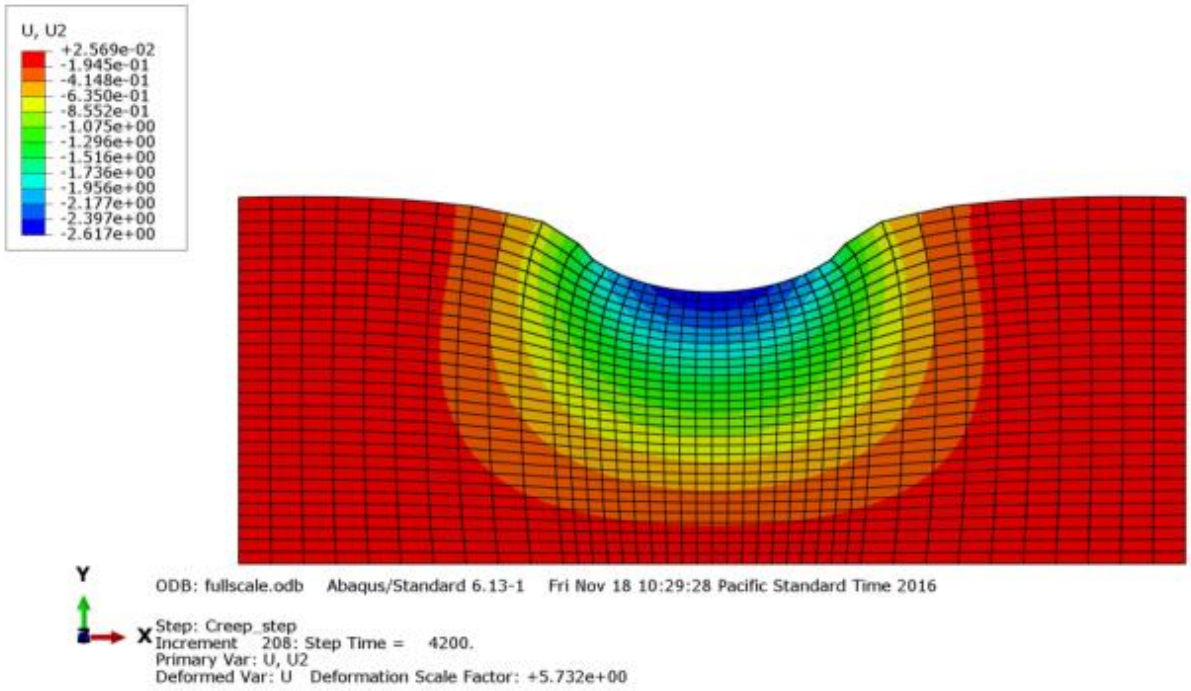

Figure 29 Predicted vertical deformation in FM1_0.05% after 20,000 cycles

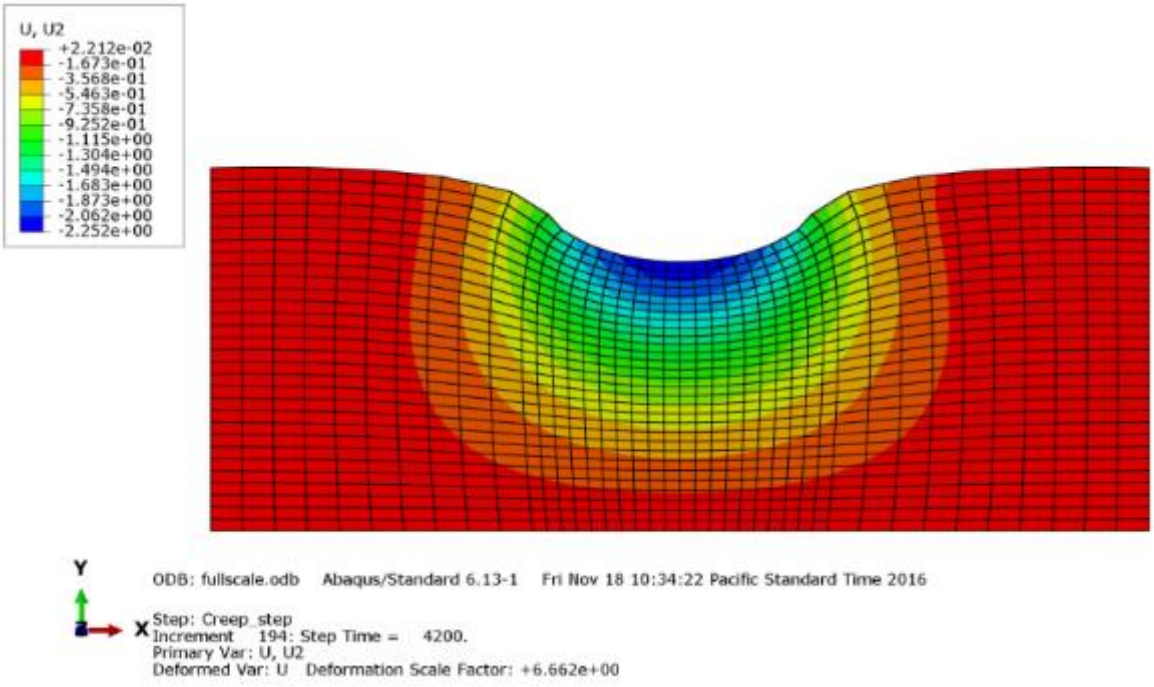

Figure 30 Predicted vertical deformation in FM2_0.015% after 20,000 cycles

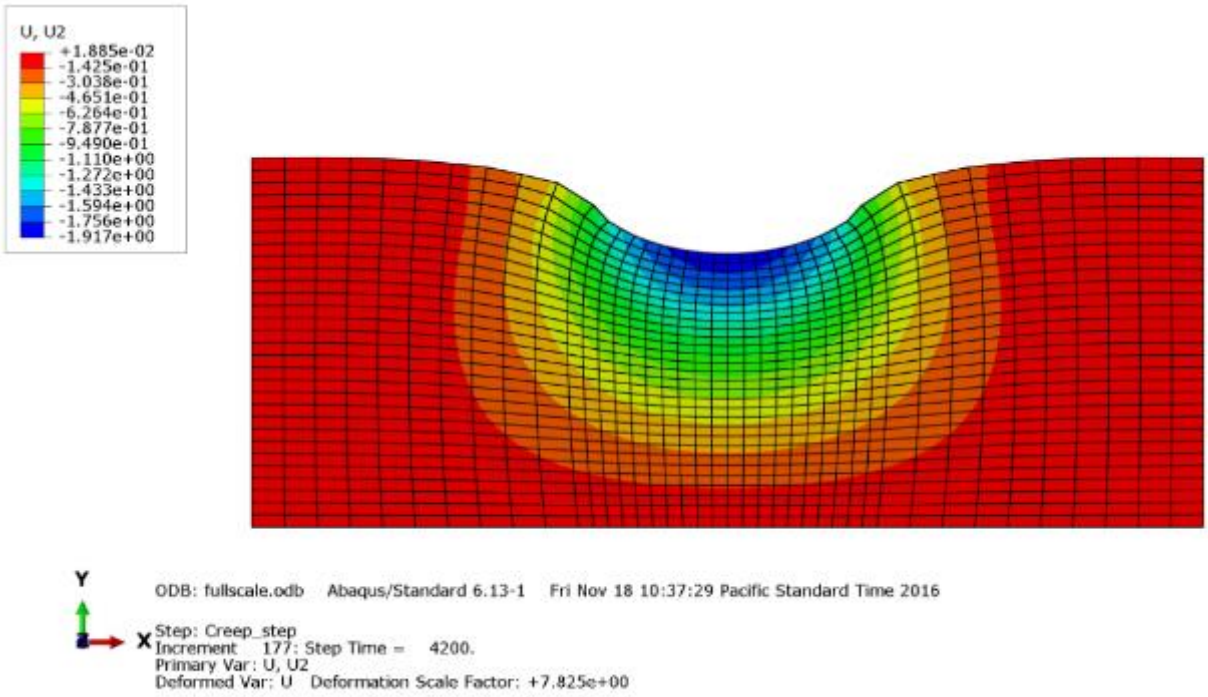

Figure 31 Predicted vertical deformation in FM3_0.16% mix after 20,000 cycles

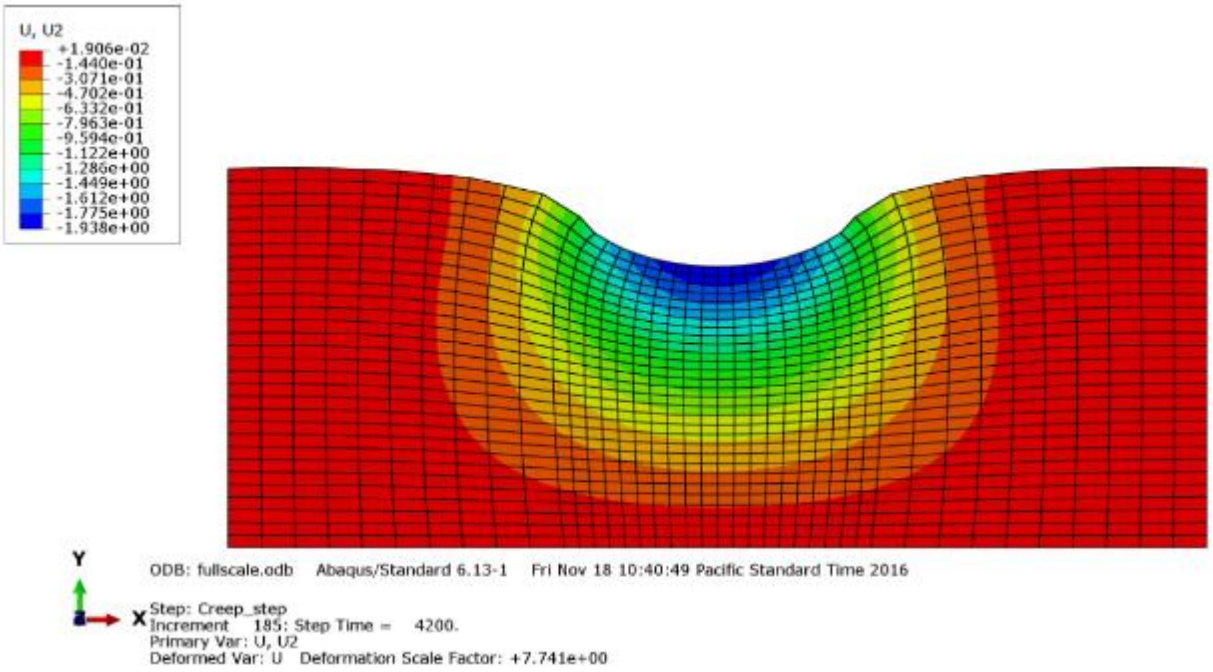

Figure 32 Predicted vertical deformation in LM1_0.2% mix after 20,000 cycles

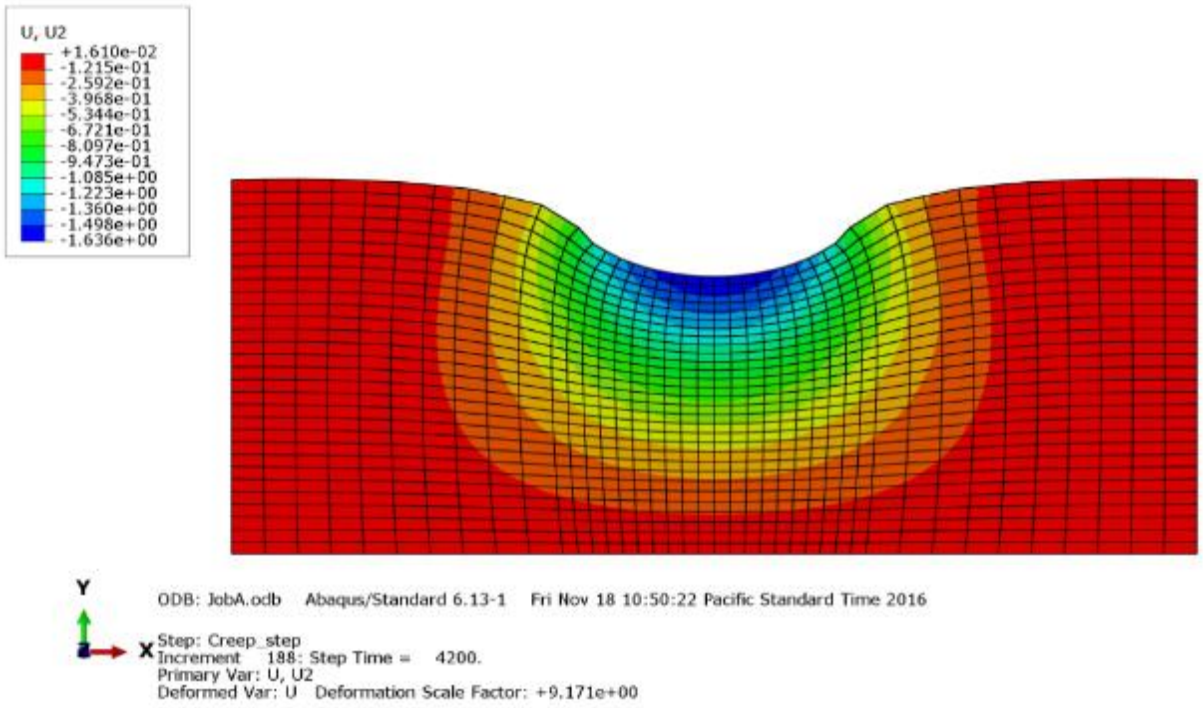

Figure 33 Predicted vertical deformation in LM2_0.3% mix after 20,000 cycles

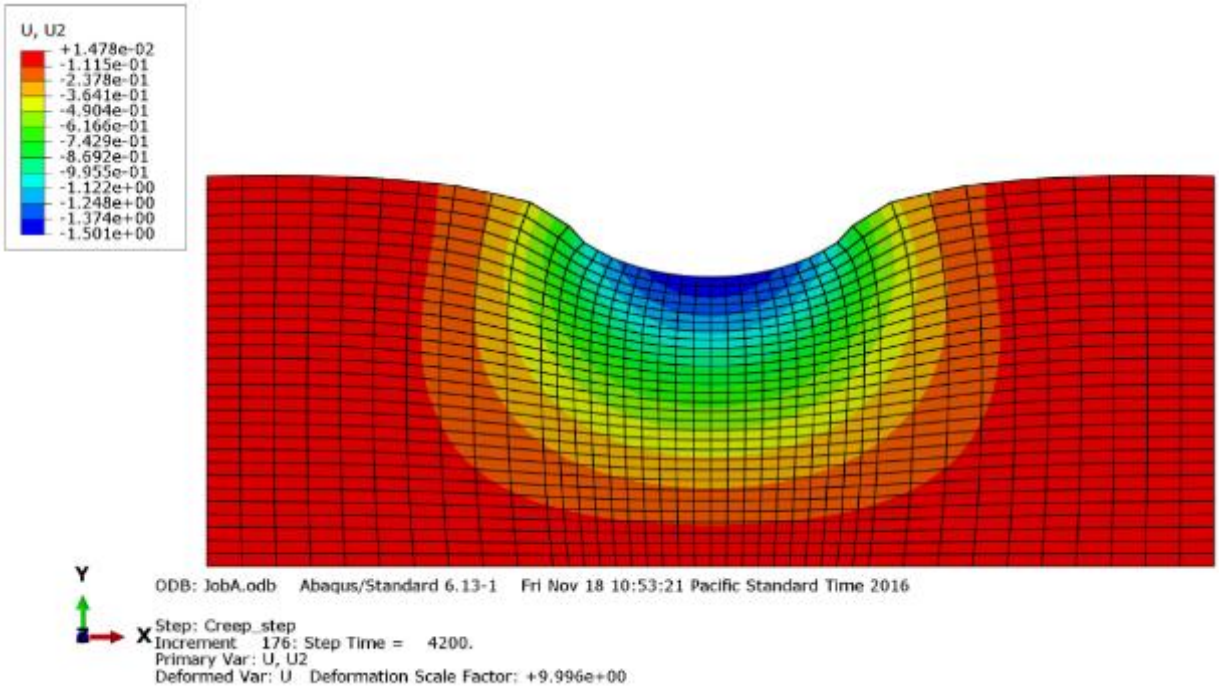

Figure 34 Predicted vertical deformation in LM3_0.4% mix after 20,000 cycles

Table 12 shows the final creep parameters for all asphalt mixes with the predicted rut values. The linear trend line in Figure 35 shows a good fit for the measured and predicted values with R^2 of 0.99 after model calibration.

Table 12 Final Material Parameters used in Modeling

Mix	Final material parameters			Rutting Depth (in) measured in HWTT	Rutting Depth (in) Predicted by Abaqus
	A	n	m		
Control Mix	0.0074	1.45	-0.72	0.122	0.120
FM1_0.15%	0.0079	1.45	-0.76	0.104	0.103
FM2_0.05%	0.0061	1.45	-0.74	0.089	0.089
FM3_0.16%	0.0061	1.45	-0.77	0.078	0.075
LM1_0.2%	0.0065	1.45	-0.78	0.077	0.076
LM1_0.3%	0.0064	1.45	-0.81	0.066	0.064
LM1_0.4%	0.0053	1.45	-0.79	0.060	0.059

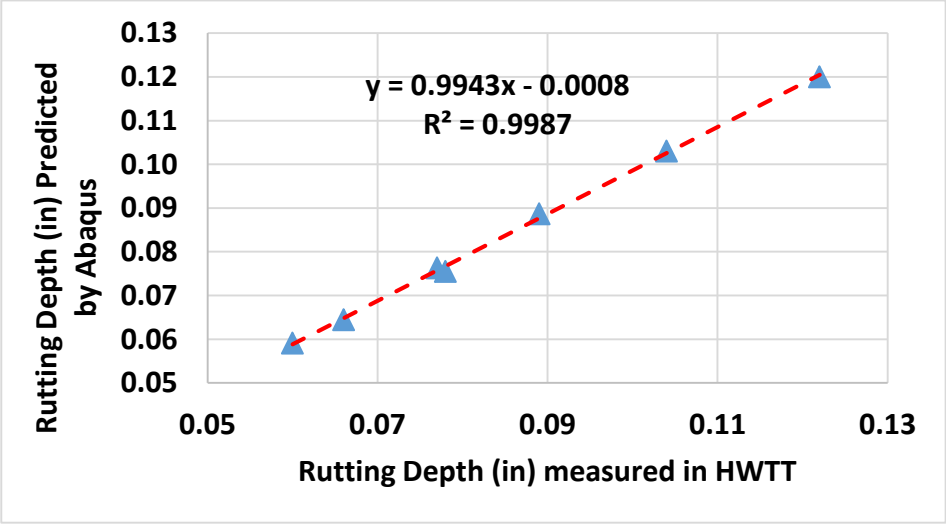

Figure 35 Measured vs. Predicted Rutting at different passes with the final material parameters

Once the model is calibrated and obtaining the final creep parameters, a comparison of rutting depths among fiber mixes can be made at any scale and for longer terms. A comparison has been made for a higher number of cycles (100,000 cycles) to see the effectiveness of fiber mixes in mitigating rutting for the long term performance. As can be seen in Figure 36, fiber mixes with 0.2% or higher have accumulated rut depths less than half of what occurred in the control mix.

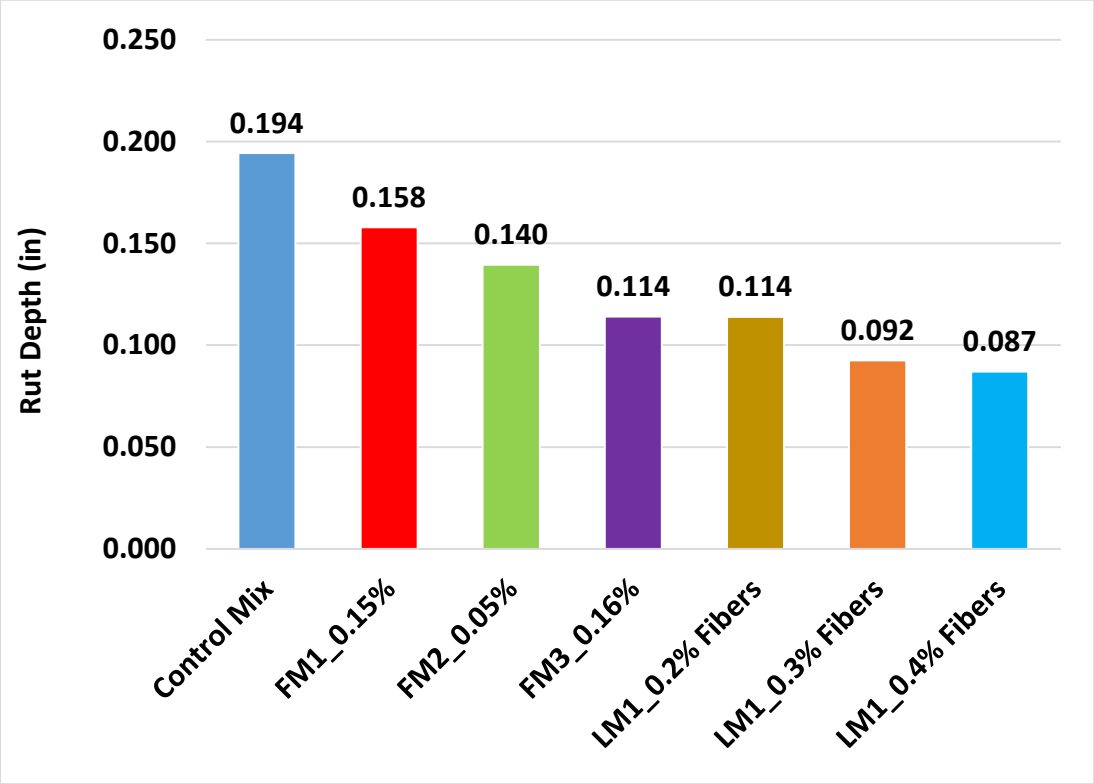

Figure 36 Predicted Rut depths of all mixes after 100,000 cycles

Summary

Visco-plastic deformation is the main cause of rutting in asphalt pavements. The finite element software, Abaqus, used to simulation the Hamburg Wheel tracking test. A

two-dimensional plane strain models are used in the simulation. The initial elastic material properties, modulus of elasticity and Poisson's ratio, were determined form the dynamic modulus test. The creep parameters A, n and m developed from the repeated load creep test. The continuous loading time and creep power law used in the finite element modeling.

Since, there wasn't a good fit in the relationship between the predicted and measured rutting, an adjustment of creep parameter A and m for the fiber mixes was required. The calibrated parameters can be used for future finite element pavement in-situ performance simulation.

7. Evaluation and Quantification of Fiber Dispersion

There is a need to quantify the level of dispersion of fibers in the mix as it plays a major role in the mix performance. Fibers should be well distributed inside the mixture to get the benefits of using them. The primary approach stemmed from previous research using X-Ray Tomography technology to analyze asphalt mix internal structure. The technology was also used to investigate the crack propagation in HMA mixes.

7.1 X-ray Tomography

Brief review of some of these studies are presented here. Bahia et al. stated that the two dimensional (2-D) imaging techniques is efficient approach to characterize the microstructure of the HMA, and it can capture the structure of the aggregates inside the mix (Masad et al., 1999). This technique could be used to introduce an elaborated method to characterize the internal structure and correlated it to the rutting resistance performance. The researchers used a processed digital images for different samples with different gradations and binder contents under different compaction efforts. The results show that there is a correlation between the internal structure indices and rutting resistance. Also, the indices were successfully used to capture the effect of compaction effort, gradation quality, and binder modification on the mixture internal structure.

Masad et al. (1999) used the 2D imaging techniques to investigate the difference in the internal structure of asphalt mixes compacted by linear kneading compactor (LKC) and Superpave gyratory compactor (SGC). In order to study the internal structure of these mixes, the distribution and orientation of aggregates and the aggregate to aggregate contacts were used as quantifying measures. The results revealed that the LKC specimens are relatively

randomly distributed. However, the SGC specimens tend to be more orientated toward the horizontal direction.

In a following study, Masad et al. (1999) measured the orientation of aggregates in asphalt mixes that have different compaction efforts (different number of gyrations) and in field cores. The researchers found that the anisotropy in gyratory samples became more noticeable with the increase in the number of gyrations (compaction effort) up to a certain point. After that the anisotropy level decreased and the orientation of the aggregates became more randomly distributed.

Tashman et al. (2001) examined the relationship between the compaction effort and the aggregate orientation. In this study, the authors used samples compacted by Superpave gyratory compactor and compared them to field core samples. The results indicated that the aggregate anisotropic distribution was less in the SGC specimens than the field cores, and the imaging analysis showed a tendency for coarse aggregates to move toward the edge in SGC specimens. The researchers also compared samples before and after triaxial compression tests at high temperatures, and they analyzed the CT images to characterize the change in the air voids. The results showed a uniform air-voids distribution in the horizontal direction and a non-uniform distribution in the vertical direction from field cores studied using CT.

X-ray CT has also been used to detect the cracks in asphalt mixes by using computerized tomography techniques to detect the development of the crack (Braz et al., 2004; Offrel et al., 2002). However, there is no enough research on the use of X-ray

tomography techniques to investigate the distribution of some additives inside asphalt mixes such as: rubbers and fibers.

Field core samples were prepared for X-ray Tomography test to examine the dispersion of the fibers in the mix. The scanning was performed with high-resolution at the X-ray CT scan facility at the University of Texas at Austin (UTCT). In this machine, X-ray beams are radiated from all directions to the specimen. Passing X-ray through the specimen can decrease the X-ray intensity and this variation is measured by detectors in the plane of specimen. By processing the data of detectors gray scales cross sections of the specimen are constructed. Data from detectors determine the attenuation coefficient of sample that is function of density, atomic number and X-ray energy. By combining these images (slices) the 3D image of sample can be obtained. The thickness of each image is related to X-ray beam and detector plane.

Figure 37 shows the final image of fiber#1 field cores. These images were analyzed based on above explanation. As can be seen, no fiber was detectable in these images. The size and density of fiber were less than the capacity of X-ray machine. Furthermore, by using X-ray machine with low energy range the X-ray beam cannot penetrate specimen. Since the results did not reveal any significant conclusion and fibers were not actually detected. It was decided to abandon the test and do not continue for other mixes.

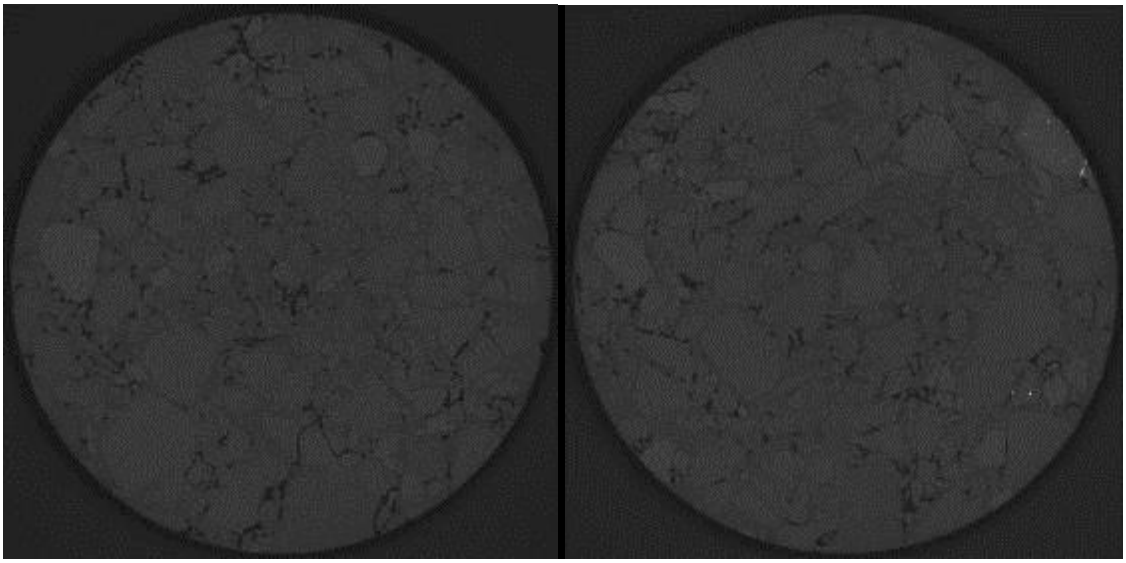

Figure 37 Fiber #1 modified asphalt specimen used for high resolution X-ray CT scanning

7.2 Lab Trials for Extraction of Fibers

At the laboratory, it is not difficult to control a precise content of fibers that need to be added to the asphalt mixture. However, in the field it is challenging to regulate the fiber content per each ton of asphalt mixture during the construction. Since, Idaho Transportation Department built three test sections that designed with specific fiber content and type for each one. It was essential to determine the exact fiber content and check the variability in the fiber dispersion. The initial experimental procedure for this research was planned based on the assumption that each asphalt mix has the desired fiber content with uniform distribution. However, the high variation in test results revealed the distribution of added fiber was not uniform. Therefore, it was necessary to measure the fiber content in asphalt mixes. For this purpose, two different methods were followed to separate the fiber from asphalt mixes.

The first method included two steps. In the first step, asphalt binder was extracted from asphalt mixes according to AASHTO T-164. In the second step, fiber-aggregate mixture from the extraction was ignited in NCAT ignition oven at the temperature of 1200 ^{o}F (650°C). Laboratory tests showed this temperature can burn 99 percent of fiber, whereas ignition in lower temperatures led to a considerable amount of fiber leftover after ignition. Figure 38 presents the schematic steps of this method.

Figure 38 Schematic Steps of Proposed Method to Identify Fiber Content

Measured fiber content from this method was much higher than target values which indicated that considerable amount of fine aggregate was burned during second step in the ignition oven at 1200 ^{o}F (650°C). Therefore, a new method was evaluated to measure the fiber content in asphalt mix. This method was similar to the first but instead of using an ignition oven, calcium chloride solvent was used to separate fiber and aggregate. Light fibers that suspended in the solvent could be collected from the surface of solvent. Finally, collected fibers were washed to remove remaining fine aggregate in their structure. The

fiber collected in this way was dried to constant mass in the oven at the temperature of 212±40 °F. Figure 39 presents the final result of this procedure for mixes with fiber #2.

Figure 39 (a) Aggregate-Fiber Mix after Extraction (AASHTO T-164) (b) Collected Fiber #2

Table 13 illustrates the fiber content for fiber #2 mix. The proposed lab method showed that the measured fiber content is approximately close to the target values.

Table 13 Results of Fiber Content for Fiber #2

Measured Asphalt Content from Extraction Method(AASHTO T-164)	4.9%
Target Asphalt Content (JMF)	4.8%
Measured Fiber Content	0.0172%
Target Fiber Content for fiber #2	0.015%

The proposed lab method was not successful for the other two types of fibers. In the case of fiber #3, the fibers were heavier than the solution, so they settled with the aggregate. For the case of fiber #1 mixes, the fiber structure completely trapped the fine

aggregate, making the separation of fiber and aggregate difficult by means of this method. Further study is needed in this area.

7.3 UV light (New proposed method)

The author looked into different approaches to detect the fiber dispersion in the mix, since X-ray tomography did not detect the fibers' dispersion, and no other successful application has been found. The author proposed and investigated a new method that employed the application an optical image processing technique in conjunction with using UV light to detect the fiber dispersion.

Fluorescence is beneficial in a number of safety applications, in investigative medicine, and as a scientific research tool. The new developed approach is based upon the use of the fluorescent materials to detect the fibers inside the mixture. Which is basically coating the fibers with fluorescent material that can be easy to detect under the UV light. Among many fluorescence materials, two types of fluorescent dyes were investigated. The first one is the Triphenylmethane dye which has a blue color under the UV light. The second one, was a pyrene-based dye (pyranine) which is commonly used for the yellow highlighters. The pyrene-based dye found to be more visible than the Triphenylmethane dye. Figure 40 shows fiber #2 coated with the pyrene-based dye.

Figure 40 Fiber #2 before and after coating with a pyrene based dye (a) under day light (b) under UV light

The procedure of this method is as follows. First fibers submerged in the pyrene based dye, then leave it for 24 hours to be completely dry. Later, the asphalt loose mixture was heated to the compaction temperature then fibers added gradually to the heated loose mixture during the mixing in the laboratory drum at the specified dosage. Fiber modified asphalt samples were compacted in the superpave gyratory compactor. After cooling down, the cylindrical samples were cut at five specified depths as shown in Figure 41 below. Then photos of the sample slices were taken under the UV light. At this point, it was straightforward to visualize the fibers under the UV light, and roughly it can be seen whether fibers have uniform distribution or not. However, in order to quantify the level of dispersion of fibers, further analysis is required.

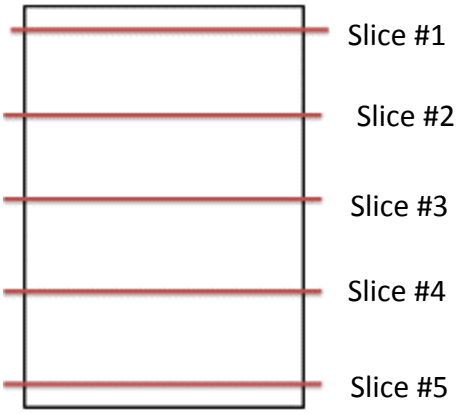

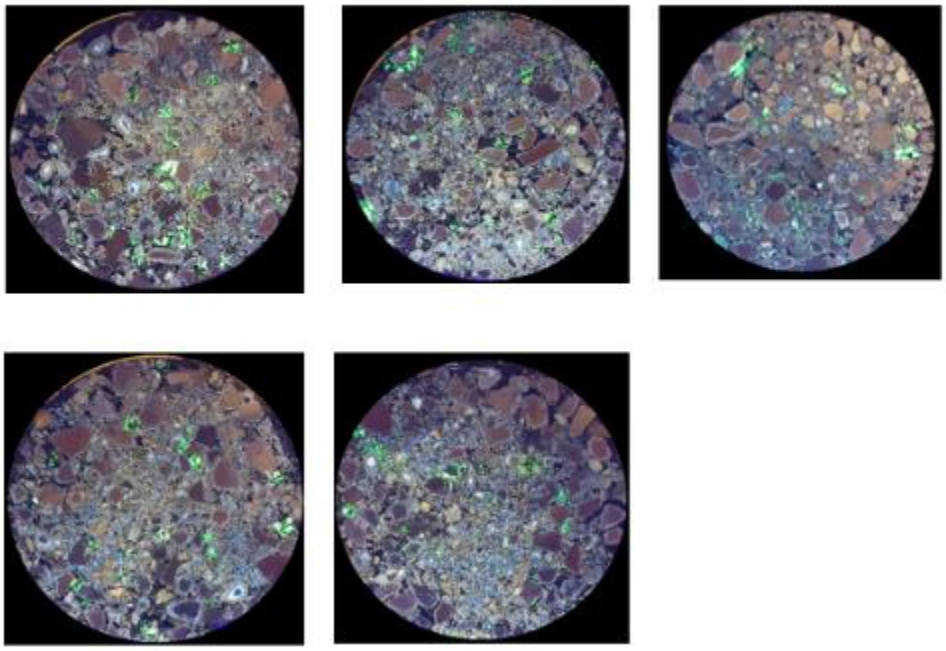

Figure 41 Photos of a fiber modified specimen's slices under the UV light

In order to quantify the level of dispersion of fibers inside the asphalt mixture, photos that were taken under the UV light can be analyzed using an image processing and analysis software such as ImageJ. The software has the capability to detect the areas of the coated

fibers that have distinguished color than the asphalt binder and aggregates. The software also has the ability to locate each area and define the centroid coordinate of each fiber's area. Figure 42 shows the data points for each fiber area. Once the coordinates of the fiber areas are determined, the level of dispersion can be evaluated by plotting the X and Y coordinates as shown in Figure 43.

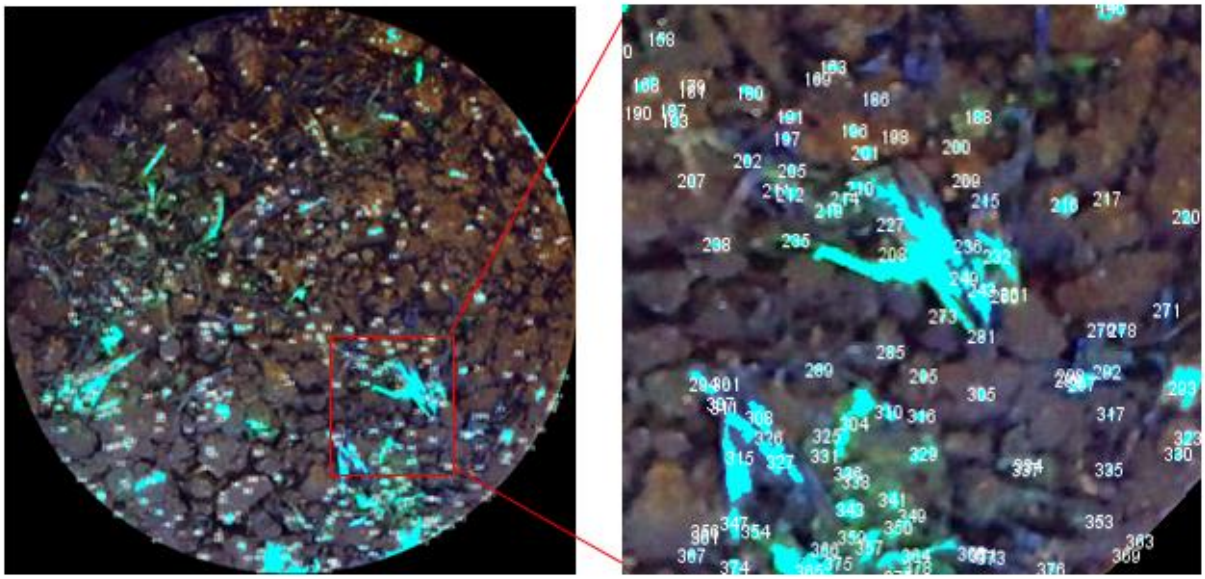

Figure 42 Fibers' areas as labeled in the software

Since there are no specifications or criteria to evaluate the level of dispersion inside the asphalt mixtures, the author set up a threshold for the coefficient of variation that determine the level of dispersion of fibers. Two approaches were evaluated for determining the COV. The first one is by dividing the area of the sample into four quarters as shown in Figure 44. The number of objects or areas of fiber can be counted in each quarter. If the coefficient of variation is less than or equal 58%, then fibers have uniform distribution. The other approach is to divide the slice into two areas, one is at half of the radius and the other

is between the radius and half of the radius. If one area has fibers equal or more than one third of the total area, then the fibers are well dispersion. The role of one third of fiber's existence in specific area can translated as COV from the total average area of 47%. Table 14 shows an example of determining the level of dispersion for each slice.

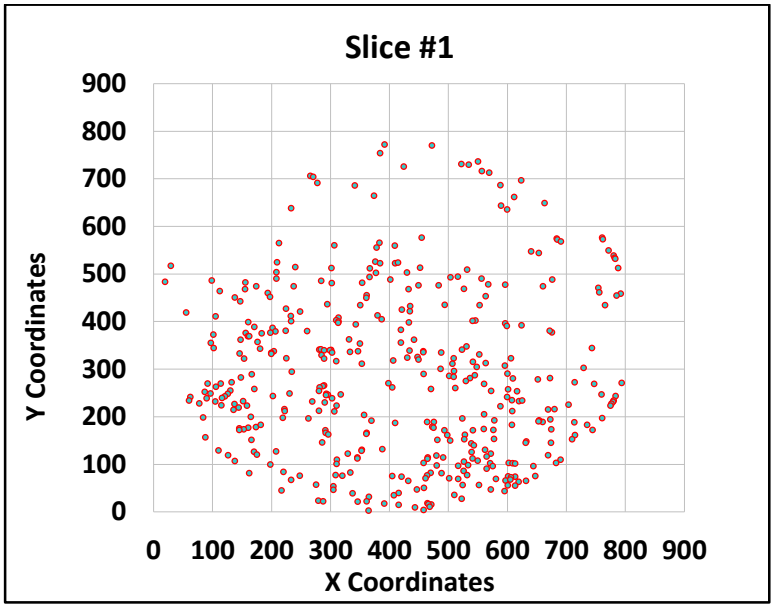

Figure 43 Data points for fiber distribution in one of the slices_LM1_0.2%

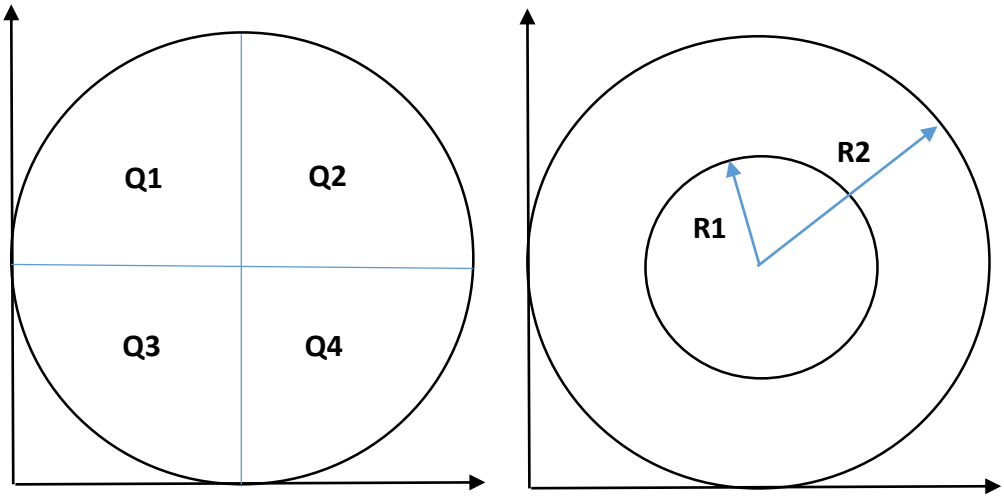

Figure 44 Divided sample areas to account for fiber dispersion

Table 14 Evaluation of fiber dispersion in Slice #1

Total data points = 411				
Area label	Counted area of fibers	Average Area	STDEV	**COV**
Q1	52	102.75	56.91	**55.39%**
Q2	165			
Q3	137			
Q4	57			

Total data points = 411				
Area label	Counted area of fibers	Average Area	STDEV	COV
<R1	260	205.50	77.07	37.51%
<R2,>R1	151			

Table 15 shows a summary of fiber dispersion evaluation of two fiber modified asphalt mixes. The two samples have 0.2% of fiber #1 and 0.4% of fiber #3 respectively. The evaluation shows that both samples have a uniform distribution and no clumping occurred during the mixing.

Table 15 Summary of fiber dispersion in one sample

Slice #	Sample 1 (0.2% fibers)		Sample2 (0.4% fibers)	
	COV_q	COV_r	COV_q	COV_r
Slice #1	44%	25%	20%	17%
Slice #2	55%	28%	57%	24%
Slice #3	90%	35%	18%	33%
Slice #4	64%	97%	25%	28%
Slice #5	86%	26%	46%	41%
Average	**68%**	**42%**	**33%**	**28%**

8. Summary, Conclusions and Recommendations

8.1 Summary

The main objective of this research was to evaluate the effectiveness of using fibers to improve performance of the Hot-Mix Asphalt (HMA). Three different types of fibers that are referred to as #1, #2 and #3 were used in this study. Fiber #1 is a blend of polyolefin and aramid fibers from Forta Fi Corporation. Fiber #2 is wax treated aramid fibers from Surface Tech Company (commercial name ACE fibers). Fiber #3 is glass fibers from Nycon Corporation. Concurrently, three field test sections using these fibers along with a control unmodified section were constructed at US30 in south Idaho. The field test sections were to monitor the performance of these fiber modified sections over long period of time under the actual prevailing climate and traffic conditions. The fiber content in each section was in accordance to the vendors' recommendation. The field monitoring will be over several years and therefore it is not included in this study. Hence the study focused on the laboratory evaluation of mixtures laid in the field. To optimize on the fiber content, an extended laboratory program was conducted using varied fiber contents. However, the extended lab program was limited to Fiber #1. The mix design of the fiber-modified mixes followed the original unmodified control mix. It was assumed that the fibers will not affect the volumetric mix design due to its very low content by mix weight.

The laboratory research program included evaluation of rutting, fatigue cracking, and low temperature cracking properties of the mixtures. For rutting, the tests performed were the Flow Number (FN), Hamburg Wheel Tracking (HWT). Potential of the mix to resist fatigue

was evaluated using the fracture work density measured at the Indirect Tension Test (IDT) at normal temperature (68 °F) as well as the semi-circular bending test of notched samples to determine the fracture parameter (J_c). Resistance to low temperature cracking was evaluated by the IDT at low temperature (14 °F).

To predict the expected field performance of the laid mixes, the research utilized the AASHTOWare Pavement ME Design software. Mix properties required by the software were determined during the lab study. Data input for the software related to pavement structure, climate and traffic were obtained for Idaho Transportation Department (ITD).

A new test protocol was established to study the healing characteristics of fiber modified asphalt mixtures. The semi-circular bending test was adopted for the healing study. It was conducted at a temperature of 70 ^{o}F, and involved rest periods at the operating test temperature coupled with a thermal treatment.

The finite element method (FEM) was used to simulate the rutting performance in the Hamburg Wheel Tracking (HWT) test. A FEM model was developed and calibrated using the lab results of HWT at 20,000 cycles. Due to the limited Abaqus software license available in the lab, it was not possible to conduct simulation for the full scale pavements over long period of time.

Furthermore, an attempt to evaluate the degree of fiber dispersion in each mix using X-ray Tomography was made, but it did not reveal any meaningful results. A new proposed method that involved dying the fibers with florescent material and optical imaging with UV light was developed. Images were analyzed by an image analysis software to quantify the level of dispersion of the fibers.

8.2 Conclusions

Based on the results of the laboratory testing of the investigated mixes in this research, and the developed FEM model, the following conclusions are drawn:

1. Density analysis of field cores as well as reproduced lab specimens from loose plant mixes revealed that the addition of fibers did not alter the mix design volumetric properties. The volumetric analysis showed that all fiber modified mixes have comparable properties to the unmodified mixture.
2. An extended laboratory program to optimize the fiber content using Fiber #1 indicated that the maximum fiber content that may be added, without altering the mix properties, is 0.4% by total weight of the mix. Additional fibers above this limit led to a decrease in the mix density and higher air voids. It was found that at 0.5% fiber content, the workability of the asphalt mixture decrease, and a higher number of gyrations is required to achieve the same density and height of the unmodified compacted samples. The possible explanation is that more asphalt binder would be needed to coat the fibers and to maintain the mixture's properties.
3. Rutting resistance measured by Flow Number and Hamburg Wheel Track tests of the fiber field mixes was comparable to the control mix. The rutting performance did not improve regardless of the type of fiber added based on the vendor's recommendation. Statistical analysis confirmed that there was no significant difference in the rutting performance for the investigated field mixes. Additional

laboratory investigation revealed that fibers might improve the performance of asphalt mixtures at higher dosages than the one provided and recommended by the fiber vendors. The laboratory results indicated that, regardless of the fiber type, a 0.3% by total weight of the mix is the minimum fiber content that can show significant improvement in the mixture performance. All investigated fibers have a comparable performance, and this is due to the high tensile strength of these fibers.

4. For the fatigue cracking resistance measured by both the Fracture Work Density (FWD) and the fracture parameter J_c, the dosage of fibers added to the asphalt mixes in the field did not improve cracking resistance as was reported in previous studies. These results can be explained by lack of tensile stress on the fibers until the pavement experience excessive stresses that lead to cracking of the mix. At higher dosages, it was observed that fibers provide extra tensile strength and improved performance. At low temperatures, the fracture work densities of the fiber mixes were statistically comparable to the control mix and had no significant difference. The expected advantage of the fibers in resisting cracking was not observed even at higher dosages.
5. A new test protocol to evaluate healing characteristics of asphalt mixtures with and without fibers was developed. The average fatigue life of the asphalt mixtures increased when a rest period was introduced during the testing. Improved performance was observed with the thermal treatment applied during the rest period. Healing was found to reverse the accumulated damage. Fibers

contribution was to accelerate the self-healing process. Hence, the average fatigue life increased when samples were left to rest during testing. The self-healing was even more efficient when resting was combined with thermal treatment.

6. A finite element model (FEM) to simulate rutting performance in Hamburg wheel tracking test was developed. The nonlinear visco-plastic behavior of asphalt mixtures was modeled using Abaqus software. The developed model was calibrated using the laboratory data and can be used for further development to evaluate the rutting for in-situ pavement performance simulation.
7. An attempt to evaluate the degree of fiber dispersion in asphalt mixes using X-ray Tomography was made, but it did not detect fibers within the mix due to the fact that the density of fibers was similar to the asphalt binder and fine aggregates.
8. A new method to evaluate and quantify the fiber dispersion in the mix in the lab was developed. The method utilizes optical image processing technique in conjunction with UV light. It was found to be more successful to evaluate the fiber dispersion in the mix.

8.3 Recommendations for Future Work:

To further explore the potential of using fibers in dense graded asphalt mixtures, the following issues need to be further investigated:

1. Only three types of fibers were investigated in this research. Use of other types of fibers that are commercially available need to be investigated.

2. There was only one mix design employed in this study. It will be worthwhile to look into the effect of various mix designs on the type and content of fiber selected.
3. The developed FEM model need to be extended to evaluate the rutting performance of a full scale pavement structure under real traffic and climate conditions. This can be facilitated using a full license version of the Abaqus FEM software and high speed computers.
4. Further in-depth investigation is needed to evaluate the practicality of the developed method of using UV light and image processing techniques to evaluate and quantify the fiber dispersion in the mix. This might lead to developing a practical method that can be used for quality control in the field during construction.

References

Advanced Asphalt Technologies, LLC. *A Precision of the Dynamic Modulus and Flow Number Tests Conducted with the Asphalt Mixture Performance Tester.* NCHRP Report 702, Washington, D.C., 2011

Ahmed, A. I. "Laboratory Investigation into the impact of Polypropylene Fiber Content on Temperature Susceptibility of Dense Graded Mixtures." Al-Qadisiya Journal for Engineering Sciences, Vol. 5, No. 4 (2012): 424-438.

Alrajhi, A. "Fiber Dosage Effects in Asphalt Binders and Hot Mix Asphalt Mixtures." Master's thesis, Arizona State University, 2012.

American Association of State Highway and Transportation Officials. *AASHTO T209: Theoretical Maximum Specific Gravity (G_{mm}) and Density of Hot Mix Asphalt (HMA)*. Washington, D. C.: American Association of State Highway and Transportation Officials, 2014.

American Association of State Highway and Transportation Officials. *AASHTO T166: Bulk Specific Gravity (G_{mb}) of Compacted Hot Mix Asphalt (HMA) Using Saturated Surface-Dry Specimens*. Washington, D. C.: American Association of State Highway and Transportation Officials, 2014.

American Association of State Highway and Transportation Officials. AASHTO T342: *Determining Dynamic Modulus of Hot Mix Asphalt (HMA)*. Washington, D. C.: American Association of State Highway and Transportation Officials, 2014.

American Association of State Highway and Transportation Officials. *AASHTO TP 79-13: Standard Method of Test for Determining the Dynamic Modulus and Flow Number*

for Asphalt Using the Asphalt Mixture Performance Tester (AMPT). Washington, D.C.: American Association of State Highway and Transportation Officials, 2015.

American Association of State Highway and Transportation Officials. AASHTO TP 63-09: *Determining Rutting Susceptibility of Hot Mix Asphalt (HMA) Using the Asphalt Pavement Analyzer (APA)*. Washington, D. C.: American Association of State Highway and Transportation Officials, 2010.HWT

American Association of State Highway and Transportation Officials. *AASHTO T 322-07 (2011): Standard Method of Test for Determining the Creep Compliance and Strength of Hot Mix Asphalt (HMA) Using the Indirect Tensile Test Device*. Washington, D.C.: American Association of State Highway and Transportation Officials, 2015.

Anderson, T. L., Fracture Mechanics Fundamentals and Applications, 2nd ed., Boca Raton, FL. CRC press. 1995.

Ayyed Mahdi Abtahi 1, S. E. *Hybrid Reinforcement of Asphalt-Concrete Mixtures Using Glass and Polypropylene Fibers.* Journal of Engineered Fibers and Fabrics, Vol. 8, 2013.

AASHTOWare Pavement ME Design (Version 2.1) [Computer software]. Washington DC: AASHTO.

Barros J.A.O., Dalfré G.M. and Dias J.P.S.E. "Numerical simulation of continuous RC slabs strengthened using NSM technique", 2nd International Conference on Concrete Repair, Rehabilitation and Retrofitting (ICCRRR 2008), 24-26 November 2008.

Bayomy, F., S. El-Badawy, and A. Awed. *Implementation of the MEPDG for Flexible Pavements in Idaho*. Boise, ID: Idaho Transportation Department, FHWA-ID-12-193, 2012.

Bayomy, F., R. Nielsen, T. Weaver, S. J Jung, and A. Abu Abdo. *Evaluation of Mix Resistance to Fracture and Fatigue Cracking.* National Institute for Advanced Transportation Technology, University of Idaho: Final Report ITD NIATT Project KLK479-483 Phase B, 2010.

Bayomy, F. and A. A. Abdo. *Performance Evaluation of Idaho HMA Mixes Using Gyratory Stability.* Boise, ID: Idaho Transportation Department, ITD Project No. SPR-0004(022) RP 175, 2007.

Bennert, T. *Advanced Characterization Testing of Fiber Reinforced Hot Mix Asphalt*, Rutgers University, Piscataway, N.J., Sep. 2012.

Bhasin, A., Narayan, A., Little, D., (2009), *Laboratory Investigation of a Novel Method to Accelerate Healing in Asphalt Mixtures Using Thermal Treatment* (Report 476660-00005-1),

Braz D., Lopes R. T. and Motta L. M. G. "Research on fatigue cracking growth parameters in asphaltic mixtures using computed tomography." *Nuclear Instruments and Methods in Physics Research*, B, 213 (2004): 498–502.

Chen, H., Q. Xu, S. Chen, and Z. Zhang. "Evaluation and design of fiber-reinforced asphalt mixtures." *Materials and Design*, Vol. 30, No. 7, 2009: 2595–2603.

Cox, B. N. "Scaling for bridged cracks." Mechanics of Materials, 15, 87-98. 1993.

De S. Bueno, B., da Silva, W. R., de Lima, D. C., & Minete, E. “Engineering Properties of Fiber Reinforced Cold Asphalt Mixes.” *Journal of Environmental Engineering*, Vol. 10, No. 129 (October 2003): 952–955.

Edgar, R. *Ten Year Performance of Asphalt Additive Test Sections: Lava Butte-Fremont Highway Junction Section*, Report FHWA-IR-RD-99-08, Federal Highway Administration, Washington, D.C., 1998.

Federal Highway Administration (2001), *Microdamage Healing in Asphalt and Asphalt Concrete, Volume 1: Microdamage and Microdamage Healing.* (Publication No. FHWA-RD-98-141), Mclean, VA, Research, Development, and Technology Turner-Fairbank Highway Research Center.

Forta Fi, Forta Fi Blends, “Unique Blends for Hot Mix, Warm Mix and Hot/Cold Patch Asphalt.” http://www.forta-fi.com/forta-fi-blends/ Accessed July 28, 2015

Gibson, N., X. Qi, A. Shenoy, G. Al-Khateeb, M.E. Kutay, A. Andriescu, K. Stuart, Y. Youtcheff, and T. Harman, *Performance Testing for Superpave and Structural Validation*, Report FHWA-HRT-11-045, FHWA, McLean, Va., 2012.

Gibson, N., and X. Li, “Cracking Characterization of Asphalt Mixtures with Fiber Reinforcement Using Cyclic Fatigue and Direct Tension Strength Tests,” paper submitted to Transportation Research Board for 94th Annual Meeting, Jan. 2015.

Guo, N. S., & Zhao, Y. H. *Effect of Fiber Content on Viscoelasticity of Asphalt Concrete Institute of Road and Bridge Engineering* , Dalian Maritime University , Dalian, China, PH (576-581), 2007.

Huang, B., Chen, X., and Shu, X. “Effects of electrically conductive additives on laboratory-measured properties of asphalt mixtures.” Journal of Materials in Civil Engineering, Vol. 21, No. 10 (2009): 612-617.

Huang, H. and T.D. White. “Dynamic Properties of Fiber Modified Overlay Mixture,” Transportation Research Record 1545, Transportation Research Board, National Research Council, Washington, D.C., (1996): 98–104.

Huang B., Mohammad L.N., Rasoulian M., “3-D Numerical Simulation of Asphalt Pavement at Louisiana Accelerated Loading Facility (ALF)”, Transportation Research Record, National Research Council, Washington, D.C., 2001.

Idaho Transportation Department. *Standard Specification for Highway Construction*. Boise, Idaho: Idaho Transportation Department, 2012. http://itd.idaho.gov/manuals/Manual%20Production/SpecBook/SpecHome.htm Accessed in July 2015.

Jahromi, S. and khodaii, A. “Carbon Fiber Reinforced Asphalt Concrete”, *Arabian Journal for Science and Engineering*, Vol. 33, 2008: 355-354.

Jiang, Y. and R.S. McDaniel. *Evaluation of Cracking and Seating Technique and Use of Polypropylene Fibers in Bituminous Mixtures on I-74*, Final Report, Indiana Department of Transportation, West Lafayette, 1992.

J. Hua, “Finite Element Modeling and Analysis of Accelerated Pavement Testing Devices and Rutting Phenomenon”, Ph.D. Thesis, Purdue University, 2000

Kaloush, K., Biligiri, K., Zieada, W., Rodezno, M., & Reed, J. "Evaluation of Fiber-Reinforced Asphalt Mixtures Using Advanced Material Characterization Tests." *ASCE Journal of Testing and Evaluation,* Vol. 38, No. 4, 2010

Kim, R. (2009) *Modeling of Asphalt Concrete*, Reston, Virginia: the American Society of Civil Engineers.

Lee, S. J. "Fatigue Cracking Resistance of Fiber-Reinforced Asphalt Concrete." *Textile Research Journal*, Vol. 2, No. 75 (2005): 123–128.

Li, V.C., and Wu, H.C. "Conditions for pseudo strain hardening in fiber reinforced brittle matrix composites." Journal of Applied Mechanics Review, 45(8), 390-398, 1992.

Masad E., Muhunthan B., Shashidhar N., and Harman T., "Internal structure characterization of asphalt concrete using image analysis." *Journal of Computing in Civil Engineering*, Vol. 13, No. 2 (1999): 88–95.

Masad E., Muhunthan B., Shashidhar N., and Harman T., "Quantifying laboratory compaction effects on the internal structure of asphalt concrete." *Transportation Research Record*, 1681 (1999): 179–185

Mahrez, A., Karim. M., and Katman, H. "Prospect of Using Glass Fiber Reinforced Bituminous Mixes." *Journal of the Eastern Asia Society for Transportation Studies (EASTS, Bangkok),* Vol. 5, 2003: 784-807.

McDaniel, R. Fiber Additives in Asphalt Mixtures. Washington, D.C. Transportation Research Board, NCHRP Synthesis 475, 2015.

McDaniel, R.S. and A. Shah. *Asphalt Additives to Control Rutting and Cracking*, Final Report, FHWA/IN/JTRP- 2002/29, Joint Transportation Research Program, West Lafayette, Ind., Jan. 2003.

Mobasher, B. *Mechanics of Fiber and Textile Reinforced Cement Composites*. Boca Raton, FL: Taylor & Francis Group. 2003.

Mobasher, B. Li, C.Y., "Mechanical Properties of Hybrid Cement Based Composites," *ACI Materials J*., Vol. 93, No.3, pp.284-293, 1996.

Mobasher, B., Desai , R. Shah, A. Peled, "Mechanical Properties of Concrete Reinforced with AR-Glass Fibers, Proc. of the 7th Int. Symp. on Brittle Matrix Composites (BMC7), Warsaw, October 13-15, 2003

Mondschein, P., Valentin, J., & Vavřička, J. *Laboratory Performance Assessment of Fiber*. International Conference of Bituminous Mixtures and Pavements, Thessaloniki, Greece, June 2011

Nycon, *Nycon-E,* "High Dispersion Fiberglass." http://nycon.com/wp-content/uploads/2013/08/NyconESheet011712.pdf Accessed July 28, 2015.

Offrel P. and Magnusson R. "Computerized tomography as a tool for crack analysis in asphalt layers." *Journal of Road Materials and Pavement Design*, Vol. 3, No. 1 (2002): 49–72.

Putman, B. J. "Effects of Fiber Finish on the Performance of Asphalt Binders and Mastics." *Hindawi Publishing Corporation Advances in Civil Engineering,* Vol. 2011: Article ID 172634, 11.

Pyeong Jun Yoo, B. S. (2011). "Toughening Characteristics of Plastic Fiber-reinforced Hot-Mix Asphalt Mixtures." KSCE Journal of Civil Engineering, Vol. 16, No. 5 (2011): 751-758.

Read J. M. "New method for measuring crack propagation in asphalts." *International Journal of Pavement Engineering,* Vol.1, No. 1 (2003): 15–34

Sefidmazgi N., Tashman L., Bahia H. "Internal Structure Characterization of Asphalt Mixtures for Rutting Performance Imaging Analysis", *Association of Asphalt Paving Technologists* Vol. 13, No. 1 (2012)

Soranakom, C*. Mutli-Scale Modeling of Fiber and Fabric Reinforced Cement Based Composites*. A Ph.D dissertation Retrieved from Arizona State University, 2008.

Su, K. and Hachiya, Y. *Examination of Fiber – Added Recycled Asphalt Concretes for Surface Course in Airport Pavements*. First International Conference on Transportation Infrastructure. Beijing, China, 2008.

Suzuki, T., and Sakai, M. "A model for crack-face bridging" International Journal of Fracture. 65(4). 329-344, 1994.

Surface-Tech, "ACE Fiber-Engineered Fibers for Asphalt Pavement." http://www.surface-tech.com/ace-fibers-1.html Accessed July 28, 2015.

Taher Baghaee Moghaddam, M. R. "A review on fatigue and rutting performance of asphalt mixes." *Scientific Research and Essays* Vol. 6(4), 2013: 670-682.

Tashman L., Masad E., Peterson B. and Saleh H. "Internal structure analysis of asphalt mixes to improve the simulation of Superpave gyratory compaction to field

conditions.*" Journal of the Association of Asphalt Paving Technologists*, Vol.70, (2001): 605–645.

Tapkin, S. "The effect of polypropylene fibers on asphalt performance." *Building and Environment*, No. 43, (2008): 1065–1071.

TEX-242-F. 2009, "Test Procedure for Hamburg Wheel Tracking Test", ftp://ftp.dot.state.tx.us/pub/txdot-info/cst/TMS/200-F_series/pdfs/bit242.pdf. Accessed August 20, 2015.

Uzarowski, L. (2007). The development of asphalt mix creep parameters and finite element modeling of asphalt rutting.

Van Breukelen, G. *Analysis of covariance (ANCOVA). In N. Salkind (Ed.), Encyclopedia of research design*. (pp. 21-27). Thousand Oaks, CA: SAGE Publications, Inc. doi: http://dx.doi.org/10.4135/9781412961288.n10 Accessed July 2015.

Wen, H. and Kim, R.Y. "Simple Performance Test for Fatigue Cracking and Validation with West rack Mixtures.*" Transportation Research Record*, Vol. 1789 (1), (2002): 66-72.

Wen, H. "Use of Fracture Work Density Obtained from Indirect Tensile Testing for the Mix Design and Development of a Fatigue Model." *International Journal of Pavement Engineering*, Vol. 14, No.6 (2013): 561-568.

White T.D., Haddock J.E., Hand A. J. T. and Fang H., "Contributions of Pavement Structural Layers to Rutting of Hot Mix Asphalt Pavements", Transportation Research Board, National Research Council, National Cooperative Highway Research Program, NCHRP Report 468, Washington, D.C., 2002.

Xu, Q., Chen, H., & Prozzi, J. a. “Performance of fiber reinforced asphalt concrete under environmental temperature and water effects.” *Construction and Building Materials*, Vol. 10, No. 24 (2010): 203–210.

Appendix A
Mix Design and Fiber Characteristics

Project:	Montperlier to Dingle	Date:	July 8, 2014
Asphalt Supplier:	Staker Parson	Class of Mixture:	Superpave "SP5"
Virgin Grade	PG70-28	Asphalt Grade:	PG70-28
Stripping Agents:	Evotherm	Testing By:	NCF/DJ
Aggregate Source:	BL93	Product Number:	50.402

Figure 41 Selected PG grade for the ITD Superpave SP5

Sieve Size	A Pile 20%	B Pile 14%	C Pile 14.5%	Sand 4.0%	Rap 47.0%	BD-Pile 0.5%	JMF Blended Gradation	JMF Specification	Blank Neat Gradation	Average Neat Gradation
1" / 25mm	100	100	100	100	100	100	100	100	100	100
3/4" / 19mm	100	100	100	100	98	100	99	94-100	99	99
1/2" / 12.5mm	45	100	100	100	87	100	83	78-88	83	83
3/8" / 9.5mm	8	80	100	100	73	100	66	61-71	66	67
No. 4 / 4.75mm	2	7	88	92	44	100	39	34-44	39	40
No. 8 / 2.36mm	2	3	59	73	29	100	26	23-30	26	26
No.16 / 1.18mm	2	3	42	64	21	100	20	16-24	20	21
No. 30 / 600um	2	2	30	55	17	100	15	11-19	15	17
No. 50 / 300um	2	2	20	24	14	100	11	8-14	11	12
No. 100 / 150um	1	2	13	2	10	100	7	4-10	8	8
No. 200 / 75um	1.1	1.4	8.8	1.2	5.7	100	* 4.5	3.0-6.0	4.6	4.7
* Use of bag house will maintain the -#200 material to 4.5% as designed due to breakdown.										

Figure 42 Aggregate Gradation Data

Laboratory Gyratory Values	Min	Target	Max	ITD Spec.
Total Asphalt by Weight of Mix % (Pb)	4.5	4.8	5.10	
Aspalt by Weight of Mix Hot Plant	1.67	1.97	2.27	
Rap Asphalt by Weight of Mix 58.9%	2.83	2.83	2.83	
Air Voids % (Va)	5.0	4.0	3.0	4.0
Voids in Mineral Aggregate (VMA)	13.8	13.6	13.4	13.0
Voids Filled with Asphalt (VFA)		70.4%		65% - 75%
Dust Ratio(PCS 39% passing #4 / 0.8%-1.6%)	1.1%	1.1%	1.0%	0.8-1.6
Bulk Specific Gravity (Gmb)	2.326	2.338	2.35	
Unit Weight lb./cu.ft.	144.8	145.5	146.3	
Theo Max Spec Gravity (Gmm)	2.45	2.436	2.423	
Theo Max Spec Gravity lb./cu.ft.	152.5	151.6	150.8	
% Gmm @ Nini(8 gyrations)		86.3%		89%max
% Gmm @ Ndes(100 gyrations)		95.9%		96%max
% Gmm @ Nmax(160 gyrations)		97.6%		98%max
Effective Specific Gravity of Blend (Gse)		2.618		
Specific Gravity of Aggregate (Gsb provided by ITD)		2.576		
Fine Aggregate Angularity		48%		45.0%
NCAT Aspalt Correction Factor		-0.21		
Sand Equivalency (SE)		48		45% Min
Flat and Elongation		3%		10% Max
Percent Fracture 1 Face		97%		95%
Percent Fracture 2 Face		96%		90%
Laboratory Mixing Temperature(deg in F)		300 deg		
Laboratory Compaction Temperature(deg in F)		275 deg		
Plant Mixing Temperature(deg in F)	295 deg		305 deg	
Field Compaction Temperature(deg in F)	268 deg		280 deg	
Superpave Design Sample Wt.		4600 g		

Figure 43 Job Mix Formula (JMF)

National Center for Asphalt Technology
NCAT
at AUBURN UNIVERSITY

Project: Hk Contractors
Date: 5/19/2014
Sample ID: Dingle RAP

Superpave Asphalt Binder Grading Summary
AASHTO M320

Original Binder				
Test, Method			Test Results	Specification
Rotational Viscosity @ 135°C, AASHTO T 316, PaS			0.45	≤ 3 PaS
Dynamic Shear Rheometer AASHTO T 315				
Test Temperature, °C	G*, kPa	Phase Angle δ, °	G* / sinδ, kPa	
64	1.56	85.5	1.56	≥ 1.00 kPa
70	0.76	87.0	0.76	
Rolling Thin Film (RTFO) Aged Binder, AASHTO T 240				
Mass Change, %			na	≤ 1.00%
Dynamic Shear Rheometer AASHTO T 315				
Test Temperature, °C	G*, kPa	Phase Angle δ, °	G* / sinδ, kPa	
64	3.21	83.3	3.24	≥ 2.20 kPa
70	1.39	85.4	1.39	
Dynamic Shear Rheometer AASHTO T 315*				
Test Temperature, °C	G*, kPa	Phase Angle δ, °	G* sinδ, kPa	
16	8833	43.3	6059	≤ 5,000 kPa
19	5634	46.69	4099	
Bending Beam Rheometer (BBR) AASHTO T313*				
Test Temperature, °C				
-12	Stiffness, Mpa		108	≤ 300 Mpa
	m-value		0.351	≥ 0.300
-18	Stiffness, Mpa		282	
	m-value		0.309	
True Grade	66.7 -28.4			
PG Grade	64 - 28			

* intermediate and low temperature tests performed using RTFO aged RAP binder

1. DSR Original: T_{max}
   Temperature at which G*/sinδ = 1.00 kPa — 67.7
2. DSR RTFO: T_{max}
   Temperature at which G*/sinδ = 2.20 kPa — 68.7
3. DSR PAV: T_{int}
   Temperature at which G*sinδ = 5,000 kPa — 17.5
4. BBR PAV: T_{min}
   Tempearautre at which S(t) = 300 Mpa — -28.4
   Temperature at which m = 0.300 — -29.3

Figure 44 Superpave Asphalt Binder Grading Summary

Appendix B
Laboratory Performance Test Data

Table 16 Averaged Dynamic Modulus Test Results of fiber Mixes

Temp. (°F)	Frequency (Hz)	CM_No Fibers			FM1_0.05%			FM2_0.015%			FM3_0.16%		
		Modulus (ksi)	SD	COV (%)	Modulus (ksi)	SD	COV (%)	Modulus (ksi)	SD	COV (%)	Modulus (ksi)	SD	COV (%)
40	25	2268	93.58	4.13	2241	122.83	5.48	2305	83.38	3.62	2342	209.8	8.96
40	10	2059	85.04	4.13	2052	105.12	5.12	2099	74.18	3.53	2141	197.3	9.22
40	5	1896	78.51	4.14	1905	100.08	5.25	1950	78.48	4.03	1948	165.7	8.50
40	1	1505	59.57	3.96	1551	85.23	5.50	1584	84.24	5.32	1605	155.9	9.72
40	0.5	1345	49.71	3.70	1399	80.97	5.79	1428	87.16	6.10	1403	127.0	9.05
40	0.1	979	37.15	3.80	1058	60.63	5.73	1073	77.29	7.20	1024	118.8	11.61
70	25	984	27.24	2.77	1057	51.43	4.87	1061	79.62	7.51	1084	110.3	10.18
70	10	795	16.56	2.08	874	43.67	5.00	875	67.68	7.74	881	93.1	10.56
70	5	665	14.74	2.22	742	37.15	5.00	744	64.69	8.69	746	80.5	10.78
70	1	402	12.38	3.08	468	21.89	4.67	470	55.03	11.71	465	62.4	13.41
70	0.5	320	11.75	3.67	379	17.95	4.74	379	52.33	13.79	373	57.3	15.38
70	0.1	168	7.18	4.28	204	10.41	5.12	200	41.73	20.87	201	43.5	21.66
100	25	266	8.72	3.28	316	11.68	3.69	311	43.64	14.03	307	46.0	14.99
100	10	190	7.01	3.70	226	6.53	2.89	220	37.85	17.19	218	37.9	17.37
100	5	138	5.65	4.09	165	4.61	2.79	160	32.59	20.37	158	31.0	19.60
100	1	60	2.96	4.93	73	2.60	3.57	70	17.81	25.38	71	18.4	25.79
100	0.5	41	2.23	5.37	51	2.00	3.92	49	13.06	26.72	50	13.8	27.36
100	0.1	20	5.64	27.80	22	0.66	2.94	22	5.37	24.69	23	6.0	26.00
130	25	77	8.58	11.21	98	8.94	9.10	93	8.02	8.67	88	13.0	14.75
130	10	49	5.33	10.91	59	13.91	23.48	56	7.42	13.13	51	10.1	19.64
130	5	37	7.25	19.51	43	5.06	11.88	37	5.08	13.58	34	7.0	20.38
130	1	16	3.71	23.91	18	1.76	9.85	16	1.37	8.76	16	6.0	38.15
130	0.5	11	2.68	24.48	13	1.16	8.97	11	0.69	6.06	13	2.2	17.55
130	0.1	6	1.31	22.57	7	0.34	4.58	6	0.27	4.22	7	1.0	13.26

Table 17 Multiple Comparisons of Fiber Modified Mixes for Dynamic Modulus at 70 F and 1 Hz test by ANCOVA Analysis (p-value)

Mixes		(p-value) of E*
CM	FM1	0.002*
	FM3	0.053
	FM2	0.095
FM1	CM	0.002*
	FM3	0.959
	FM2	0.923
FM2	CM	0.053
	FM1	0.959
	FM2	0.909
FM3	CM	0.095
	FM1	0.923
	FM3	0.909

Table 18 Flow Number Test Results of Fiber Mixes

Mixes		Flow Numbers	Avg. Flow Numbers	Standard Deviation	COV (%)
CM	1	1534	1891	966.86	51.12
	2	1154			
	3	2986			
FM1	1	2823	2079	744.00	35.78
	2	2080			
	3	1335			
FM2	1	2442	2415	573.98	23.77
	2	2975			
	3	1828			
FM3	1	2050	2453	361.58	14.74
	2	2749			
	3	2560			

Table 19 Multiple Comparisons of Fiber Modified Mixes for Flow Number test by ANCOVA Analysis (p-value)

Mixes		(p-value) of FN test
CM	FM1	0.803
	FM3	0.465
	FM2	0.399
FM1	CM	0.803
	FM3	0.570
	FM2	0.478
FM2	CM	0.465
	FM1	0.570
	FM2	0.927
FM3	CM	0.399
	FM1	0.478
	FM3	0.927

Table 20 Multiple Comparisons of Fiber Modified Mixes for HWT Final Rut Depth by ANOVA Analysis (p-value)

Mixes		(p-value) Of Rut Depth
CM	FM1	0.366
	FM3	0.064
	FM2	0.140
FM1	CM	0.366
	FM3	0.202
	FM2	0.459
FM2	CM	0.140
	FM1	0.459
	FM2	0.519
FM3	CM	0.064
	FM1	0.202
	FM3	0.519

Table 21 Fracture Work Density for IDT Test at 68°F

Mixes		Fracture Work	Average	Standard	COV
CM	1	17.42	16.39	0.97	5.93
	2	16.26			
	3	15.49			
FM1	1	16.02	16.38	1.00	6.13
	2	15.60			
	3	17.51			
SM2	1	20.29	18.53	1.57	8.49
	2	18.05			
	3	17.26			
FM3	1	14.30	15.83	2.48	15.63
	2	18.69			
	3	14.51			

Table 22 Vertical Failure Deformation for IDT Test at 68°F

Mixes		Vertical Failure Deformation (inch)	Average (inch)	Standard Deviation (inch)	COV (%)
CM	1	0.0739	0.0639	0.0088	13.75
	2	0.0596			
	3	0.0580			
FM1	1	0.0643	0.0651	0.0011	1.69
	2	0.0648			
	3	0.0663			
FM2	1	0.0700	0.0681	0.0037	5.43
	2	0.0704			
	3	0.0638			
FM3	1	0.0576	0.0663	0.0075	11.31
	2	0.0697			
	3	0.0714			

Table 23 IDT Strength for Mixes at 68°F

Mixes		IDT Strength (psi)	Average (psi)	Standard Deviation (psi)	COV (%)
CM	1	339	273	58.79	21.53
	2	255			
	3	225			
FM1	1	304	284	18.44	6.49
	2	279			
	3	268			
FM2	1	297	295	11.70	3.96
	2	306			
	3	283			
FM3	1	241	274	61.89	22.59
	2	345			
	3	235			

Table 24 Multiple Comparisons of Fiber Modified Mixes for Fracture Work Density at Intermediate Temperature by ANCOVA Analysis (p-value)

Mixes		**(p-value) of Fracture Work Density**
CM	**FM1**	0.759
	FM3	0.748
	FM2	0.129
FM1	**CM**	0.759
	FM3	0.533
	FM2	0.219
FM2	**CM**	0.748
	FM1	0.533
	FM2	0.079
FM3	**CM**	0.129
	FM1	0.219
	FM3	0.079

Table 25 Multiple Comparisons of Fiber Modified Mixes for Vertical Failure Deformation at Intermediate Temperature by ANCOVA Analysis (p-value)

Mixes		(p-value) of Vertical Failure Deformation
CM	FM1	0.567
	FM3	0.559
	FM2	0.397
FM1	CM	0.567
	FM3	0.996
	FM2	0.792
FM2	CM	0.559
	FM1	0.996
	FM2	0.783
FM3	CM	0.397
	FM1	0.792
	FM3	0.783

Table 26 Multiple Comparisons of Fiber Modified Mixes for IDT Strength at Intermediate Temperature by ANCOVA Analysis (p-value)

Mixes		(p-value) of Failure Deformation
CM	FM1	0.396
	FM3	0.847
	FM2	0.452
FM1	CM	0.396
	FM3	0.494
	FM2	0.896
FM2	CM	0.452
	FM1	0.896
	FM2	0.571
FM3	CM	0.847
	FM1	0.494
	FM3	0.571

Table 27 J_c Test Results of Fiber Mixes

Mixes		J_c (psi)	Average J_c (psi)	Standard Deviation (psi)	COV (%)
CM	1	2.428	2.041	0.487	23.84
	2	1.355			
	3	2.341			
FM1	1	3.534	2.058	1.098	53.34
	2	1.737			
	3	0.903			
FM2	1	2.970	2.120	0.674	31.78
	2	2.793			
	3	1.446			
FM3	1	2.311	2.463	0.804	32.63
	2	3.514			
	3	1.563			

Table 28 Multiple Comparisons of Fiber Modified Mixes J_c at Intermediate Temperature by ANCOVA Analysis (p-value)

Mixes		(p-value) of J_c
CM	**FM1**	0.985
	FM3	0.574
	FM2	0.560
FM1	**CM**	0.985
	FM3	0.725
	FM2	0.696
FM3	**CM**	0.574
	FM1	0.725
	FM2	0.940
FM2	**CM**	0.560
	FM1	0.696
	FM3	0.940

Table 29 Fracture Work Density for IDT Test at 14°F

Mixes		Fracture Work Density (psi)	Average (psi)	Standard Deviation (psi)	COV (%)
CM	1	12.43	11.81	2.00	16.90
	2	9.58			
	3	13.42			
FM1	1	14.77	11.62	2.74	23.56
	2	10.32			
	3	9.79			
FM2	1	9.31	11.19	3.85	34.46
	2	8.63			
	3	15.62			
FM3	1	12.33	12.46	0.76	6.10
	2	13.28			
	3	11.78			

Table 30 Multiple Comparisons of Fiber Modified Mixes for Fracture Work Density at Low Temperature by ANCOVA Analysis (p-value)

Mixes		(p-value) of Vertical Failure Deformation
CM	**FM1**	0.646
	FM3	0.223
	FM2	0.734
FM1	**CM**	0.646
	FM3	0.113
	FM2	0.905
FM3	**CM**	0.223
	FM1	0.113
	FM2	0.134
FM2	**CM**	0.734
	FM1	0.905
	FM3	0.134

Table 31 Multiple Comparisons of Fiber Modified Mixes for Creep Compliance at Low, Intermediate and High Time-Temperature Level by ANCOVA Analysis (p-value)

Mixes		(p-value) of Creep Compliance at Low Level	(p-value) of Creep Compliance at Intermediate Level	(p-value) of Creep Compliance at High Level
CM	**FM1**	0.409	0.101	0.865
	FM3	0.773	0.172	0.255
	FM2	0.419	0.828	0.774
FM1	**CM**	0.409	0.101	0.865
	FM3	0.577	0.735	0.306
	FM2	0.970	0.138	0.653
Fm3	**CM**	0.773	0.172	0.255
	FM1	0.577	0.735	0.306
	FM2	0.612	0.232	0.168
Fm2	**CM**	0.419	0.828	0.774
	FM1	0.970	0.138	0.653
	FM3	0.612	0.232	0.168

Table 32 SCB Fatigue test G1

Type of Mixture	Number of cycles to failure		
	Test Type 1: Without rest periods	Test Type 2: With rest periods but without heating	Test Type 3: With rest periods and heating
Control	9210	11637	15053
0.2% Fiber #1	9909	13750	17516
0.4% Fiber #1	11464	13031	18683

Table 33 SCB Fatigue test G2

Type of Mixture	Number of cycles to failure		
	Test Type 1: Without rest periods	Test Type 2: With rest periods but without heating	Test Type 3: With rest periods and heating
Control	11289	15670	17720
0.2% Fiber #1	14013	25490	28304
0.4% Fiber #1	15812	18526	20506

Table 34 Example of fiber areas' coordinates in Slice #1_LM1_0.2%

Area #	Area	Mean	StdDev	Min	Max	XM	YM	Slice
1	2	219.5	2.121	218	221	3287.5	2458.997	1
2	1	188	0	188	188	3304.5	2458.5	1
3	1	228	0	228	228	3361.5	2458.5	1
4	1	222	0	222	222	3287.5	2456.5	1
5	1	206	0	206	206	3288.5	2449.5	1
6	1	220	0	220	220	3293.5	2425.5	1
7	1	235	0	235	235	3004.5	2416.5	1
8	2	230	1.414	229	231	3484.998	2373.5	1
9	2	244	4.243	241	247	3360.5	2124.994	1
10	2	227	1.414	226	228	3457.002	2121.5	1
11	1	232	0	232	232	3468.5	2120.5	1
12	7	229.286	3.498	226	235	3470.079	2115.086	1
13	1	235	0	235	235	2513.5	2009.5	1
14	3	216.667	6.506	210	223	2483.521	2006.834	1
15	1	238	0	238	238	2808.5	1955.5	1
16	2	224.5	0.707	224	225	2842.999	1939.5	1
17	1	220	0	220	220	2845.5	1939.5	1
18	1	219	0	219	219	2786.5	1903.5	1
19	1	203	0	203	203	2758.5	1897.5	1
20	1	247	0	247	247	2731.5	1877.5	1
21	1	245	0	245	245	2731.5	1874.5	1
22	1	232	0	232	232	2732.5	1872.5	1
23	1	231	0	231	231	2249.5	1870.5	1
24	1	231	0	231	231	2251.5	1870.5	1
25	2	227	1.414	226	228	2249.999	1861.5	1
26	1	235	0	235	235	2832.5	1801.5	1
27	1	215	0	215	215	2811.5	1796.5	1
28	2	234	2.828	232	236	2833.996	1796.004	1
29	1	214	0	214	214	2805.5	1791.5	1
30	1	226	0	226	226	2782.5	1786.5	1
31	2	240	0	240	240	2777	1785.5	1
32	1	244	0	244	244	3153.5	1785.5	1
33	2	235.5	0.707	235	236	2872.5	1780.999	1
34	1	230	0	230	230	2867.5	1780.5	1
35	1	233	0	233	233	2858.5	1758.5	1
36	1	234	0	234	234	2862.5	1758.5	1
37	1	236	0	236	236	2862.5	1753.5	1
38	6	216.667	9.048	200	224	2859.994	1743.012	1
39	1	248	0	248	248	2439.5	1738.5	1

40	1	232	0	232	232	2852.5	1735.5	1
41	1	227	0	227	227	2462.5	1734.5	1
42	1	244	0	244	244	1460.5	1698.5	1
43	1	207	0	207	207	2842.5	1685.5	1
44	1	224	0	224	224	2470.5	1664.5	1
45	2	217	1.414	216	218	2473.002	1662.998	1
46	1	222	0	222	222	2480.5	1663.5	1
47	2	219	2.828	217	221	2473.005	1660.5	1
48	1	229	0	229	229	2499.5	1659.5	1
49	1	223	0	223	223	2476.5	1658.5	1
50	1	239	0	239	239	2518.5	1658.5	1
51	1	230	0	230	230	2860.5	1657.5	1
52	2	221.5	3.536	219	224	2462.994	1656.5	1
53	1	235	0	235	235	2516.5	1656.5	1
54	2	214	0	214	214	2470.999	1655.5	1
55	2	226.5	2.121	225	228	2462.003	1654.5	1
56	1	217	0	217	217	2468.5	1654.5	1
57	1	218	0	218	218	2496.5	1653.5	1
58	3	217.333	14.154	201	226	2461.155	1652.192	1
59	2	223	2.828	221	225	2473.004	1652.5	1
60	1	229	0	229	229	2501.5	1652.5	1
61	1	229	0	229	229	2457.5	1651.5	1
62	1	218	0	218	218	2472.5	1650.5	1
63	1	233	0	233	233	2517.5	1649.5	1
64	2	206.5	6.364	202	211	2462.989	1648.5	1
65	6	218.667	5.61	213	227	2467.324	1646.011	1
66	1	234	0	234	234	2519.5	1648.5	1
67	1	231	0	231	231	2459.5	1646.5	1
68	1	224	0	224	224	2461.5	1646.5	1
69	1	218	0	218	218	2455.5	1643.5	1
70	1	227	0	227	227	2464.5	1642.5	1
71	1	220	0	220	220	2464.5	1640.5	1
72	3	227.667	2.887	226	231	2462.831	1638.508	1
73	1	223	0	223	223	2516.5	1639.5	1
74	1	246	0	246	246	3230.5	1629.5	1
75	1	207	0	207	207	2900.5	1611.5	1
76	1	238	0	238	238	2842.5	1610.5	1
77	1	235	0	235	235	2846.5	1608.5	1
78	1	230	0	230	230	2848.5	1605.5	1
79	2	242	5.657	238	246	2771.008	1599.5	1
80	2	237.5	0.707	237	238	1826.001	1596.5	1

81	1	233	0	233	233	1828.5	1590.5	1
82	1	247	0	247	247	2261.5	1584.5	1
83	1	233	0	233	233	2683.5	1578.5	1
84	3	236.667	9.609	228	247	2705.848	1577.49	1
85	3	238.333	5.774	235	245	2784.829	1576.5	1
86	1	231	0	231	231	2787.5	1577.5	1
87	2	234.5	3.536	232	237	2568.995	1566.5	1
88	3	239.667	7.506	232	247	2241.521	1556.5	1
89	1	247	0	247	247	2266.5	1556.5	1
90	1	234	0	234	234	2269.5	1556.5	1
91	3	238.667	5.859	232	243	2237.503	1555.163	1
92	1	235	0	235	235	2343.5	1554.5	1
93	1	229	0	229	229	3348.5	1550.5	1
94	1	232	0	232	232	2826.5	1483.5	1
95	3	246.667	1.528	245	248	2761.166	1481.169	1
96	1	233	0	233	233	2857.5	1481.5	1
97	1	232	0	232	232	2860.5	1481.5	1
98	2	211	4.243	208	214	2846.993	1478.993	1
99	5	242.8	9.471	226	248	2758.722	1475.535	1
100	1	234	0	234	234	2862.5	1475.5	1
101	1	248	0	248	248	2837.5	1448.5	1
102	1	229	0	229	229	2779.5	1442.5	1
103	1	231	0	231	231	2781.5	1442.5	1
104	1	239	0	239	239	2783.5	1439.5	1
105	1	248	0	248	248	2880.5	1438.5	1
106	1	243	0	243	243	2882.5	1438.5	1
107	1	229	0	229	229	2779.5	1437.5	1
108	1	236	0	236	236	2781.5	1437.5	1
109	3	246.667	1.528	245	248	2835.501	1436.835	1
110	2	242	4.243	239	245	2853.007	1437.5	1
111	2	228.5	20.506	214	243	2883.968	1435.5	1
112	1	231	0	231	231	2781.5	1434.5	1
113	1	240	0	240	240	2834.5	1434.5	1
114	1	244	0	244	244	2880.5	1433.5	1
115	1	248	0	248	248	2830.5	1432.5	1
116	1	234	0	234	234	2881.5	1431.5	1
117	1	207	0	207	207	2771.5	1430.5	1
118	3	226	4.583	221	230	2769.165	1429.161	1
119	1	230	0	230	230	2648.5	1428.5	1
120	2	204	11.314	196	212	2772.98	1428.5	1
121	1	217	0	217	217	2780.5	1428.5	1

122	1	247	0	247	247	2646.5	1427.5	1
123	1	228	0	228	228	2782.5	1427.5	1
124	2	247.5	0.707	247	248	2779.001	1419.999	1
125	1	248	0	248	248	2821.5	1415.5	1
126	1	246	0	246	246	2770.5	1412.5	1
127	4	246.5	3	242	248	3181.997	1410.991	1
128	12	241.083	2.275	236	244	1741.332	1404.663	1
129	1	245	0	245	245	3179.5	1406.5	1
130	1	228	0	228	228	2774.5	1405.5	1
131	1	245	0	245	245	3177.5	1405.5	1
132	1	234	0	234	234	3162.5	1404.5	1
133	3	241.333	2.887	238	243	3178.5	1403.836	1
134	1	248	0	248	248	3167.5	1402.5	1
135	1	244	0	244	244	1743.5	1400.5	1
136	2	219.5	9.192	213	226	2771.985	1399.985	1
137	2	237	0	237	237	2883.5	1397.999	1
138	1	226	0	226	226	2840.5	1397.5	1
139	1	232	0	232	232	2772.5	1396.5	1
140	1	236	0	236	236	2798.5	1396.5	1
141	2	231.5	0.707	231	232	2789.001	1394.999	1
142	1	235	0	235	235	2791.5	1395.5	1
143	5	240.6	2.51	237	243	2768.901	1393.099	1
144	2	235.5	2.121	234	237	2807.003	1394.003	1
145	2	240	1.414	239	241	2795.002	1393.5	1
146	2	238	0	238	238	2799	1393.5	1
147	1	242	0	242	242	2801.5	1393.5	1
148	3	246.333	0.577	246	247	2846.833	1392.833	1
149	1	239	0	239	239	2792.5	1392.5	1
150	1	234	0	234	234	2762.5	1391.5	1
151	1	235	0	235	235	2778.5	1391.5	1
152	3	233.333	2.887	230	235	2781.164	1390.829	1
153	3	233	1.732	231	234	2761.835	1388.5	1
154	1	233	0	233	233	2763.5	1389.5	1
155	1	236	0	236	236	2765.5	1389.5	1
156	1	231	0	231	231	2766.5	1387.5	1
157	1	222	0	222	222	2837.5	1387.5	1
158	3	240	3.464	236	242	2341.508	1384.172	1
159	2	226.5	12.021	218	235	2762.018	1382.982	1
160	2	236.5	7.778	231	242	2346.988	1376.988	1
161	3	230.333	3.055	227	233	2835.163	1374.171	1
162	2	235	4.243	232	238	2836.993	1368.5	1

163	1	211	0	211	211	2820.5	1364.5	1
164	1	224	0	224	224	2822.5	1364.5	1
165	1	230	0	230	230	2825.5	1361.5	1
166	1	209	0	209	209	2805.5	1356.5	1
167	2	244	1.414	243	245	2703.002	1354.998	1
168	1	210	0	210	210	2809.5	1354.5	1
169	1	228	0	228	228	3049.5	1353.5	1
170	2	225	4.243	222	228	2185.007	1349.5	1
171	1	236	0	236	236	2845.5	1345.5	1
172	1	246	0	246	246	2847.5	1339.5	1
173	2	217	11.314	209	225	2759.5	1311.982	1
174	1	234	0	234	234	2762.5	1311.5	1
175	1	241	0	241	241	2774.5	1309.5	1
176	1	238	0	238	238	2791.5	1309.5	1
177	1	240	0	240	240	2793.5	1309.5	1
178	1	247	0	247	247	3153.5	1308.5	1
179	1	244	0	244	244	2814.5	1306.5	1
180	1	241	0	241	241	3146.5	1306.5	1
181	2	241.5	6.364	237	246	3151.009	1306.5	1
182	1	233	0	233	233	2760.5	1304.5	1
183	3	237	3.464	233	239	3139.827	1298.164	1
184	1	207	0	207	207	3144.5	1297.5	1
185	1	236	0	236	236	3137.5	1296.5	1
186	1	196	0	196	196	2246.5	1295.5	1
187	3	190.667	6.658	183	195	2764.82	1294.498	1
188	3	224	4.359	219	227	3147.174	1292.489	1
189	2	208	14.142	198	218	2746.976	1291.976	1
190	2	187.5	6.364	183	192	2245.5	1291.011	1
191	2	227.5	0.707	227	228	2761.001	1291.5	1
192	1	232	0	232	232	3138.5	1291.5	1
193	3	215.667	4.619	213	221	2750.488	1290.159	1
194	1	202	0	202	202	2758.5	1290.5	1
195	2	228	1.414	227	229	3150.998	1290.002	1
196	1	227	0	227	227	3153.5	1290.5	1
197	4	220.5	6.856	211	226	3138.021	1288.021	1
198	1	186	0	186	186	2246.5	1288.5	1
199	3	225	2	223	227	3145.502	1285.502	1
200	1	235	0	235	235	3152.5	1286.5	1
201	2	213.5	9.192	207	220	3152.015	1284.5	1
202	1	212	0	212	212	2217.5	1283.5	1
203	1	208	0	208	208	2219.5	1283.5	1

204	1	217	0	217	217	3141.5	1283.5	1
205	1	224	0	224	224	3147.5	1283.5	1
206	1	209	0	209	209	2214.5	1282.5	1
207	2	200.5	9.192	194	207	2245.5	1281.983	1
208	1	248	0	248	248	2741.5	1281.5	1
209	1	248	0	248	248	2744.5	1281.5	1
210	1	234	0	234	234	2765.5	1281.5	1
211	1	237	0	237	237	2983.5	1281.5	1
212	5	237.6	5.983	233	248	2987.71	1279.892	1
213	3	223	5	218	228	3141.494	1281.173	1
214	1	199	0	199	199	2212.5	1280.5	1
215	1	248	0	248	248	2665.5	1276.5	1
216	2	240	11.314	232	248	2675.5	1274.983	1
217	1	248	0	248	248	2977.5	1275.5	1
218	1	245	0	245	245	2997.5	1275.5	1
219	1	248	0	248	248	2730.5	1273.5	1
220	3	185	4	181	189	2219.493	1271.5	1
221	1	245	0	245	245	2526.5	1271.5	1
222	2	242	2.828	240	244	2730.004	1271.5	1
223	1	248	0	248	248	2528.5	1268.5	1
224	1	186	0	186	186	2245.5	1265.5	1
225	1	233	0	233	233	2981.5	1264.5	1
226	2	240.5	10.607	233	248	2532.5	1260.984	1
227	1	231	0	231	231	2753.5	1261.5	1
228	1	237	0	237	237	2982.5	1261.5	1
229	2	221.5	17.678	209	234	2757.5	1260.028	1
230	1	234	0	234	234	2761.5	1256.5	1
231	1	243	0	243	243	2947.5	1256.5	1
232	2	214	4.243	211	217	3146.993	1256.5	1
233	1	224	0	224	224	3087.5	1253.5	1
234	2	241	0	241	241	2860	1252.5	1
235	3	229.333	1.528	228	231	3092.836	1251.832	1
236	1	234	0	234	234	2725.5	1251.5	1
237	1	227	0	227	227	2989.5	1249.5	1
238	1	248	0	248	248	2534.5	1248.5	1
239	2	238.5	12.021	230	247	2874.982	1248.018	1
240	2	220	5.657	216	224	3095.5	1248.009	1
241	1	232	0	232	232	2995.5	1247.5	1
242	3	235.333	0.577	235	236	2992.834	1243.167	1
243	3	240.667	3.055	238	244	2864.83	1238.493	1
244	1	213	0	213	213	3073.5	1239.5	1

245	2	243.5	2.121	242	245	2741.5	1237.997	1
246	1	248	0	248	248	2747.5	1238.5	1
247	1	237	0	237	237	2942.5	1238.5	1
248	1	242	0	242	242	2176.5	1237.5	1
249	1	231	0	231	231	2987.5	1237.5	1
250	2	227.5	6.364	223	232	2985.5	1235.99	1
251	3	224	5.292	220	230	3074.487	1235.83	1
252	1	228	0	228	228	2988.5	1235.5	1
253	1	226	0	226	226	2944.5	1233.5	1
254	3	227.333	2.887	224	229	2949.493	1233.5	1
255	1	231	0	231	231	2952.5	1233.5	1
256	2	228	4.243	225	231	2959.007	1232.993	1
257	1	227	0	227	227	2979.5	1233.5	1
258	1	245	0	245	245	2817.5	1232.5	1
259	1	244	0	244	244	2819.5	1232.5	1
260	2	235	1.414	234	236	2939.998	1232.002	1
261	6	231.333	3.141	227	236	2982.68	1232.168	1
262	2	215.5	16.263	204	227	2955.026	1231.026	1
263	1	233	0	233	233	2178.5	1230.5	1
264	1	238	0	238	238	2824.5	1230.5	1
265	1	231	0	231	231	2961.5	1230.5	1
266	3	240	1	239	241	2939.167	1228.501	1
267	1	215	0	215	215	2965.5	1229.5	1
268	4	242	2.449	239	244	2831.999	1227.248	1
269	3	199	13	191	214	2959.178	1226.858	1
270	1	232	0	232	232	2971.5	1227.5	1
271	2	226	0	226	226	2975	1226.5	1
272	2	229	4.243	226	232	2979.993	1225.993	1
273	1	234	0	234	234	2975.5	1223.5	1
274	1	216	0	216	216	2963.5	1222.5	1
275	1	226	0	226	226	2966.5	1222.5	1
276	1	245	0	245	245	3177.5	1221.5	1
277	1	239	0	239	239	3174.5	1220.5	1
278	1	226	0	226	226	2807.5	1216.5	1
279	1	227	0	227	227	2817.5	1212.5	1
280	1	245	0	245	245	2820.5	1211.5	1
281	1	224	0	224	224	3067.5	1211.5	1
282	2	226.5	6.364	222	231	3167.01	1210.01	1
283	3	221	3.606	218	225	3153.171	1207.84	1
284	1	208	0	208	208	3059.5	1206.5	1
285	2	194	9.899	187	201	3156.017	1205.017	1

286	1	222	0	222	222	3057.5	1203.5	1
287	1	194	0	194	194	3156.5	1202.5	1
288	1	237	0	237	237	3167.5	1201.5	1
289	1	224	0	224	224	3127.5	1194.5	1
290	1	228	0	228	228	3122.5	1188.5	1
291	1	224	0	224	224	3126.5	1186.5	1
292	1	240	0	240	240	2912.5	1179.5	1
293	1	227	0	227	227	2981.5	1177.5	1
294	1	233	0	233	233	2192.5	1174.5	1
295	5	232.6	7.733	227	246	2950.076	1172.726	1
296	1	229	0	229	229	2892.5	1172.5	1
297	2	213.5	17.678	201	226	3132.5	1171.971	1
298	1	228	0	228	228	3105.5	1166.5	1
299	2	229.5	0.707	229	230	3125.001	1166.5	1
300	1	240	0	240	240	3086.5	1165.5	1
301	1	226	0	226	226	2961.5	1164.5	1
302	1	239	0	239	239	3084.5	1164.5	1
303	4	232	5.292	227	239	2912.498	1159.996	1
304	2	221.5	6.364	217	226	3095.5	1156.989	1
305	2	217.5	4.95	214	221	3792.992	1157.5	1
306	1	226	0	226	226	3788.5	1156.5	1
307	1	234	0	234	234	3110.5	1155.5	1
308	1	231	0	231	231	3123.5	1155.5	1
309	1	222	0	222	222	3094.5	1152.5	1
310	3	233.667	7.506	226	241	3076.49	1114.178	1
311	1	233	0	233	233	2657.5	1105.5	1
312	1	236	0	236	236	2482.5	1050.5	1
313	4	237.75	7.089	229	244	2954.26	1013.005	1
314	2	235	0	235	235	2992	995.5	1
315	4	208	3.83	203	211	3019.739	991.495	1
316	1	218	0	218	218	3024.5	992.5	1
317	1	223	0	223	223	3026.5	992.5	1
318	1	209	0	209	209	3001.5	991.5	1
319	3	224.333	3.215	222	228	3015.161	990.502	1
320	1	217	0	217	217	3028.5	991.5	1
321	1	216	0	216	216	3005.5	987.5	1
322	1	226	0	226	226	3010.5	987.5	1
323	1	228	0	228	228	3031.5	985.5	1
324	2	246.5	2.121	245	248	2312.003	915.5	1
325	2	239	1.414	238	240	2314.998	915.5	1
326	1	247	0	247	247	2951.5	913.5	1

327	4	234.75	5.315	229	241	2317.985	911.003	1
328	1	244	0	244	244	2323.5	911.5	1
329	1	239	0	239	239	2314.5	904.5	1
330	1	244	0	244	244	2297.5	903.5	1
331	1	230	0	230	230	2305.5	902.5	1
332	1	232	0	232	232	2313.5	901.5	1
333	1	235	0	235	235	2308.5	900.5	1
334	1	231	0	231	231	2310.5	900.5	1
335	1	248	0	248	248	2901.5	893.5	1
336	1	233	0	233	233	2986.5	883.5	1
337	1	223	0	223	223	2982.5	882.5	1
338	1	229	0	229	229	3554.5	876.5	1
339	1	248	0	248	248	3163.5	865.5	1
340	1	221	0	221	221	2900.5	846.5	1
341	1	232	0	232	232	2864.5	838.5	1
342	3	214.667	11.015	202	222	2859.528	834.155	1
343	1	248	0	248	248	2926.5	834.5	1
344	9	243.333	3.873	236	248	2459.84	828.845	1
345	1	245	0	245	245	2783.5	826.5	1
346	1	245	0	245	245	2297.5	821.5	1
347	1	226	0	226	226	1968.5	809.5	1
348	2	241.5	3.536	239	244	1966.996	801.5	1
349	1	246	0	246	246	2565.5	776.5	1
350	6	246.333	1.862	243	248	2659.162	750.169	1
351	1	236	0	236	236	2659.5	748.5	1
352	2	247	0	247	247	2950.5	734	1
353	5	234.6	7.765	226	247	2682.896	698.714	1
354	4	240.75	1.258	239	242	2460.5	693.748	1
355	1	215	0	215	215	2452.5	693.5	1
356	1	222	0	222	222	2463.5	693.5	1
357	1	245	0	245	245	2459.5	688.5	1
358	1	234	0	234	234	2453.5	686.5	1
359	1	242	0	242	242	2460.5	683.5	1
360	1	228	0	228	228	2460.5	677.5	1
361	1	228	0	228	228	3437.5	672.5	1
362	1	247	0	247	247	3023.5	671.5	1
363	1	231	0	231	231	3449.5	663.5	1
364	2	240	9.899	233	247	3289.015	649.5	1
365	1	245	0	245	245	2569.5	621.5	1
366	1	239	0	239	239	2562.5	607.5	1
367	1	245	0	245	245	2557.5	605.5	1

368	1	202	0	202	202	2582.5	587.5	1
369	1	247	0	247	247	3111.5	554.5	1
370	2	246.5	0.707	246	247	3141.999	535.999	1
371	1	248	0	248	248	3138.5	534.5	1

Appendix C
AASHTOWare Pavement ME Design inputs and Modeling data

This Appendix presents data that were used for AASHTOWare Pavement ME Design. Some data, e.g. asphalt layer properties, were measured directly in the lab. However, other data, such as Traffic, Pavement structure, Layers properties, and project location were provided by the Idaho Transportation Department.

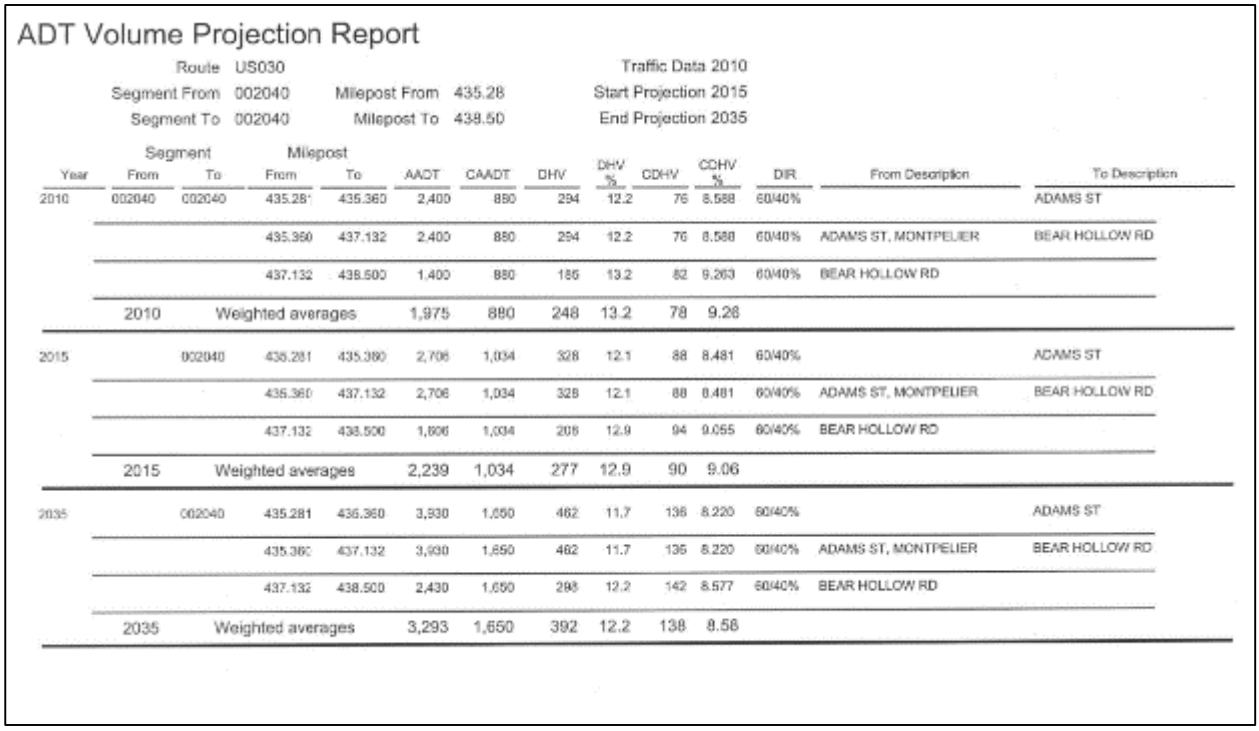

ADT Volume Projection Report

Route US030 Traffic Data 2010
Segment From 002040 Milepost From 435.28 Start Projection 2015
Segment To 002040 Milepost To 438.50 End Projection 2035

Year	Segment From	Segment To	Milepost From	Milepost To	AADT	CAADT	DHV	DHV %	CDHV	CDHV %	DIR	From Description	To Description
2010	002040	002040	435.281	435.360	2,400	880	294	12.2	76	8.588	60/40%		ADAMS ST
			435.360	437.132	2,400	880	294	12.2	76	8.588	60/40%	ADAMS ST, MONTPELIER	BEAR HOLLOW RD
			437.132	438.500	1,400	880	185	13.2	82	9.263	60/40%	BEAR HOLLOW RD	
	2010		Weighted averages		1,975	880	248	13.2	78	9.28			
2015		002040	435.281	435.360	2,706	1,034	328	12.1	88	8.481	60/40%		ADAMS ST
			435.360	437.132	2,706	1,034	328	12.1	88	8.481	60/40%	ADAMS ST, MONTPELIER	BEAR HOLLOW RD
			437.132	438.500	1,606	1,034	208	12.9	94	9.055	60/40%	BEAR HOLLOW RD	
	2015		Weighted averages		2,239	1,034	277	12.9	90	9.06			
2035		002040	435.281	435.360	3,930	1,650	462	11.7	136	8.220	60/40%		ADAMS ST
			435.360	437.132	3,930	1,650	462	11.7	136	8.220	60/40%	ADAMS ST, MONTPELIER	BEAR HOLLOW RD
			437.132	438.500	2,430	1,650	288	12.2	142	8.577	60/40%	BEAR HOLLOW RD	
	2035		Weighted averages		3,293	1,650	392	12.2	138	8.58			

Figure 45 AADT Volume Projection Report

Route: US030 Segment From: 002040 Milepost From: 435.281 Truck Density: 3 - Heavy

Traffic Data 2010 Segment To: 002040 Milepost To: 438.500

Initial	Passenger AADT	Commercial AADT	AADT	Accumulating ESALs up to 2035, starting in 2015
	1,095	880	1,975	

Year	Passenger AADT	Commercial AADT	Rigid Pavement ESALs (in thousands)				Flexible Pavement ESALs (in thousands)			
			Both Directions		One Way		Both Directions		One Way	
			Year	Cumulative	Year	Cumulative	Year	Cumulative	Year	Cumulative
2015	1,205	1,034	1,434	1,434	717	717	721	721	360	360
2016	1,226	1,065	1,493	2,927	746	1,463	750	1,471	375	735
2017	1,248	1,096	1,552	4,479	776	2,239	784	2,255	392	1,127
2018	1,270	1,126	1,608	6,087	804	3,043	814	3,069	407	1,534
2019	1,292	1,157	1,668	7,755	834	3,877	849	3,918	425	1,959
2020	1,314	1,188	1,730	9,485	865	4,742	880	4,798	440	2,399
2021	1,336	1,219	1,793	11,278	896	5,638	912	5,710	456	2,855
2022	1,358	1,250	1,856	13,134	928	6,566	949	6,659	474	3,329
2023	1,380	1,280	1,916	15,050	958	7,524	982	7,641	491	3,820
2024	1,402	1,311	1,981	17,031	991	8,515	1,019	8,660	510	4,330
2025	1,424	1,342	2,048	19,079	1,024	9,539	1,053	9,713	527	4,857
2026	1,445	1,373	2,115	21,194	1,057	10,596	1,087	10,800	544	5,401
2027	1,467	1,404	2,183	23,377	1,091	11,687	1,127	11,927	564	5,965
2028	1,489	1,434	2,246	25,623	1,123	12,810	1,162	13,089	581	6,546
2029	1,511	1,465	2,316	27,939	1,158	13,968	1,203	14,292	602	7,148
2030	1,533	1,496	2,386	30,325	1,193	15,161	1,240	15,532	620	7,768
2031	1,555	1,527	2,458	32,783	1,229	16,390	1,276	16,808	638	8,406
2032	1,577	1,558	2,530	35,313	1,265	17,655	1,319	18,127	660	9,066
2033	1,599	1,588	2,603	37,916	1,302	18,957	1,357	19,484	678	9,744
2034	1,621	1,619	2,677	40,593	1,339	20,296	1,395	20,879	697	10,441
2035	1,643	1,650	2,752	43,345	1,376	21,672	1,439	22,318	720	11,161

Figure 46 Projected Equivalent Single Axle Loading of the Project

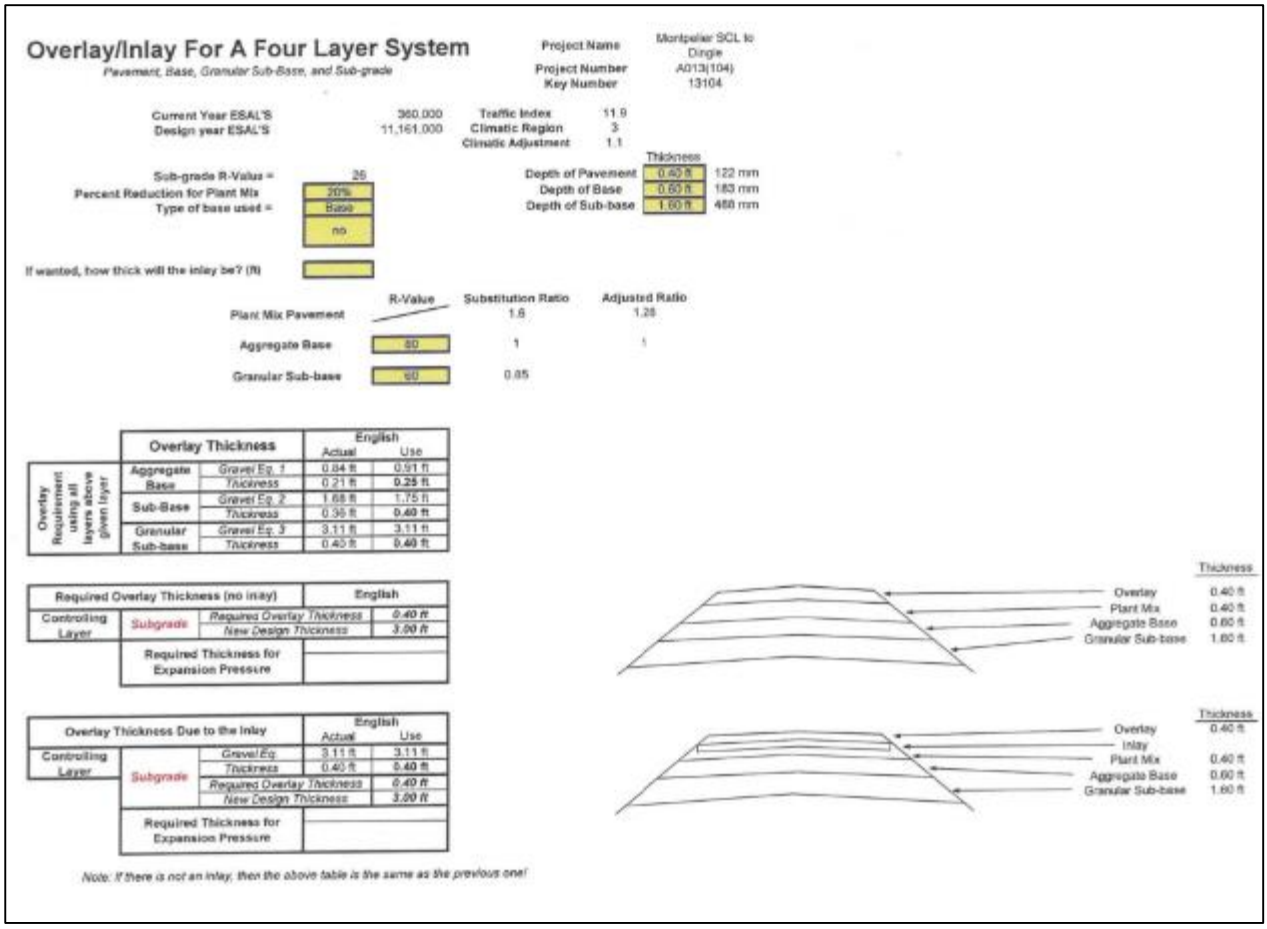

Figure 47 Pavement structure Design of the test sections

Table 35 Traffic Input Data for the project

Initial Two-Way AADTT	1034
Number of Lanes in Design Direction	1
Percentage of Trucks in Design Direction (%)	61
Percentage of Trucks in Design Lane (%)	100

Table 36 Monthly Adjustment Factors (MAF) for North Mixes

	Vehicle Class									
	4	**5**	**6**	**7**	**8**	**9**	**10**	**11**	**12**	**13**
January	0.261	0.776	0.844	0.632	0.457	1.005	0.886	0.632	1.333	1.104
February	0.417	0.792	0.724	0.632	0.519	1.078	0.886	0.632	1.333	1.254
March	0.313	0.857	0.724	0.632	0.561	1.125	0.818	0.632	1.333	1.045
April	0.417	0.890	0.784	0.632	0.685	1.078	0.852	1.263	1.333	0.955
May	0.470	0.976	0.965	0.947	0.872	1.059	1.023	0.632	1.333	0.716
June	1.096	0.586	0.724	0.947	0.830	0.447	0.648	1.263	0.444	0.388
July	2.922	1.389	1.749	2.526	1.889	1.041	1.295	1.895	0.889	0.896
August	2.452	1.291	2.111	2.211	1.806	1.064	1.159	1.895	0.889	0.896
September	2.191	1.335	1.508	1.579	1.599	1.157	1.193	1.263	0.444	1.015
October	0.626	1.156	0.603	0.316	1.287	1.040	1.261	1.263	0.889	1.284
November	0.470	1.052	0.603	0.316	0.893	1.036	1.023	0.632	0.889	1.194
December	0.365	0.901	0.663	0.632	0.602	0.870	0.955	0.000	0.889	1.254

Table 37 Vehicle Class Distribution for North Mixes

	Vehicle Class									
	4	**5**	**6**	**7**	**8**	**9**	**10**	**11**	**12**	**13**
AADTT Distribution by Vehicle Class (%)	2.15	21.28	1.90	0.36	5.51	61.01	3.43	0.19	0.27	3.91

Table 38 Number of Axles per Truck Class for North Mixes

Vehicle Class	Axle Type			
	Single	Tandem	Tridem	Quad
4	1.59	0.34	0.00	0.00
5	2.00	0.00	0.00	0.00
6	1.00	1.00	0.00	0.00
7	1.00	0.22	0.83	0.10
8	2.52	0.60	0.00	0.00
9	1.25	1.87	0.00	0.00
10	1.03	0.85	0.95	0.26
11	4.21	0.29	0.01	0.00
12	3.24	1.16	0.07	0.01
13	3.32	1.79	0.14	0.02

Table 39 Complex Shear Modulus and Phase Angle of PG 70-28 Binder Used

PG 70-28		
Temp. (°F)	**G* (psi)**	**Delta (°)**
40	1,445.15	58.22
70	273.56	59.61
100	16.11	61.85
130	1.94	67.88

Table 40 Tensile Strength at 14 F (psi)

CM	730.14
FM1	705.70
FM2	689.59
FM3	726.76

Table 41 Avg. Creep compliance of Control mix (1/psi)

time (S)	-4°F	14°F	32°F
1	2.34292E-07	3.11519E-07	4.64867E-07
2	2.4551E-07	3.28663E-07	5.18723E-07
5	2.57697E-07	3.56704E-07	5.98653E-07
10	2.68573E-07	3.83264E-07	6.90494E-07
20	2.81021E-07	4.14287E-07	8.11314E-07
50	2.99141E-07	4.64419E-07	1.03319E-06
100	3.18799E-07	4.97916E-07	1.25197E-06

Table 42 Avg. Creep compliance of FM1 mix (1/psi)

time (S)	-4°F	14°F	32°F
1	2.24E-07	2.64E-07	4.08E-07
2	2.25E-07	2.74E-07	4.37E-07
5	2.45E-07	2.98E-07	5.06E-07
10	2.52E-07	3.17E-07	5.84E-07
20	2.62E-07	3.34E-07	6.91E-07
50	2.84E-07	3.62E-07	8.44E-07
100	2.99E-07	3.85E-07	1.03E-06

Table 43 Avg. Creep compliance of FM2 mix (1/psi)

time (S)	-4°F	14°F	32°F
1	2.19E-07	3.04E-07	4.8E-07
2	2.31E-07	3.19E-07	5.37E-07
5	2.43E-07	3.45E-07	6.38E-07
10	2.55E-07	3.69E-07	7.41E-07
20	2.66E-07	4.14E-07	8.7E-07
50	2.81E-07	4.64E-07	1.11E-06
100	2.93E-07	5.34E-07	1.36E-06

Table 44 Avg. Creep compliance of FM3 mix (1/psi)

time (S)	-4°F	14°F	32°F
1	2.37E-07	3.09E-07	4.6E-07
2	2.47E-07	3.2E-07	5.11E-07
5	2.58E-07	3.44E-07	5.82E-07
10	2.71E-07	3.72E-07	6.62E-07
20	2.79E-07	4.07E-07	7.74E-07
50	3.01E-07	4.52E-07	9.67E-07
100	3.16E-07	5.08E-07	1.17E-06

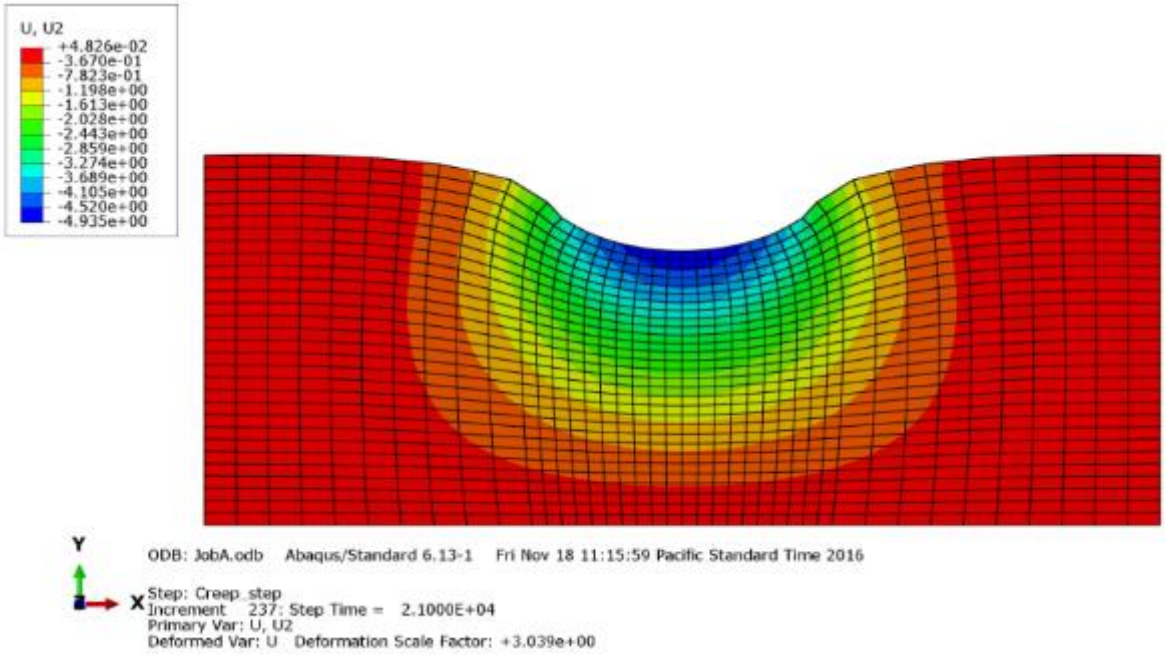

Figure 45 Predicted vertical deformation in the Control mix after 100,000 cycles

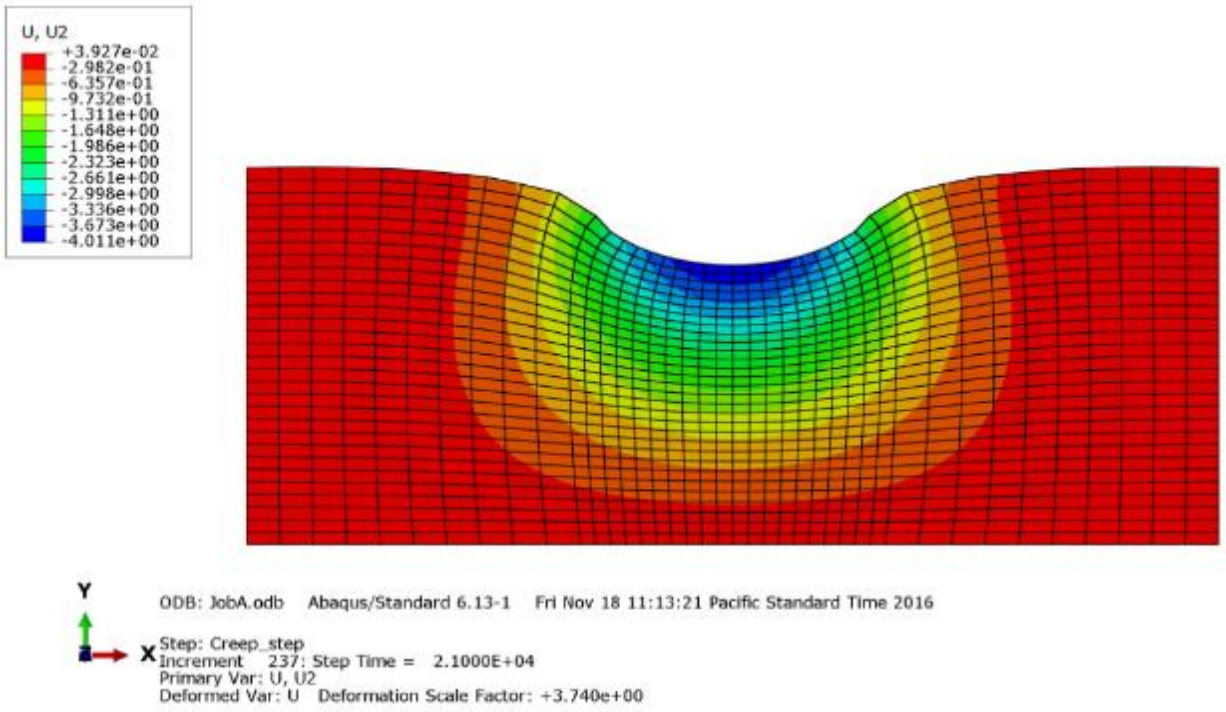

Figure 46 Predicted vertical deformation in FM1_0.05% after 100,000 cycles

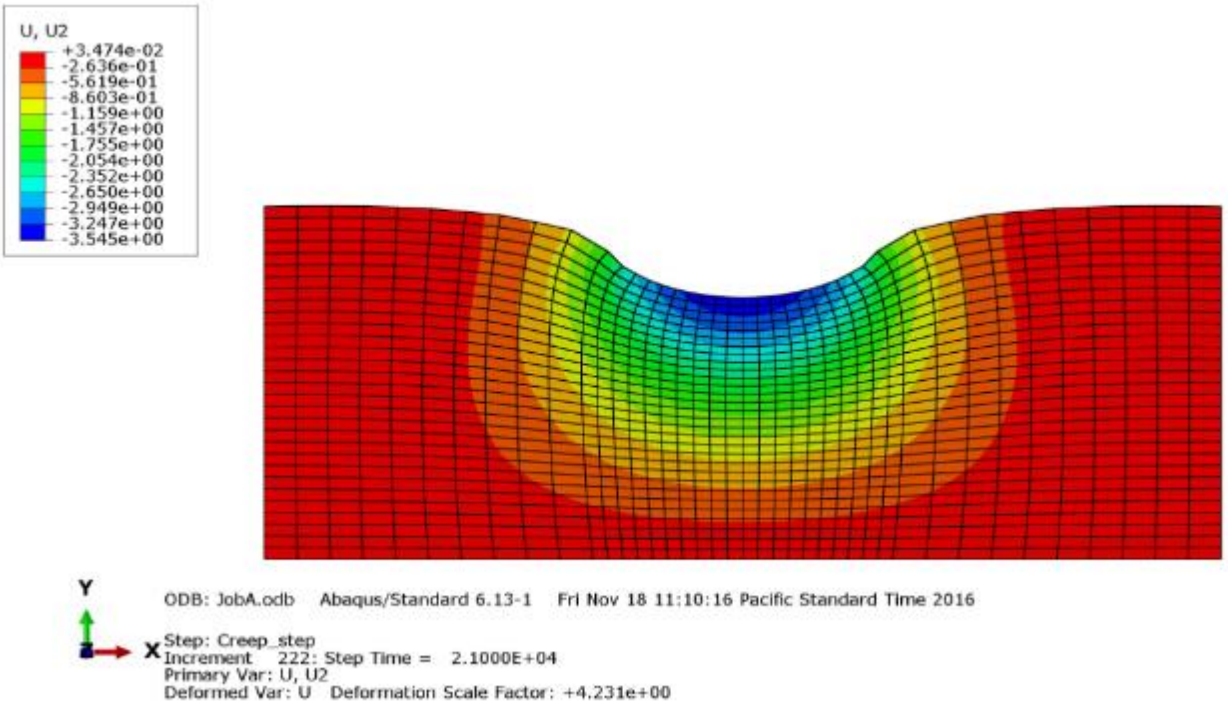

Figure 47 Predicted vertical deformation in FM2_0.015% after 100,000 cycles

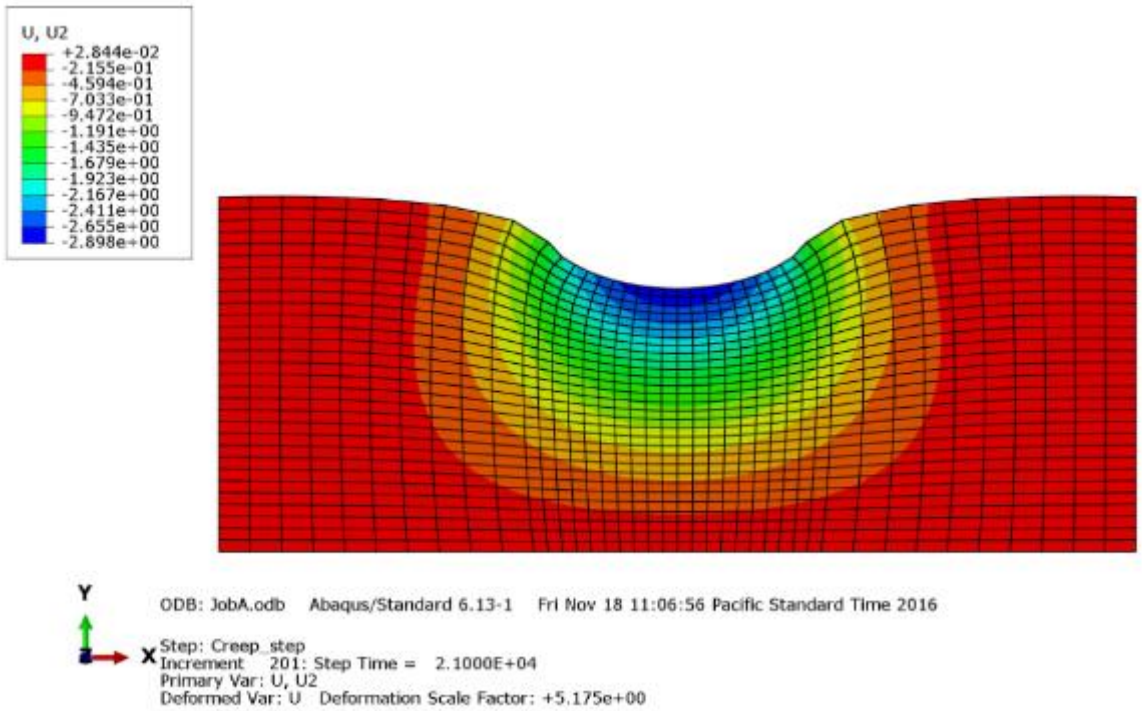

Figure 48 Predicted vertical deformation in FM3_0.16% after 100,000 cycles

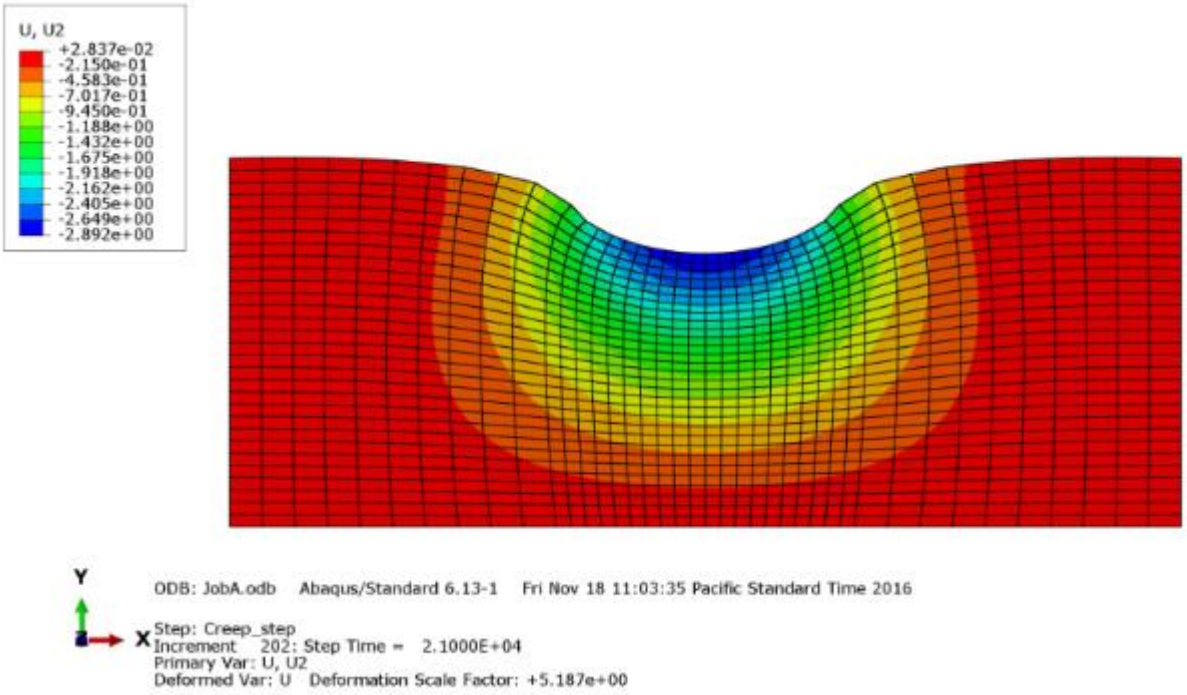

Figure 49 Predicted vertical deformation in LM1_0.2% mix after 100,000 cycles

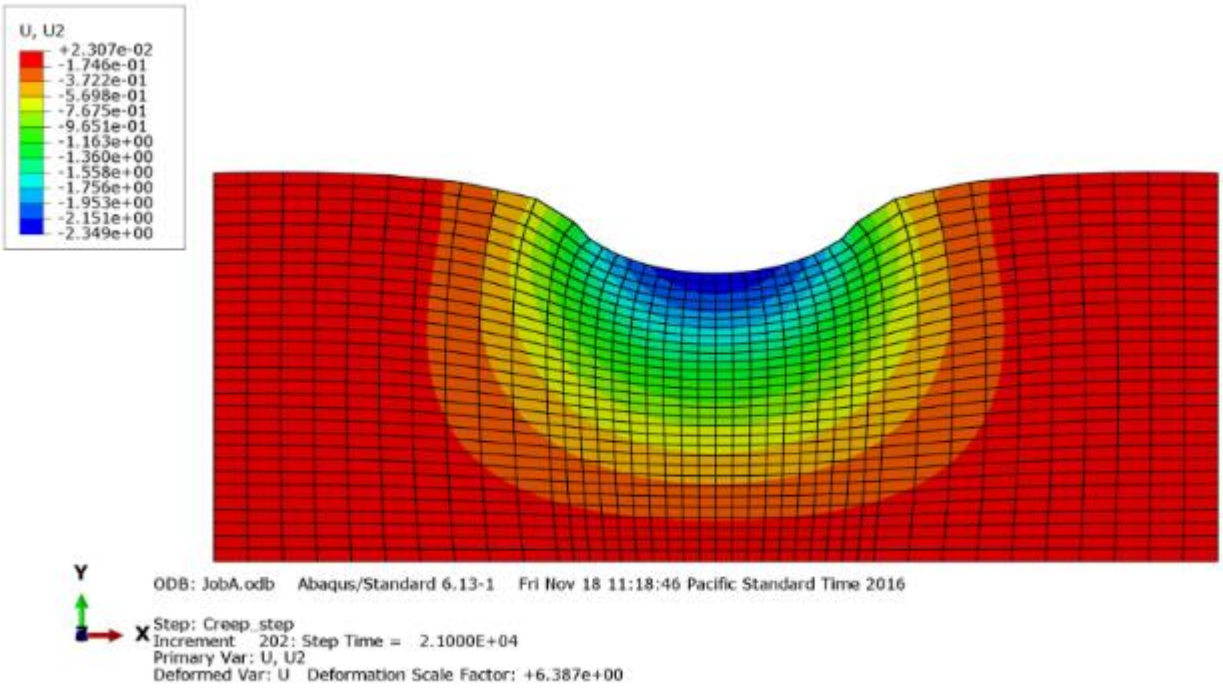

Figure 50 Predicted vertical deformation in LM2_0.3% after 100,000 cycles

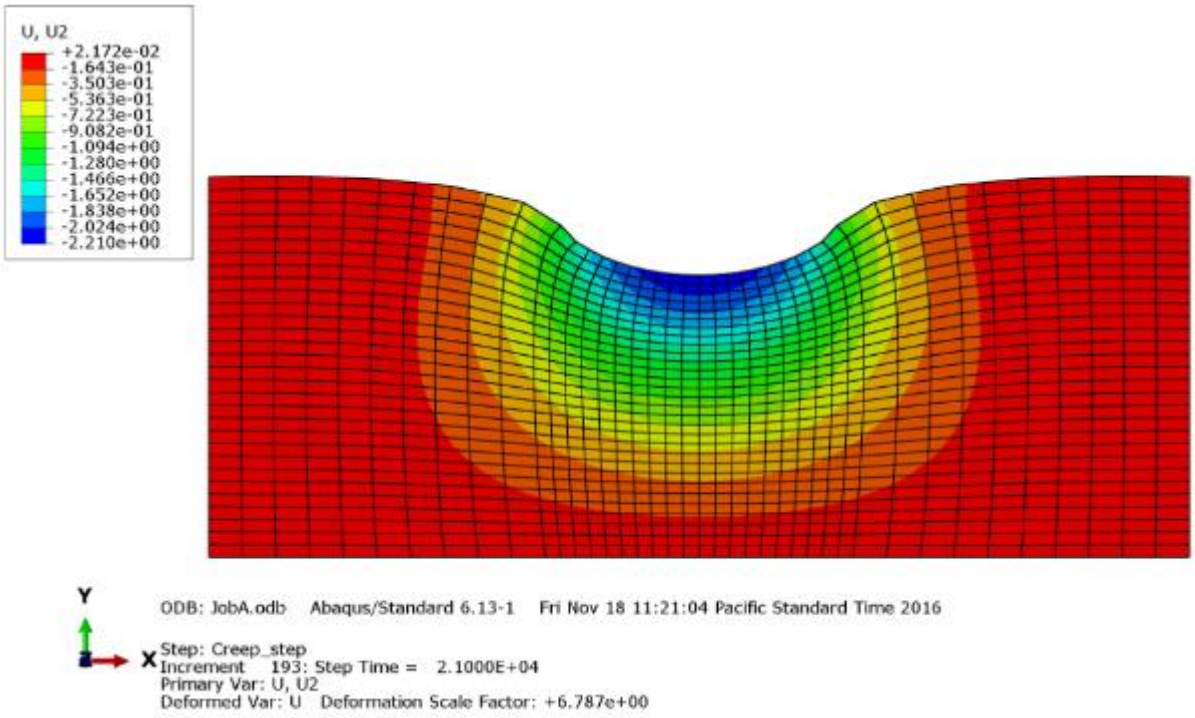

Figure 51 Predicted vertical deformation in LM3_0.3% after 100,000 cycles